PB84-199371

Evaluation of the Efficiency of Industrial Flares: Test Results

Energy and Environmental Research Corp.
Irvine, CA

Prepared for

Industrial Environmental Research Lab.
Research Triangle Park, NC

May 84

U.S. Department of Commerce
National Technical Information Service
NTIS

PB84-199371

EPA-600/2-84-095
May 1984

EVALUATION OF THE EFFICIENCY OF INDUSTRIAL FLARES: TEST RESULTS

By

J. H. Pohl, R. Payne, and J. Lee

ENERGY AND ENVIRONMENTAL RESEARCH CORPORATION
18 Mason
Irvine, California 92714

EPA Contract No. 68-02-3661

EPA Project Officer: Bruce A. Tichenor
Industrial Processes Branch
Industrial Environmental Research Laboratory
Research Triangle Park, North Carolina 27711

INDUSTRIAL ENVIRONMENTAL RESEARCH LABORATORY
OFFICE OF RESEARCH AND DEVELOPMENT
U.S. ENVIRONMENTAL PROTECTION AGENCY
RESEARCH TRIANGLE PARK, NC 27711

REPRODUCED BY
NATIONAL TECHNICAL
INFORMATION SERVICE
U. S. DEPARTMENT OF COMMERCE
SPRINGFIELD, VA. 22161

TECHNICAL REPORT DATA

(Please read Instructions on the reverse before completing)

1. REPORT NO. EPA-600/2-84-095	2.	3. RECIPIENT'S ACCESSION NO. PB8 4 199371
4. TITLE AND SUBTITLE Evaluation of the Efficiency of Industrial Flares: Test Results		5. REPORT DATE May 1984
		6. PERFORMING ORGANIZATION CODE
7. AUTHOR(S) J.H. Pohl, R. Payne, and J. Lee		8. PERFORMING ORGANIZATION REPORT NO.
9. PERFORMING ORGANIZATION NAME AND ADDRESS Energy and Environmental Research Corporation 18 Mason Irvine, California 92714		10. PROGRAM ELEMENT NO.
		11. CONTRACT/GRANT NO. 68-02-3661
12. SPONSORING AGENCY NAME AND ADDRESS EPA, Office of Research and Development Industrial Environmental Research Laboratory Research Triangle Park, NC 27711		13. TYPE OF REPORT AND PERIOD COVERED Final; 10/80 - 2/84
		14. SPONSORING AGENCY CODE EPA/600/13

15. SUPPLEMENTARY NOTES IERL-RTP project officer is Bruce A. Tichenor, Mail Drop 54; 919/541-2991. EPA-600/2-83-070 is an earlier related (Phases 1 and 2) report.

16. ABSTRACT

The report gives results of Phases 3 and 4 of a four-phase research program to quantify emissions from, and efficiencies of, industrial flares. Phase 1 consisted of the experimental design; Phase 2, the design of the test facilities; Phase 3, development of the test facilities; and Phase 4, data collection and analysis. The combustion efficiency of large pilot-scale flares was measured. The flame structure and combustion efficiencies were correlated with operating conditions of the flare, the size of the flare head, and properties of the flared gases. The combustion efficiency was correlated with the ratio of heating value of the gas flared to the heating value required to maintain a stable flame, and was independent of the flame head size. In turn, the heating value required to maintain a stable flame was correlated with the reciprocal of an estimated flame temperature based on properties of the flared gas. The length of the flame, entrainment into the flame, and liftoff distances were also correlated, using combinations of the Richardson Number, jet theory, and properties of the flared gas.

17. KEY WORDS AND DOCUMENT ANALYSIS

a. DESCRIPTORS		b. IDENTIFIERS/OPEN ENDED TERMS	c. COSATI Field/Group
Pollution	Analyzing	Pollution Control	13B
Exhaust Gases		Stationary Sources	21B
Efficiency		Industrial Flares	14G
Flames			
Measurement			
Surveys			14B

18. DISTRIBUTION STATEMENT Release to Public	19. SECURITY CLASS *(This Report)* Unclassified	21. NO. OF PAGES 204
	20. SECURITY CLASS *(This page)* Unclassified	22. PRICE

EPA Form 2220-1 (9-73)

NOTICE

This document has been reviewed in accordance with U.S. Environmental Protection Agency policy and approved for publication. Mention of trade names or commercial products does not constitute endorsement or recommendation for use.

ABSTRACT

The U.S. Environmental Protection Agency has contracted with Energy and Environmental Research Corporation to conduct a research program which will result in the quantification of emissions from, and efficiencies of, industrial flares. The study is being conducted in four phases:

I - Experimental Design
II - Design of Test Facilities
III - Development of Test Facilities
IV - Data Collection and Analysis

EPA Report No. 600/2-83-070 provides the results of Phases I and II of the study; the results of Phases III and IV are reported herein.

Measurements were made of the combustion efficiency of large pilot-scale flares. The flame structure and combustion efficiencies were correlated with operating conditions of the flare, size of the flare head, and properties of the flared gases. The combustion efficiency was correlated with the ratio of heating value of the gas flared to the heating value required to maintain a stable flame, and was independent of the flame head size. In turn, the heating value required to maintain a stable flame was correlated with the reciprocal of an estimated flame temperature based on properties of the flared gas. Other correlations for the length of the flame, entrainment into the flame, and liftoff distances were developed using combinations of the Richardson Number, jet theory, and the properties of the flared gas.

TABLE OF CONTENTS

Section Page

List of Figures vii

List of Tables ix

1.0 INTRODUCTION 1-1

1.1 Flare Flames 1-1
1.2 Amount of Gases Flared in the United States 1-1
1.3 Emissions from Flares 1-2
1.4 Approach of This Study 1-5

2.0 CONCLUSIONS 2-1

2.1 Technical Summary 2-1

3.0 TEST METHODOLOGY 3-1
3.1 Flare Test Facilities (FTF). 3-1
3.2 Test Procedure 3-6
3.3 Data Reduction 3-13

4.0 FLAME STRUCTURE 4-1

4.1 Test Conditions 4-2
4.2 Mechanism of Combustion 4-6
4.3 Flame Length . . . . 4-13 ← 15
4.4 Entrainment 4-20
4.5 Flame Liftoff 4-23
4.6 Flame Stability 4-26

5.0 COMBUSTION EFFICIENCY OF FLARE FLAME 5-1

5.1 Study Conditions 5-1
5.2 Comparison with Other Studies 5-1
5.3 Correlations 5-3
5.4 Commercial Flare Heads 5-7
5.5 High Velocity 5-7
5.6 Steam 5-7

TABLE OF CONTENTS
(Continued)

Section Page

APPENDIX A: EPA Flare Test Facility at EER . . . . A-i

APPENDIX B: Testing Methodology B-1

APPENDIX C: Data Summary Table C-1

APPENDIX D: Integrated Combustion Efficiencies D-1

APPENDIX E: Examples of Test Data E-1

APPENDIX F: Graphs of Local Combustion Efficiencies and Dilution Factors F-1

APPENDIX G: Quality Assurance G-1

LIST OF FIGURES

Figure No.		Page
2-1	EPA flare test facility at EER	2-2
2-2	Diagram of sampling locations	2-11
2-3	Region of flame instability	2-12
2-4	Combustion efficiency near the limits of flame stability	2-14
3-1	Design of retention ring for 3-inch flare head	3-3
3-2	Flow patterns determined by smoke tests	3-5
3-3	Influence of hood position on closure of a carbon balance using mass fluxes measured in the hood	3-8
3-4	Influence of hood position on combustion efficiency measured in the hood	3-9
3-5	Verification of carbon mass balance for hood measurements.	3-11
3-6	Comparison of SO_2 and CO_2 used as tracers	3-12
4-1	Comparison of the range of conditions tested in this study and those of commercial flare flames	4-8
4-2	Correlation of lengths of flames studied with Reynolds number	4-10
4-3	Surface rate of combustion of flare flames	4-11
4-4	Volumetric combustion intensity of flare flames	4-12
4-5	Comparison of flame lengths predicted by available studies with those observed in this study	4-16
4-6	Comparison of a Hottel and Hawthorne correlation with the flame length of this study	4-17
4-7	Comparison of flame lengths predicted by a buoyance correlation with observed flame lengths of this study	4-18
4-8	Correlation of flame lengths in this study	4-19
4-9	Empirical correction for radiation loss from flare flames.	4-21
4-10	Entrainment of air into flare flames	4-22
4-11	Correlation of entrainment rate for flare flames	4-24

LIST OF FIGURES
(Continued)

Figure No.		Page
4-12	Correlation of entrainment rate for flare flames	4-25
4-13	Liftoff of flare flames without pilot flames	4-27
4-14	Correlation of liftoff distances for flames without pilot flames	4-28
4-15	Region of flame instability	4-30
4-16	Flame speeds of hydrocarbons	4-31
4-17	Limits of flame stability as a function of estimated temperature	4-32
5-1	Conditions to obtain 98 percent combustion efficiency for mixtures of propane and nitrogen	5-4
5-2	Combustion efficiency near the limits of flame stability	5-6
5-3	Influence of steam on combustion efficiency	5-8

LIST OF TABLES

Table No. Page

1-1 Estimate of the amount of gas flared in the United States in 1980 (Ref. 1-3) 1-3

1-2 Combustion efficiency of flare flames measured in previous studies 1-4

2-1 Combustion efficiencies of EER three-inch flare head 2-4

2-2 Combustion efficiency of three-inch EER flare head . . . . . at high velocities 2-5

2-3 Combustion efficiencies of EER six-inch flare head 2-6

2-4 Combustion efficiencies of EER twelve-inch flare head 2-7

2-5 Combustion efficiencies of twelve-inch industrial flare head #A 2-8

2-6 Combustion efficiency of twelve-inch industrial flare head #B 2-9

2-7 Combustion efficiencies of twelve-inch industrial flare head #C 2-10

4-1 Flare test conditions 4-4

4-2 Matrix for testing commercial flare heads 4-5

4-3 Test conditions for high-velocity flares 4-7

4-4 Conditions under which correlations for flames were derived 4-15

1.0 INTRODUCTION[1]

Flares are used to safely destroy industrial gases when: (1) the heating value cannot be recovered economically because of intermittent and uncertain flow, or (2) process upsets occur. Large amounts of gases are flared in the United States. However, even the approximate amount of these gases is difficult to establish, because most of the gas is released as leaks, purges and emergency vents. Such releases are poorly measured and reported. Also, the emissions of incompletely burned hydrocarbons from flare flames are not know accurately, because the amount of material flared is uncertain and the combustion efficiency of the flare flames is unknown and difficult to measure. This program has measured the combustion efficiency of pilot-size flares, whose size and operating conditions have been scaled by several different techniques.

1.1 Industrial Flares

The size, use, operating conditions, and geometry of commercial flares are diverse. Flares can be enclosed, gas-assisted, air-assisted, pressure, or pipe (without or without steam assist) (1.1 - 1.3). They can be used to destroy relatively constant purges and leaks of gases and emergency or intermittent planned releases of large amounts of gases. The size of commercial flares can vary from 1-1/2 inches in diameter to over 12 feet; operating conditions can include velocities as low as 0.005 ft/sec and as high as sonic; to suppress soot, steam is added at rates of from 0- to one-pound-of-steam-per-pound-of-fuel, water from 0- to 2-pounds-of-water-per-pound-of-fuel, or air from 0- to 6 -pounds-of-air-per-pound-of-fuel (1.1). This study was limited to measuring the combustion efficiencies of pipe flares burning propane-nitrogen mixtures at steady operating conditions with and without steam injection, in the absence of wind.

---

[1] The project's initial report (1.4), "Evaluation of the Efficiency of Industrial Flares: Background-Experimental Design-Facility" (EPA No. 600/2-83-070) provides the basis for the research reported herein. The present Introduction provides only a brief summary of the earlier report.

1.2 Amount of Gases Flared in the United States

The amount of gases flared in the United States is uncertain. A partial estimate of the amount of gas flared in industries by Klett and Galeski (1976) (1.3) indicated that 12 million tons of gases per year were flared in the United States in 1974. The initial report of this study expanded and updated this estimate and concluded that approximately 16 million tons of gas were flared per year in 1980 from the industries shown in Table 1-1 (1.4). Based on heating value, most gas is flared in the petroleum production and refining industries. However, based on the amount of gas, more gas is flared from blast furnaces than any other industrial segment.

1.3 Emissions From Flares

Direct field measurement of incompletely burned hydrocarbons from industrial flare flames are unavailable and unlikely to become available for a number of reasons. The flare stacks are high above the ground to protect materials and personnel from the intense radiation of the flames. In addition, the flames are very large and in constant motion. These factors make probing the plume of a commercial flare flame, even at a single location, extremely difficult. A remote sensing system may in the future help indicate the emissions from flare flames, but considerably work must be done before such systems are available (1.5 - 1.9).

In the absence of direct measurements of emissions on operating flare flames, measurements have been made on pilot-scale and small commercial flare heads. The heads studied have ranged from a 1/2-inch jet to a 27-inch commercial flare head(1) installed on a slip-stream of a refinery. Table 1-2 shows the range of flare heads, the operating conditions, and the combustion efficiencies measured on these heads. The studies indicated that the combustion efficiency of flares can be very high. However, the studies also showed that the combustion efficiency of flares can be low under some operating conditions.

The values of combustion efficiency measured in the previous studies were somewhat uncertain. The uncertainties were attributed to:

---

(1) Opening of a cone on an FS-6 Coanda flare head.

TABLE 1-1. ESTIMATE OF THE AMOUNT OF GAS FLARED IN THE UNITED STATES IN 1980 (Ref. 1.4)

INDUSTRY	PRODUCTION OF PRODUCT 10^6 TONS/YR	PERCENT FLARED	AMOUNT FLARED 10^6 TONS/YR	10^6 MBtu/YR
Refineries	1048	0.2	2.1	103
Petroleum Production	584	0.5	2.9	116
Blast Furnaces(a)	146	6.6	9.6	69
Coke Ovens(a)	55	0.4	0.2	11
Chemical(a) Industry	60	2.0	1.2	59
TOTAL			16.0	358

(a) Combustible gases only

TABLE 1-2. COMBUSTION EFFICIENCY OF FLARE FLAMES MEASURED IN PREVIOUS STUDIED

STUDY	DATE	FLARE SIZE (IN)	DESIGN	VELOCITY (FT/SEC)	GAS FLARED	MEASURED EFFICIENCY (%)
Palmer (1.10)	1972	0.5	Experimental Nozzle	50 - 250	Ethylene	> 97.8
Lee & Whipple (1.11)	1981	2.0	Holes in 2" Cap	1.8	Propane	96 - 100
Siegel (1.12)	1980	27.(f)	Commercial Flaregas Coanda FS-6	0.7 - 16	Refinery Gas(a)	97 - > 99
Howes, et al (1.8)	1981	6.(c)	Commercial Air Assist. Zink LH	40 - 60	Propane	92 - 100
Howes, et al (1.8)	1981	3at 4(b)	Commercial H.P.Zink LRGO	Near Sonic (estimate)	Natural Gas	> 99
McDaniel (1.13)	1983	8	Commercial Zink STF-S-8	0.03 - 62	Propylene/Nitrogen(d)	67 - 100
McDaniel (1.13)	1983	6(c)	Commercial Air Assist. Zink STF-LH-457-5	1.4 - 218	Propylene/Nitrogen(e)	55 - 100

(a) 50% hydrogen plus light hydrocarbons

(b) Three Spiders, each with an open area of 1.3 in^2

(c) Supplied through spiders; high Btu gas through area of 5.30 in^2 and low Btu gas through 11.24 in^2

(d) Heating value was varied from 209 to 2183 Btu/scf

(e) Heating value was varied from 83 to 2183 Btu/scf

(f) See footnote (1), p. 1-2

- Inability to close a material balance.
- Soot concentrations were rarely measured.
- Samples were typically taken only on the axis.
- Difficulties were caused by the intermittent nature of the flare flame.

1.4 Approach of This Study

The approach used in this study was designed to eliminate or minimize many of the uncertainties of previous studies.

- The closure of a material balance was verified using a hood to capture the entire flare plume for small flames and by using SO_2 as a tracer for large flames.
- Soot concentration was measured for all tests.
- The average concentration of incompletely burned combustion species from the flare flame was determined for the entire plume captured by a hood for small flames, and samples were simultaneously measured at five radial positions using the rake probe for large flames. These values were combined with velocities calculated from jet theory to estimate the global combustion efficiencies of each flame.
- The intermittency of the flare flames were accounted for by mixing a sample taken over a period sufficient to average flame fluctuations (20 minutes).

The experimental test matrix was designed to determine the validity of several common scaling procedures for three-, six-, and twelve-inch flare heads. The scaling criteria were constant exit velocity, constant residence time, constant Reynolds number, and constant Richardson's number.

Throughout the program, advice and consultation was sought from a Technical Advisory Committee. The committee attended meetings throughout the program to review and criticize test plans, ensure the relevance of the study and facilitate efficient technology transfer. The Advisory Committee consisted of:

Zahir Bozai
Peabody Engineering

B. C. Davis
Central Engineering Div.
Exxon Chemical Co.

John J. Dubnowski(1)
Exxon R&E

Leslie Evans
Chemical & Petroleum
Process Branch
Office of Air Quality
Planning & Standards
U.S. Environmental Protection
Agency

E. Doyle Fowler
Union Carbide

Allan Goodley
California Air Resources Board

Keith Herbert
McGill, Inc.

W. G. Hudson
Engineering & Technology
Services Division
Union Carbide Corporation

Mike Keller
John Zink Company

R. W. Ladd
Getty Refining & Marketing Co.

James G. Seebold
Chevron USA

David Shore
Flaregas Corporation

Larry Thurston
Dow Chemical Company

J. R. Venable
Rohm & Haas Texas, Incorporated

---

(1) Replaced in December 1983
by John Wang, Exxon R&E

REFERENCES

SECTION 1

1.1 Vanderlinde, L. G., "Properly Designed Mechanical Equipment Can Make Flares Smokeless," in Environmental Management Handbook for the Hydrocarbon Processing Industries, Gulf Publishing Co., Houston, Texas, 1980, pp. 132-137.

1.2 Brzustowski, T. A., "Flaring in the Energy Industry," Progress in Energy and Combustion Science, Vol. 2, 1976, pp. 129-161.

1.3 Klett, M. G., and J. B. Galeski, Flare Systems Study, EPA Report No. 600/2-75-079 NTIS Report No. PB-251664, March 1976.

1.4 Joseph, D., J. Lee, C. McKinnon, R. Payne and J. Pohl, "Evaluation of the Efficiency of Industrial Flares: Background - Experimental Design - Facility," EPA Report No. 600/2-83-070, August 1983.

1.5 Herget, W. F., Air Pollution: Ground-Based Sensing of Source Emissions in Fourier Transform Infrared Spectroscopy, J. R. Fenaro and L. J. Busile, Eds., Academic Press, 1979.

1.6 Herget, W. F., and J. D. Brasher, "Remote Fourier Transform Infrared Air Pollution Studies," Optical Engineering, 19, No. 4, 1980, pp. 508-514.

1.7 Herget, W. F., and J. D. Brasher, "Remote Measurements of Gaseous Pollution Concentrations Using a Mobile FTIR System," Applied Optics, 18, October 1979, pp. 3402-3620.

1.8 Howes, J. E., T. E. Hill, R. N. Smith, G. R. Ward and W. R. Herget, "Development of Flare Emission Measurement Methodology, Draft Report," EPA Contract No. 68-02-2682, 1981.

1.9 Armstrong, J. A., "Tethered Balloon Sampling of a Pilot-Scale Industrial Flare Plume," EPA and Denver Research Institute Cooperative Agreement No. CR-807504-01, 1983.

1.10 Palmer, P. A., "A Tracer Technique for Determining Efficiency of an Elevated Flare," E. I. DuPont de Nemours and Co., Wilmington, DE, 1972.

1.11 Lee, K. C., and G. M. Whipple, "Waste Gas Hydrocarbon Combustion in a Flare," Union Carbide Corporation, South Charleston, WV, 1981.

1.12 Siegel, K. D., "Degree of Conversion of Flare Gas in Refinery High Flares," Ph.D. Dissertation, University of Karlsruhe (Germany), February 1980.

1.13 McDaniel, M., "Flare Efficiency Study," EPA Report No. 600/2-83-052, July 1983.

2.0 CONCLUSION

2.1 Technical Summary

The EPA Flare Test Facility (FTF) was constructed at Energy and Environmental Research (EER) Corporation's El Toro test site. The FTF (Figure 2-1) includes a pad and structure for installation and testing of flare heads, screens to shield the flame from wind, parallel delivery systems to accurately meter the wide range of gas flows to the flare, a hood to sample the entire plume, a movable rake probe to simultaneously sample five radial positions, high-speed movie and photographic equipment to record the structure of the flare flame, and a room from which to control the flare and analyze gas samples.

Techniques were developed to operate, sample, analyze and reduce the data. Analysis includes visual and photographic observation of the flare flame structure, and samples of soot, O_2, CO, CO_2, total hydrocarbon, and SO_2, which was used as a tracer. The data is corrected for the measured background of combustion species and for dilution of the flare plume by ambient air. Dilution and local combustion efficiencies are calculated at each probe position and the maximum potential error in the dilution and combustion efficiencies are estimated for each data point. The local combustion efficiencies are integrated using velocity profiles estimated by jet theory to yield a global combustion efficiency for each flare flame.

The combustion efficiencies were measured for a wide range of operating conditions typical of commercial flares:

- Head type
  - 3-inch EER prototype
  - 6-inch EER prototype
  - 12-inch EER prototype
  - 3-inch EER prototype with convergent ring
  - 3-inch EER prototype with divergent ring
  - 12-inch Manufacturer A

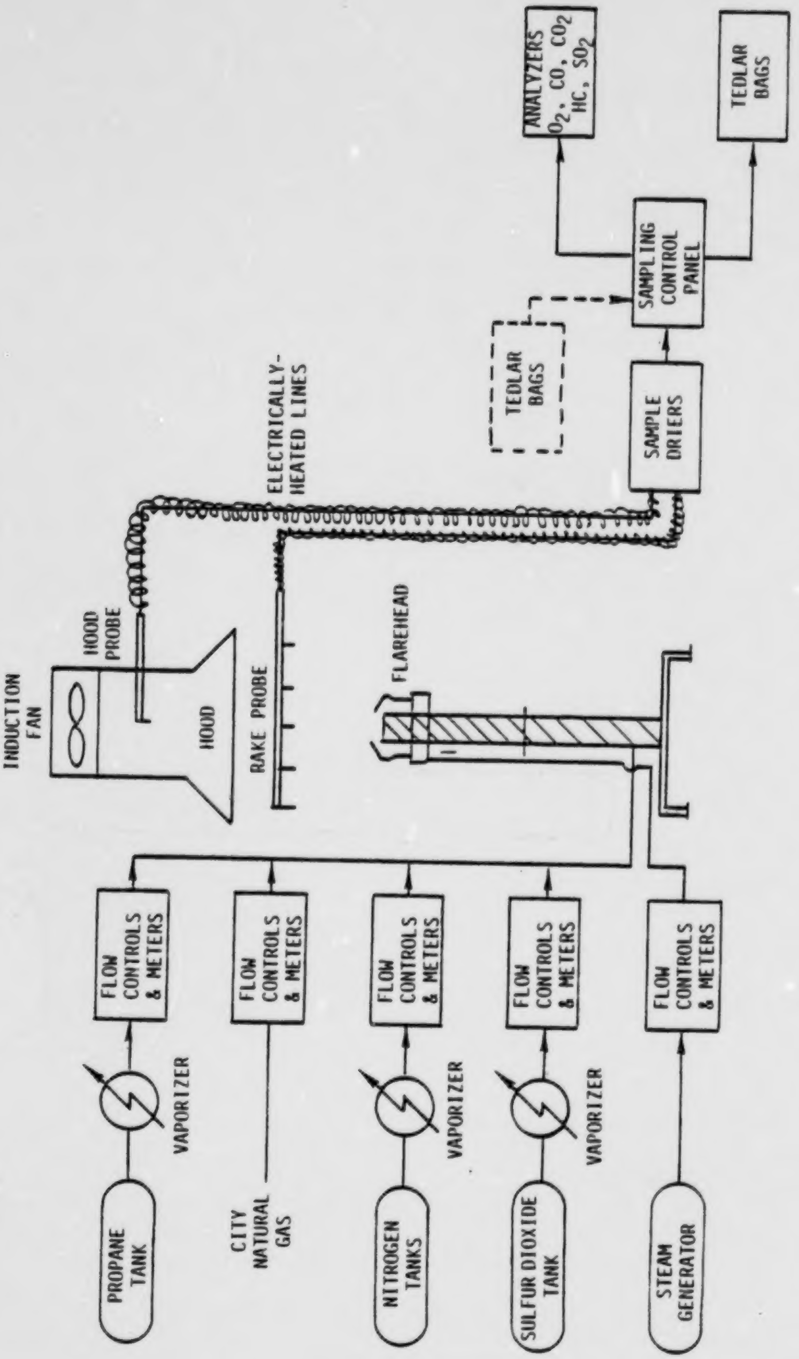
PROPANE TANK
VAPORIZER
FLOW CONTROLS & METERS
CITY NATURAL GAS
FLOW CONTROLS & METERS
NITROGEN TANKS
VAPORIZER
FLOW CONTROLS & METERS
SULFUR DIOXIDE TANK
VAPORIZER
FLOW CONTROLS & METERS
STEAM GENERATOR
FLOW CONTROLS & METERS
INDUCTION FAN
HOOD
HOOD PROBE
RAKE PROBE
FLAREHEAD
ELECTRICALLY-HEATED LINES
SAMPLE DRIERS
TEDLAR BAGS
SAMPLING CONTROL PANEL
ANALYZERS O_2, CO, CO_2 HC, SO_2
TEDLAR BAGS

Figure 2-1. EPA flare test facility at EER.

  - 12-inch Manufacturer B
  - 12-inch Manufacturer C

- Gas
  - Propane-nitrogen mixtures
  - Natural gas
- Heating value of the flared gas from 270 - 2350 Btu/ft^3
- Flow rates
  - Velocities from 0.2 - 428 ft/sec
  - Reynolds Numbers from 337 to 217,000
  - Richardson Numbers from 2.9×10^{-5} to 8×10^2

Tables 2-1 through 2-7 contain a summary of the test conditions and the combustion efficiencies. Sampling positions of the hood and rake probe are shown in Figure 2-2. In addition to the combustion efficiencies, other calculations and correlations were made:

- Combustion intensity was found to be 90,000 Btu/hr/ft^3, independent of flare or flame conditions.
- The flame length was correlated with the Richardson number.
- The liftoff distance was correlated with ratios of velocities and concentrations of combustible gas.
- The flame stability was correlated with the reciprocal of an estimated flame temperature.
- The combustion efficiency was correlated with a dimensionless heating value of the gas fired.

The term "flame stability" simply means that a flame is maintained; flame instability occurs when the jet velocity exceeds the flame velocity and the flame goes out. Figure 2-3 shows the gas heating value versus the gas exit velocity at the point of instability (i.e., at the point where the flame starts to "go out.") This point is determined by establishing a propane-nitrogen flame at a given velocity and then decreasing the flow of propane until the flame goes out. The propane flow is then increased slightly, and the combustion efficiency is measured at the conditions just prior to the point where the flame went out.

TABLE 2-1. COMBUSTION EFFICIENCIES OF EER THREE-INCH FLARE HEAD

FLARE HEAD: EER SIZE: 3-INCH

Purpose of Test	Test Number	Flame Retention Ring	(a) Actual Exit Velocity (ft/sec)	(b) Nominal Exit Velocity (ft/sec)	Low Heating Value (Btu/ft^3)	Fuel in Nitrogen (%)	Steam Ratio (lb.Steam /lb.Fuel)	Observations					Sample Method R=Rake H=Hood	(c) Probe Position (ft)	Global Combustion Efficiency (%)	Hydrocarbon Destruction Efficiency (%)
								Wind Speed (MPH)	Flame Length (ft)	Lift Off (in.)	Color	Smoke				
56 Percent C_3H_8	002	No	0.5	0.5	1311	55.8	0.0	Low	4	0	Yellow	Yes	H	10	98.37	99.87
	003		0.5	0.5	1309	55.7	0.0	Low	4	0	Yellow	Yes	R	9	98.77	99.61
	005		2.0	2.0	1318	56.1	0.0	Low	7	0	Dk.Yel	Yes	H	4	99.54	99.87
	008		2.0	2.0	1314	55.9	0.0	Low	6	0	Yellow	Yes	R	10	98.95	100.00
	012		10.0	10.0	1323	56.3	0.0	2-4	15	0	Yellow	Yes	R	15	98.78	99.25
Low Btu	013	No	0.5	0.5	273	11.6	0.0	0-1	4	0	Barely Visible	No	H	0	90.19	92.55
Effect of Steam	016	No	10.0	10.0	1323	56.3	0.142	0-8	10	0	Yellow	Little	H	7	99.83	99.96
	017		10.0	10.0	1323	56.3	0.300	0-6	10	2	Yellow	Little	H	9	99.96	99.98
	018		10.0	10.0	1321	56.2	0.500	-	9	2-4	Yellow	Little	H	9	99.89	99.99
	019		10.0	10.0	1323	56.3	1.000	-	6	4	Yellow	Little	H	9	98.94	99.59
Low Btu	020	No	12.0	12.0	620	26.4	0.0	-	-	-	Yellow	Yes	H	9	99.92	99.95
	052		2.1	2.1	376	16.0	0.0	0-3	3.5	0-3	Yel/Or	No	R	5	98.09	98.41

(a) Based on open area of flare head

(b) Based on velocity of pipe

(c) Refer to Figure 2-2

TABLE 2-2. COMBUSTION EFFICIENCY OF THREE-INCH EER FLARE HEAD AT HIGH VELOCITIES

FLARE HEAD: EER SIZE: 3-INCH

Purpose of Test	Test Number	Flame Retention Ring	(a) Actual Exit Velocity (ft/sec)	(b) Nominal Exit Velocity (ft/sec)	Low Heating Value (Btu/ft^3)	Fuel in Nitrogen (%)	Steam Ratio (lb.Steam/lb.Fuel)	Observations					Sample Method R=Rake H=Hood	(c) Probe Position (ft)	Global Combustion Efficiency (%)	Hydrocarbon Destruction Efficiency (%)
								Wind Speed (MPH)	Flame Length (ft)	Lift Off (in.)	Color	Smoke				
High-Vel, No Flame Ret. Ring	77	No	39.6	39.6	1316	56.0	0.0	0-3	24	5-9	Yellow	Yes	R	25	95.11	95.31
	78	No	80.0	80.0	1325	56.4	0.0	-	28	12-13	Yel/Or	Yes	R	33	98.40	98.57
	79	No	118.5	118.5	1307	55.6	0.058	1-5	32	18	Yel/Or	Yes	R	35	99.66	99.88
High-Vel, 56 Percent C_3H_8	80	Div.[d] 40.0%	420.5	168.2	1255	53.4	0.015	0-1	33	24	Clr/Or	No	R	34	99.20	100.00
	81		67.0	26.8	837	35.6	0.149	0-1	17.5	8-10	Orange	No	R	20	97.27	97.79
	82		248.3	99.3	1107	47.1	0.031	0-1	31	24	Orange	No	R	35	99.33	99.48
High-Vel, 100% C_3H_8	83	Div. 40.0%	144.5	57.0	2350	100.0	0.131	0-1	29.5	12	Orange	No	R	33	99.87	100.00
	93	Conv.[e] 46.3%	84.7	39.2	2348	99.9	0.122	0-5	26.5	10	Orange	No	R	31	99.74	99.98
	94		171.4	79.3	2350	100.0	0.061	0-3	34.5	12	Yel/Or	Little	R	37	99.83	99.99
High-Vel, Stable Flame Limit	95	Conv. 46.3%	114.8	53.1	792	33.7	0.087	0-2.5	23	12-18	Yellow	No	R	26	99.87	99.98
	96		274.1	126.8	1043	44.4	0.028	0-1.5	33	18-28	Yel/Or	No	R	37	99.85	99.97
High-Vel, 50 Percent C_3H_8	97	Conv. 46.3%	85.8	39.7	1156	49.2	0.142	1-5	20	8	Orange	No	R	24	99.72	99.96
	98		172.3	79.7	1133	48.2	0.071	0-2	29	7	Yel/Or	No	R	34	99.87	99.99
High-Vel, Stable Flame Limit	99	Conv. 46.3%	428.2	198.1	1027	43.7	0.018	0-1	30.5	24-36	Orange	No	R	35	99.88	99.97
High-Vel, 50 Percent C_3H_8	100	Conv. 46.3%	343.1	158.7	1149	48.9	0.020	0-4	34	24-30	Orange	No	R	37	99.84	99.93
High-Vel, 77 Percent C_3H_8	101	Conv. 46.3%	85.8	39.7	1807	76.9	0.091	1-4	25	6	Orange	No	R	29	99.73	99.96
	102		170.1	78.7	1805	76.8	0.80	1-5	30.5	12	Yel/Or	Little	R	34	99.74	99.94
	103		260.1	120.3	1795	76.4	0.060	0-1.5	37	8	Yellow	No	R	37	99.88	99.98
High-Vel, Stable Flame Limit	104	Conv. 46.3%	375.5	173.7	921	39.2	0.023	0-1.5	29.5	36-48	Orange	No	R	30	99.81	99.91
High-Vel, 100 Percent C_3H_8	105	Conv. 46.3%	243.4	112.6	2350	100.0	0.049	0-5	40	12	Orange	Little	R	42	99.77	99.95

(a) Based on open area of flare head
(b) Based on velocity of pipe
(c) Refer to Figure 2-2
(d) Div. refers to the retention ring of Figure 3-1 upside down
(e) Conv. refers to the retention ring of Figure 3-1 in the position shown

TABLE 2-3. COMBUSTION EFFICIENCIES OF EER SIX-INCH FLARE HEAD

FLARE HEAD: EER SIZE: 6-INCH

Purpose of Test	Test Number	Flame Retention Ring	Actual Exit Velocity (ft/sec)(a)	Nominal Exit Velocity (ft/sec)(b)	Low Heating Value (Btu/ft^3)	Fuel in Nitrogen (%)	Steam Ratio (lb.Steam/lb.Fuel)	Observations					Sample Method R=Rake H=Hood	Probe Position (ft)(c)	Global Combustion Efficiency (%)	Hydrocarbon Destruction Efficiency (%)
								Wind Speed (MPH)	Flame Length (ft)	Lift Off (in.)	Color	Smoke				
Combustion Efficiency 56 Percent C_3H_8	22	No	1.0	1.0	1293	55.0	0.0	0-5.5	8	0	Yellow	Yes	H	7	99.60	99.97
	26		2.8	2.8	1314	55.9	0.0	0-15	15	0	Yel/Or	Yes	H	15	99.76	99.98
Effect of Steam	27	No	2.8	2.8	1314	55.9	0.316	0-4	14	0	Lt Yel	No	H	9	99.92	99.98
56 Percent C_3H_8	30		2.9	2.9	1323	56.3	0.0	NA	12	0	Yellow	Yes	R	17	98.47	98.87
	31		10.1	10.1	1316	56.0	0.0	NA	20	0	Yellow	Yes	R	21	98.90	99.16
Effect of Steam	32	No	2.9	2.9	1316	56.0	0.563	0-5	13	0	Yellow	No	H	8	99.89	99.95
Low Btu	33	No	1.1	1.1	338	14.4	0.0	NA	4	2-4	Yel/Blu	No	H	1	96.35	99.93
	34		3.1	3.1	414	17.6	0.0	NA	6	6-12	Yel/Blu	No	H	5	98.93	99.33
	37		3.1	3.1	451	19.2	0.0	NA	8	3-6	Yellow	No	R	15	92.24	92.41
	38		11.7	11.7	613	26.1	0.0	NA	13.5	6-8	Yellow	No	R	20	98.76	98.84
	71		10.3	10.3	343	14.6	0.0	0	15	0-5	Orange	No	R	17	99.36	99.69
	73		1.0	1.0	291	12.4	0.0	0-4	5	0	Clear	No	R	10	97.97	98.27
	74		2.9	2.9	350	14.9	0.0	0-1	10	0-7	Orange	No	R	15	99.02	99.35
56 Percent C_3H_8	75	No	2.9	2.9	1321	56.2	0.9	0-2	13.5	0	Yellow	Yes	R	17	99.66	99.99
	76		1.0	1.0	1311	55.8	0.0	0-3	8	0	Orange	Yes	R	17	99.54	99.97

(a) Based on open area of flare head

(b) Based on velocity of pipe

(c) Refer to Figure 2-2

TABLE 2-4. COMBUSTION EFFICIENCIES OF EER TWELVE-INCH FLARE HEAD

FLARE HEAD: EER SIZE: 12-INCH

Purpose of Test	Test Number	Flame Retention Ring	Actual Exit Velocity (ft/sec) (a)	Nominal Exit Velocity (ft/sec) (b)	Low Heating Value (Btu/ft^3)	Fuel in Nitrogen (%)	Steam Ratio (lb.Steam /lb.Fuel)	Observations					Sample Method R=Rake H=Hood	Probe Position (ft) (c)	Global Combustion Efficiency (%)	Hydrocarbon Destruction Efficiency (%)
								Wind Speed (MPH)	Flame Length (ft)	Lift Off (In.)	Color	Smoke				
Combustion Efficiency	39	No	0.2	0.2	1309	55.7	0.0	NA	6	0	Yellow	Yes	R	13	98.29	98.70
56 Percent C_3H_8	40		2.0	2.0	1323	56.3	0.0	NA	19	0	Yellow	Yes	R	23	99.24	99.59
	43		4.1	4.1	1318	56.1	0.0	NA	23	0	Yellow	Yes	R	35	99.50	99.93
Low Btu	44	No	2.1	2.1	378	16.1	0.0	NA	12	0	Yellow	No	R	22	99.73	99.89
City Gas	45	No	0.2	0.2	980	99.4 City Gas	0.0	NA	4	0	Orange	Little	R	9	99.91	99.99
Low Btu	46	No	0.2	0.2	451	19.2	0.0	NA	4	0	Orange	Little	R	9	98.62	99.67
	47		4.1	4.1	385	16.4	0.0	NA	13	10	Orange	No	R	23	94.09	98.60
Steam, Smokeless	50	No	4.0	4.0	1323	56.3	0.457	NA	23	0	Yellow	Little	R	30	99.32	99.56

(a) Based on open area of flare head

(b) Based on velocity of pipe

(c) Refer to Figure 2-2

TABLE 2-5. COMBUSTION EFFICIENCIES OF TWELVE-INCH INDUSTRIAL FLARE HEAD A

FLARE HEAD: INDUSTRIAL A SIZE: 12-INCH

Purpose of Test	Test Number	Flame Retention Ring	(a) Actual Exit Velocity (ft/sec)	(b) Nominal Exit Velocity (ft/sec)	Low Heating Value (Btu/ft^3)	Fuel in Nitrogen (%)	Steam Ratio (lb.Steam /lb.Fuel)	Observations (c)					Sample Method R=Rake H=Hood	(c) Probe Position (ft)	Global Combustion Efficiency (%)	Hydrocarbon Destruction Efficiency (%)
								Wind Speed (MPH)	Flame Length (ft)	Lift Off (in.)	Color	Smoke				
Combustion Efficiency 56 Percent C_3H_8	62	Yes	2.0	1.9	1269	54.0	0.0	0-3	18	0	Yellow	Yes	R	22	99.12	99.67
	63		4.3	4.0	1318	56.1	0.0	0-3	24	0	Yellow	Yes	R	25	99.37	99.62
Low Btu	64	Yes	4.5	4.2	392	16.7	0.0	0-2	21	0	Yellow	No	R	23	98.49	98.98
56 Percent C_3H_8	67	Yes	4.3	4.0	1316	56.0	0.0	0-2	22	0	Yellow	Yes	R	28	99.61	99.98
	68		0.22	0.2	1309	55.7	0.0	0-2	6	0	Orange	Yes	R	8	99.78	100.00

(a) Based on open area of flare head

(b) Based on velocity of pipe

(c) Refer to Figure 2-2

TABLE 2-6. COMBUSTION EFFICIENCY OF TWELVE-INCH INDUSTRIAL FLARE HEAD B

FLARE HEAD: INDUSTRIAL B SIZE: 12-INCH

Purpose of Test	Test Number	Flame Retention Ring	(a) Actual Exit Velocity (ft/sec)	(b) Nominal Exit Velocity (ft/sec)	Low Heating Value (Btu/ft^3)	Fuel in Nitrogen (%)	Steam Ratio (lb.Steam /lb.Fuel)	Observations (c)					Sample Method R=Rake H=Hood	(c) Probe Position (ft)	Global Combustion Efficiency (%)	Hydrocarbon Destruction Efficiency (%)
								Wind Speed (MPH)	Flame Length (ft)	Lift Off (in.)	Color	Smoke				
Combustion Efficiency 56 Percent C_3H_8	84	Yes	2.9	1.9	1276	54.3	0.0	0	22.5	0	Yellow	Yes		27	99.54	99.96
	85		6.0	4.0	1316	56.0	0.0	NA	27	0	Yel/Or	Yes	R	32	99.65	99.94
	86		0.3	0.2	1314	55.9	0.0	NA	5.5	0	Orange	Yes	R	10	99.48	99.94
Low Btu	88	Yes	3.0	2.0	317	13.5	0.0	0-3.5	10.5	0	Clr/Or	No	R	15	99.21	99.78
	89		6.2	4.1	303	12.9	0.0	0-2	20	0	Orange	No	R	24	99.72	100.00
	90		0.3	0.2	315	13.4	0.0	0-3	4	0	Orange	No	R	6	99.59	99.93
Steam, Smokeless	91	Yes	5.9	3.9	1311	55.8	0.441	0-5	23	0	Orange	Very little	R	27	99.84	99.99

(a) Based on open area of flare head

(b) Based on velocity of pipe

(c) Refer to Figure 2-2

TABLE 2-7. COMBUSTION EFFICIENCY OF TWELVE-INCH INDUSTRIAL FLARE HEAD C

FLARE HEAD: INDUSTRIAL C SIZE: 12-INCH

Purpose of Test	Test Number	Flame Retention Ring	Actual Exit Velocity (ft/sec) (a)	Nominal Exit Velocity (ft/sec) (b)	Low Heating Value (Btu/ft^3)	Fuel in Nitrogen (%)	Steam Ratio (lb.Steam /lb.Fuel)	Observations (c)					Sample Method R=Rake H=Hood	Probe Position (ft) (c)	Global Combustion Efficiency (%)	Hydrocarbon Destruction Efficiency (%)
								Wind Speed (MPH)	Flame Length (ft)	Lift Off (In.)	Color	Smoke				
Combustion Efficiency 56 Percent C_3H_8	53	Yes	0.65	0.2	1309	55.7	0.0	0-2	5.5	0	Yel/Or	Yes	R	11	99.28	99.79
	54		6.50	2.0	1316	56.0	0.0	0-2	15	3-5	Yellow	Yes	R	24	99.08	99.39
	55		13.3	4.1	1328	56.5	0.0	0-2	21	0	Yel/Or	Yes	R	27	99.65	99.91
Low Btu	58	Yes	6.8	2.1	371	15.8	0.0	0-1	15	0	Yellow	No	R	18	99.52	99.80
56 Percent C_3H_8	59	Yes	13.0	4.0	1314	55.9	0.456	NA	23.5	0	Yel/Or	Little	R	27	99.55	99.70
Low Btu	60	Yes	14.63	4.5	522	22.2	0.0	0-3	15	0-12	Yellow	Little	R	25	91.16	91.96
	61		0.65	0.2	458	19.5	0.0	0-2	3	0	Yellow	Little	R	6	99.50	99.69

(a) Based on open area of flare head

(b) Based on velocity of pipe

(c) Refer to Figure 2-2

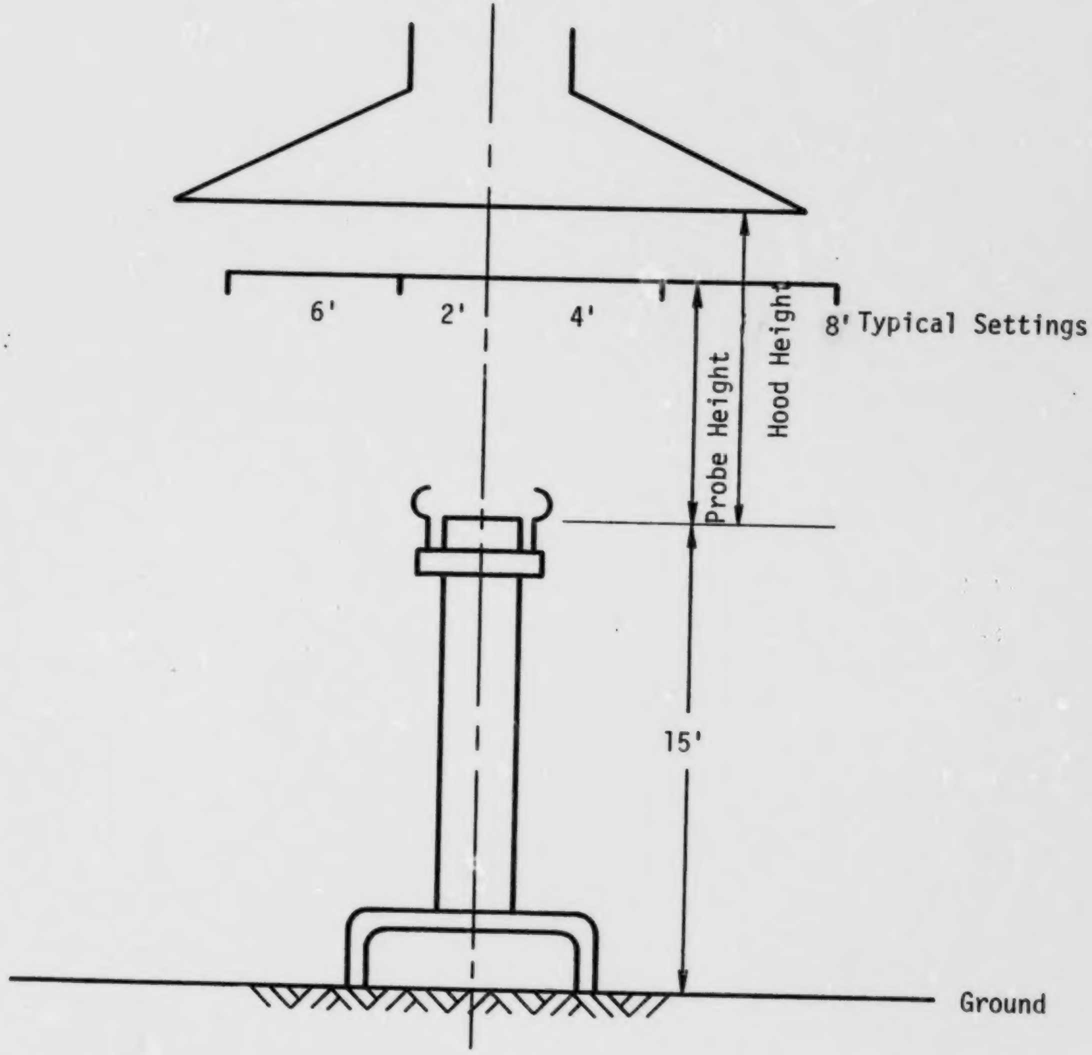
6'
2'
4'
8' Typical Settings
Probe Height
Hood Height
15'
Ground

Figure 2-2. Diagram of sampling locations.

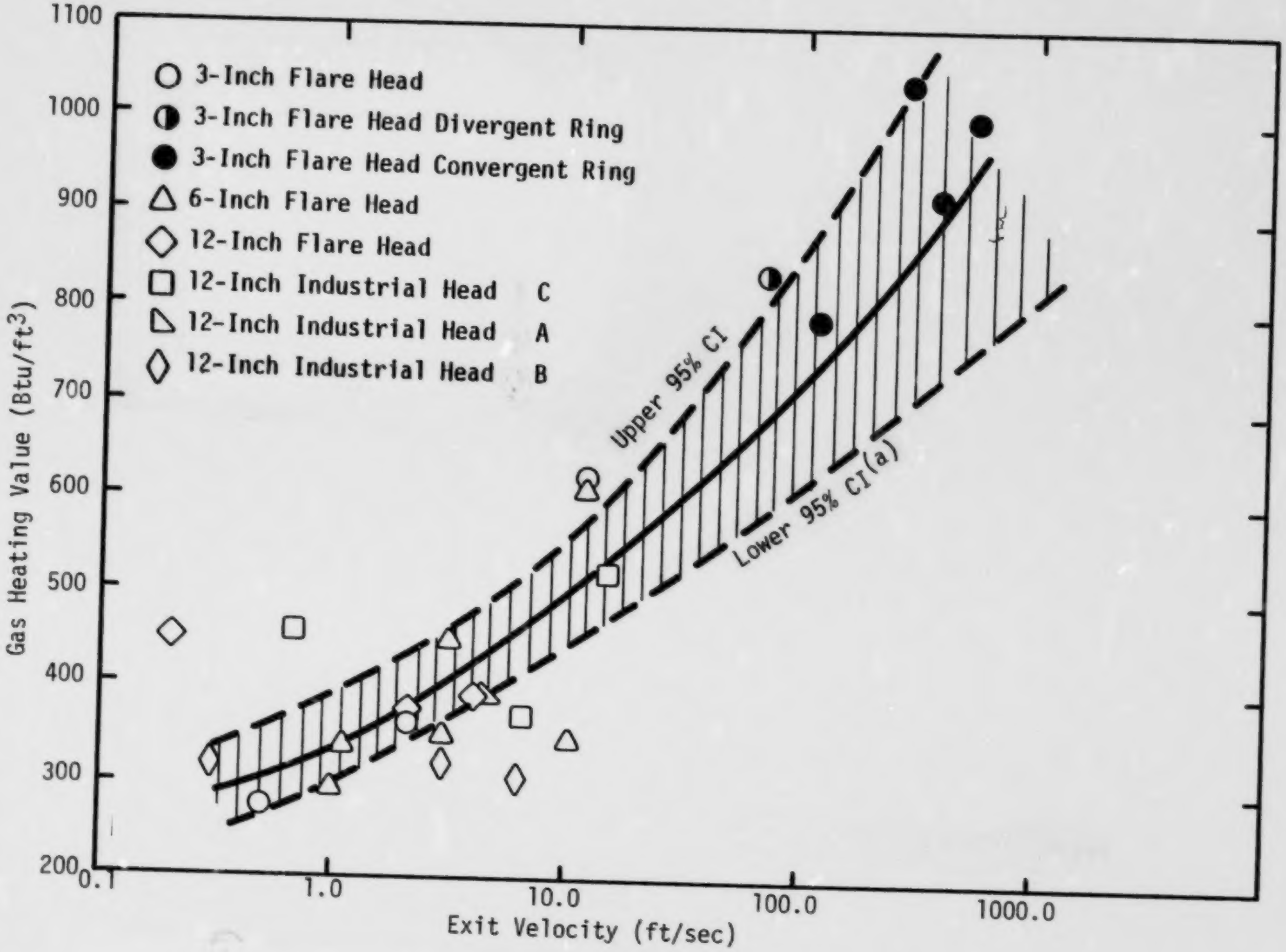

Figure 2-3. Region of flame instability.[b]

(a) Confidence interval of mean.
(b) Based on flares burning propane/nitrogen mixtures with no pilot flame.

The region shown in Figure 2-3 indicates the minimum gas heating value required to produce a stable flame at the gas exit velocity within the 95 percent confidence limits of the mean. For any given velocity, a gas with a heating value above this region would produce a stable flame; a gas with a heating value below this region would produce an unstable flame. Velocity/gas combinations in the region or below tend to produce flames with lower combustion efficiency. Thus, for any given test velocity, the minimum gas heating value for a stable flame can be determined. By dividing the actual gas heating value by the minimum value required for stability, a ratio is obtained which is greater than one (1) for stable flames, and is less than one (1) for unstable flames. Figure 2-4 plots combustion efficiencies versus this ratio and shows that high combustion efficiencies are achieved when the ratio exceeds one (1). When the ratio is one (1) or less, lower combustion efficiencies are often obtained. Note that even at a ratio less than one (1), high combustion efficiencies are sometimes achieved; this demonstrates the uncertainty associated with the stability measurements. In general, however, stable flames are efficient and unstable flames can be inefficient. Flames near the stability limit are very sensitive to perturbations, and, when perturbed, can produce high emissions of unburned material.

All conclusions are based on the data of this study and are limited to head geometries, gases and variables examined. Head geometries were limited to:

- Simple pipe flare of 3-, 6-, and 12-inches in diameter.
- Three commercial 12-inch flare heads of different design and manufacture.

The gases studied were limited:

- Propane-nitrogen mixtures with heating values of 270 - 2350 Btu/ft^3
- One test with natural gas.

The variables examined were:

- Velocities from 0.2 to 420 ft/sec
- Reynolds numbers from 340 - 217,000

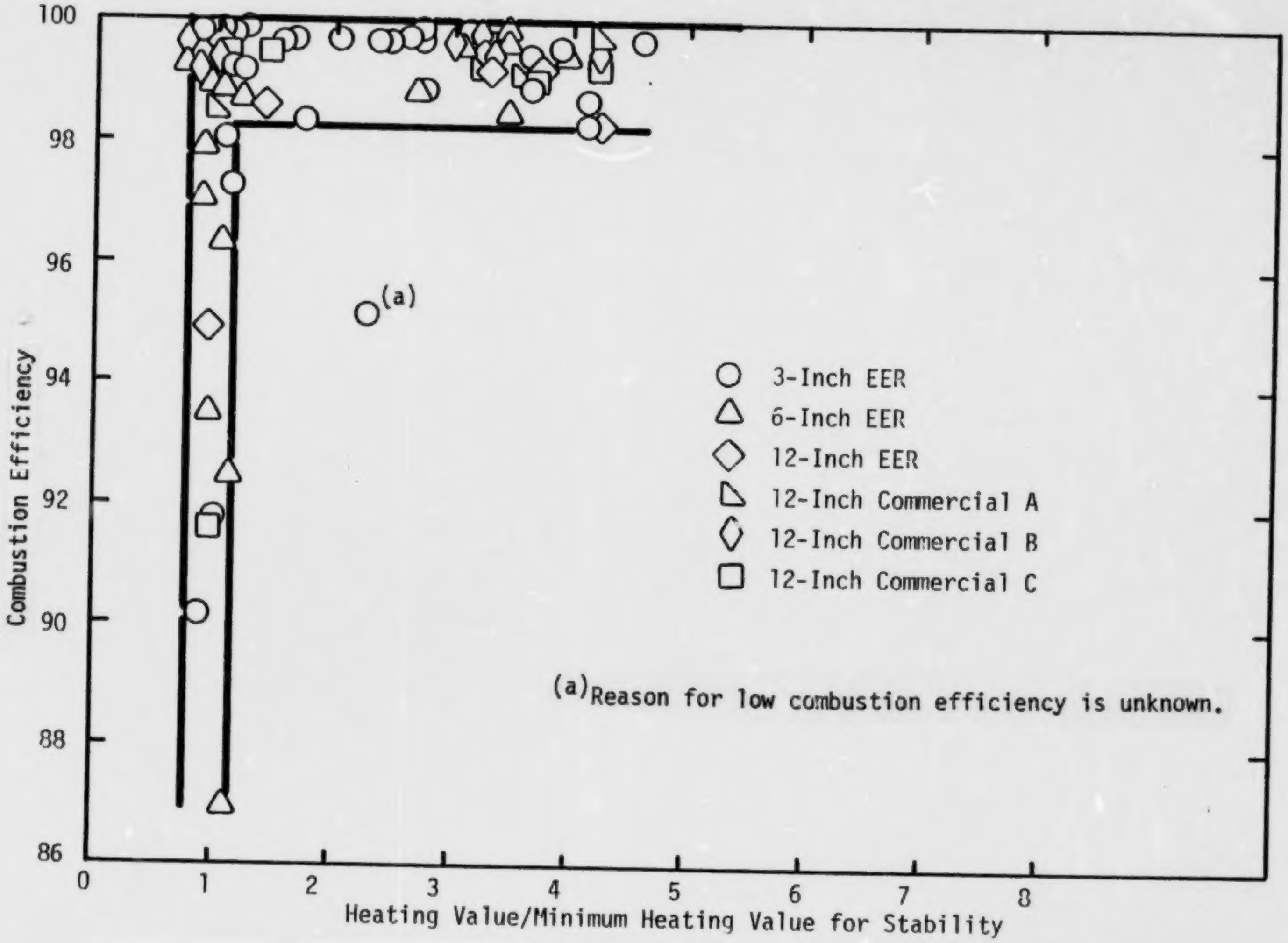

[a] Reason for low combustion efficiency is unknown.

Figure 2-4. Combustion efficiency near the lower limits of flame stability.[b]

(b) Based on flares burning propane/nitrogen mixtures with no pilot flame.

- Richardson numbers from 2.9×10^{-5} to 8×10^{2}
- Steam flow from 0 to 1 lb-steam/lb-fuel

The flare flames were shielded from the wind and combustion efficiencies were not measured in winds greater than 5 mph. The following conclusions are based on the study results:

- Flares operating with unstable flames can have low combustion efficiency.
- The combustion efficiency did not depend on flare size or geometry.
- Successful correlations were developed for flare flames:
  - Flame length was correlated with a modified Richardson number.
  - Liftoff distances were correlated with ratios of velocities and concentrations.
  - Flame stability was correlated with a pseudo flame temperature.
  - Entrainment was correlated with ratios of distances and the Richardson number or with velocity.
- Combustion efficiency was high for flares with high velocities, provided the heating value of the gas was in the region of stability.
- Steam injection completely suppressed soot production but did not appreciably alter combustion efficiency unless the flame was oversteamed (>0.5 lb-steam/lb-fuel), and then the combustion efficiency decreased.

3.0 TEST METHODOLOGY

During this program, the Flare Test Facility testing procedures and data reduction techniques were developed to characterize the emissions from several flare heads which were tested over a range of operating conditions.

3.1 Flare Test Facilities (FTF)

A Flare Test Facility was designed and built by Energy and Environmental Research Corporation at their El Toro Test Site for the Environmental Protection Agency. Details of the FTF are summarized below. A Complete description of the FTF is contained in Appendix A.

Facility Site

The FTF is located in a canyon surrounded by 70-foot cliffs. The layout of the test site includes a pad and structure for testing, screens for protecting the flare flames from wind, and a control room for operating the flare and analyzing the data. Sufficient water, compressed air, natural gas and electricity are available at the test site to operate the flare facility at gas flows up to 24,000 ft^3/hr.

Delivery Systems

Gases are supplied to the flare head and auxiliary equipment through specially designed parallel manifolds. These manifolds allow accurate determination of the flow rates over the wide range of operating conditions typical of flares. Natural gas is supplied by the local utility, through a 2-inch pipe. Natural gas can be delivered at a maximum flow rate up to 7,000 ft^3/hr. Propane is delivered and stored as liquid in a 2100 gallon tank. Vaporized propane is supplied to the flare head. At low flow rates, natural vaporization is sufficient; at higher flow rates, propane-fired vaporizers are used to increase the flow-rate of gas up to 15,000 ft^3/hr.

Nitrogen is fed to the flare head from liquid nitrogen tanks after atmospheric vaporization. Nitrogen is mixed with propane to vary the heating value of the gas flared. Nitrogen tanks and vaporizers are capable of supplying up to 9,000 ft^3/hr. Sulfur dioxide is fed from liquid cylinders through a steamheated vaporizer to the base of the flare stack. Sulfur dioxide can be supplied at a rate of 7 ft^3/hr.

Steam is produced in a 15 hp natural gas-fired boiler. The boiler is capable of supplying 400 lbs/hr of 100 psig-saturated steam.

Flare Heads

Simple pipe flare heads were designed and built by EER for testing. These heads were designed to simulate the major features of commercial flare heads; however, these heads did not include the different proprietary features of commercial flare heads used to stabilize flames and improve mixing. Three open-ended pipe flares with steam injection were used for most of the tests. These heads were 3-, 6-, and 12-inches in diameter. The steam injector was designed to provide 0.23 lbs steam/lb fuel at 20 percent of the maximum capacity (0.35 speed of sound) of the flare head. For the 56 percent propane in nitrogen mixture used in many of these tests, the maximum velocity of a 12-inch flare head would be 325 ft/sec, the flow at 20 percent maximum capacity would be 4968 lb/hr, and the maximum steam flow would be 1142.6 lb/hr. For these conditions, steam would be injected at 1289 ft/sec (Mach Number = 0.92) through sixteen 0.525-inch-diameter nozzles.

A ring was used on the 3-inch flare head to help retain the flame at high velocity. The ring was designed after consultation with the advisory panel and consisted of a convergent channel, 1.8 inches in diameter surrounded by twelve evenly spaced 1/8" holes as shown in Figure 3-1. The ring was initially installed upside down (divergent). Neither this position nor the normal position (convergent) improved the stability of the flare at high velocities. The ring did, however, increase the nozzle velocity by almost a factor of two.

Commercial flare heads were supplied for testing by three flare-head manufacturers. The specific design of the flare heads is proprietary to the manufacturers. However, each manufacturer was requested to supply a flare head with the following specifications:

- The flare head shall be a 12-inch-diameter pipe flare built according to commercial design standards of the manufacturer.

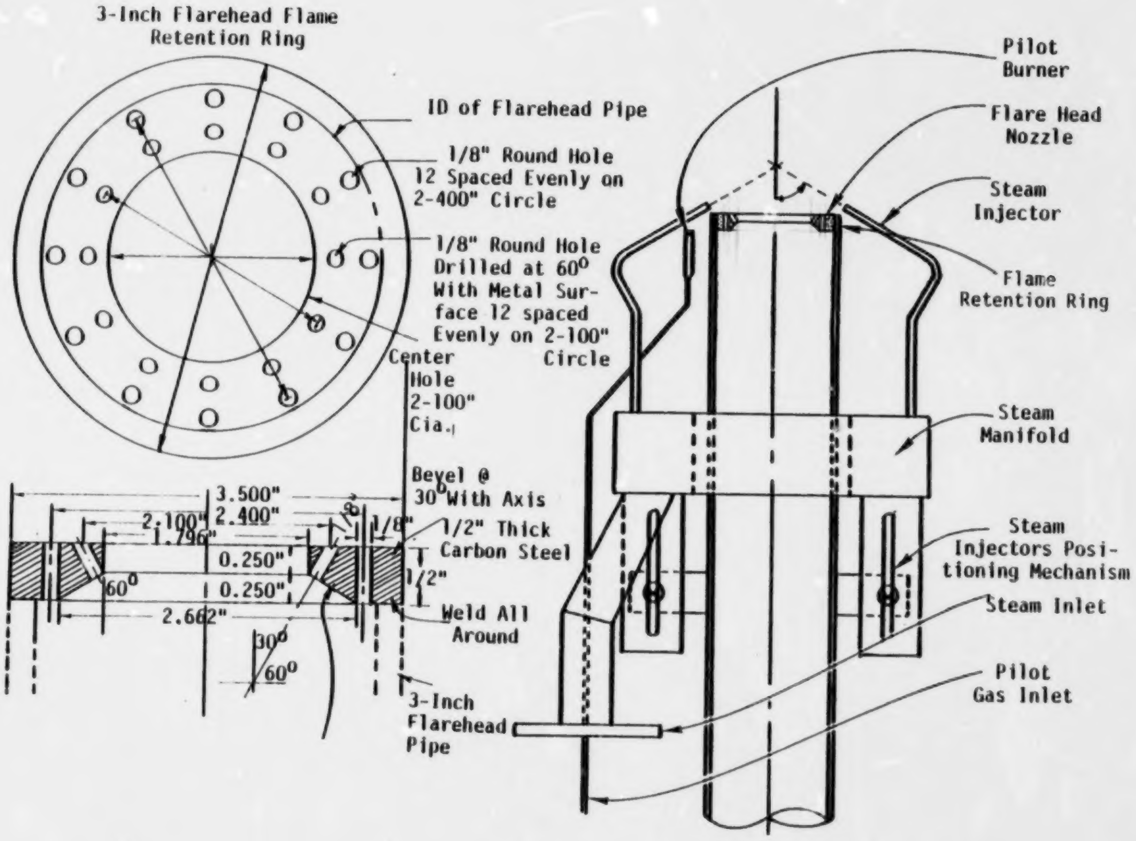
3-Inch Flarehead Flame Retention Ring
ID of Flarehead Pipe
1/8" Round Hole 12 Spaced Evenly on 2-400" Circle
1/8" Round Hole Drilled at 60° With Metal Surface 12 spaced Evenly on 2-100" Circle
Center Hole 2-100" Cia.
Bevel @ 30° With Axis
1/2" Thick Carbon Steel
1/2"
Weld All Around
3-Inch Flarehead Pipe
3.500"
2.400"
2.100"
1.796"
1/8"
1/8"
0.250"
0.250"
2.662"
60°
30°
60°
Pilot Burner
Flare Head Nozzle
Steam Injector
Flame Retention Ring
Steam Manifold
Steam Injectors Positioning Mechanism
Steam Inlet
Pilot Gas Inlet

Figure 3-1. Design of Retention Ring for 3-Inch Flare Head.

- The steam injection system shall be designed for a maximum steam flow of 13,000 lbs/hr. (This figure is based on a design exit velocity of Mach of 0.35 for a hypothetical gas in the 12-inch flare; smokeless operation to 20 percent maximum capacity; and a steam requirement of greater than 0.3 lb steam/lb fuel.)

Sampling

Samples of the effluent from the flare plume are withdrawn by two techniques. In the first, samples are withdrawn from the mixed effluent of the flare flame in the chimney of a hood designed to capture the complete plume. Pitot probes, thermocouples, and a sampling probe are positioned in the chimney of the hood. These allow the mass flow through the hood to be determined, a sample to be withdrawn for analysis, and calculation of the mass flux of incompletely burned carbon species through the hood. The second sampling technique uses a rake probe. Five individual, movable probes are positioned along the diameter of the flare plume. The entire probe assembly can be moved vertically and horizontally.

The probe in the chimney and the rake probes are designed similarly. The probes are 1-1/2" OD tubes, steam-heated to avoid condensation with interchangeable nozzles which allow isokinetic sampling. Soot is captured by filters at the end of the probe, and gases are withdrawn through a central tube into heated sampling lines. Water is removed near the probe by Perma-pure® dryers.

Ambient Control

Wind can greatly disturb the flare flame and cause difficulty in measuring emissions. The wind velocity is monitored by a three-cup anemometer, and the flame is shielded by wind-screens which have 22.7 percent open area. Flow patterns around the flare flame, as determined by smoke tracers, are shown by Figure 3-2. Trials are not conducted at high wind conditions, and many trials were conducted in the early morning or late at night to take advantage of quiescent ambient conditions.

Visual Monitors

A number of visual monitors were found useful to record the flame

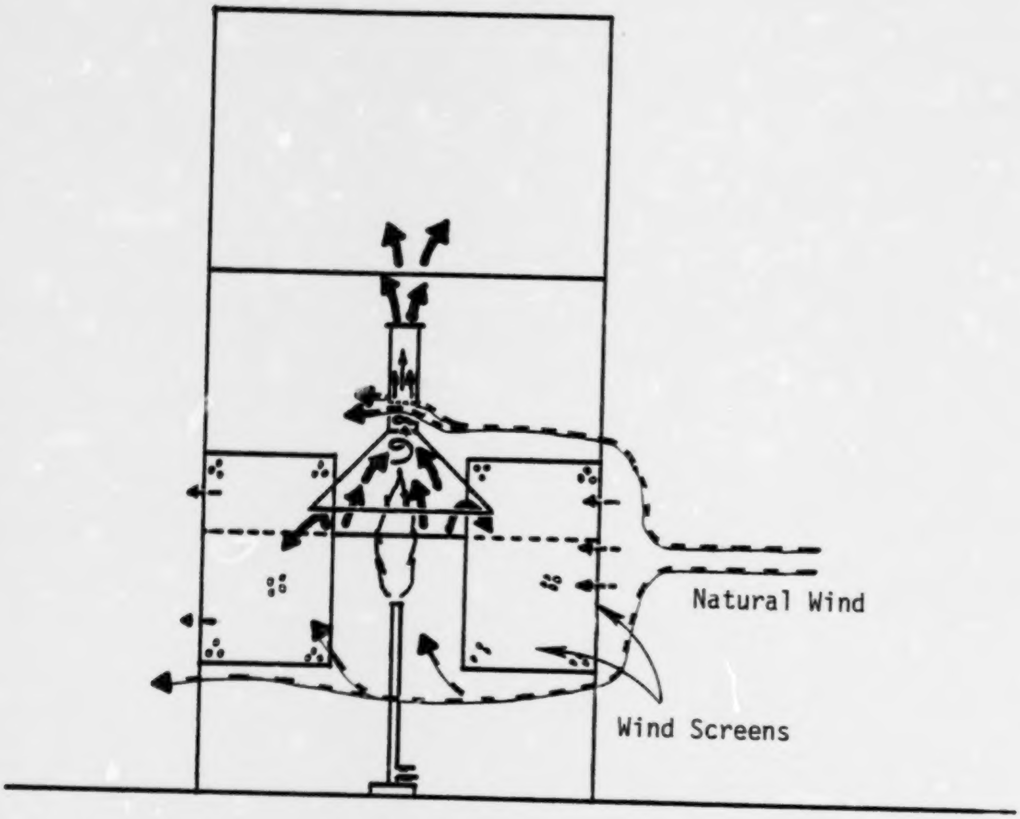
Natural Wind
Wind Screens

Figure 3-2. Flow Patterns Determined by Smoke Tests.

structure during the trials. These included:

- A video tape recorder which was used during the early trials to continuously monitor flame structure, however the usefulness of the video recording was limited by slow response times and inadequate spatial resolution, it was not used in later trials.
- Photographs of the flare flame were used to record the structure of the flame and as an aid to interpreting data. Photographs were taken with exposure times of 1 millisecond to capture the instantaneous structure of the flame and at 10 seconds to record the average shape and length of the flare flame.
- High-speed cinematography was very useful for defining the nature and evolution of flare flames at speeds of 200 frames/second. This speed was determined experimentally to be capable of identifying the development and growth of eddy structures in flare flames.

3.2 Test Procedure

The test procedure involves recording background conditions, lighting the flare flame, establishing the flame conditions, setting the sampling locations, sampling, and analyzing the sample.

Background Conditions

The background conditions influence the results of testing because of the wind and the concentration of the products of incomplete combustion in the ambient air. The wind speed is recorded and its direction noted. The operator assesses, based on previous experience, the extent to which the wind will influence the structure and emissions of the flare flame. Tests are usually conducted before noon or at night to reduce the interference from the wind.

The background composition of the ambient air is sampled before each test at the position of sampling during testing. The background sample is handled and analyzed exactly as samples from the flare plume.

The Flame

The flame is lit with a hand-held torch, and the flow conditions established. The flare structure is recorded visually and photographically, with both still and motion pictures.

Steam

Steam lines are preheated and drained prior to trials using steam injection.

Sampling

The position of the sampling probes is established from previous experiments. Figure 3-3 shows the optimum position of hood sampling as determined by a carbon balance. The position is a compromise between being so close to the flame that the hood disturbs the flare and so far from the flame that the combustion products are diluted. Figure 3-3 shows that some material is not collected by the hood at large distances above the flare head. However, Figure 3-4 shows that the calculated combustion efficiencies did not vary with sampling positions of the hood. This implies that the material which is not collected has the same composition as that which is collected.

Probe sampling also has an optimum position, however for different reasons. Positions of the probe in and near the flame may sample material which is incompletely burned. In positions far from the flame, the concentration of the gases may be so dilute that making an accurate determination of the composition of combustion products is difficult.

The soot-laden gases are drawn nearly isokinetically through a filter placed in the end of the probe to capture soot. This avoids deposition of soot on probe lines. The amount of gas is determined by a dry gas meter, and the amount of soot collected is determined as the weight of material which can be burned from a previously baked filter.

The gases are drawn through heated sample lines to Permapure® dryers where the water is removed. The dried gases are then collected in Tedlar bags. Five samples are drawn simultaneously and individually into the bags from the rake probes. Samples are taken over a 20-minute period to average out flame fluctuations. Samples are mixed in the bags prior to analysis.

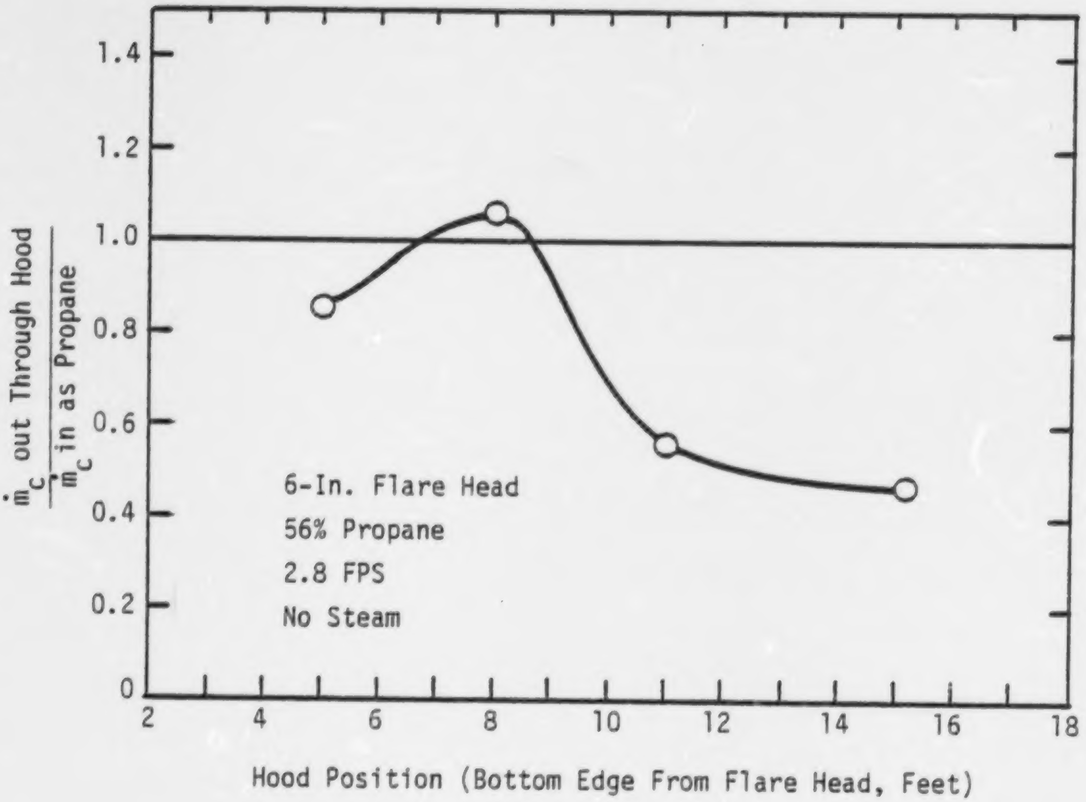

Figure 3-3. Influence of Hood Position on Closure of a Carbon Balance using Mass Fluxes Measured in the Hood.

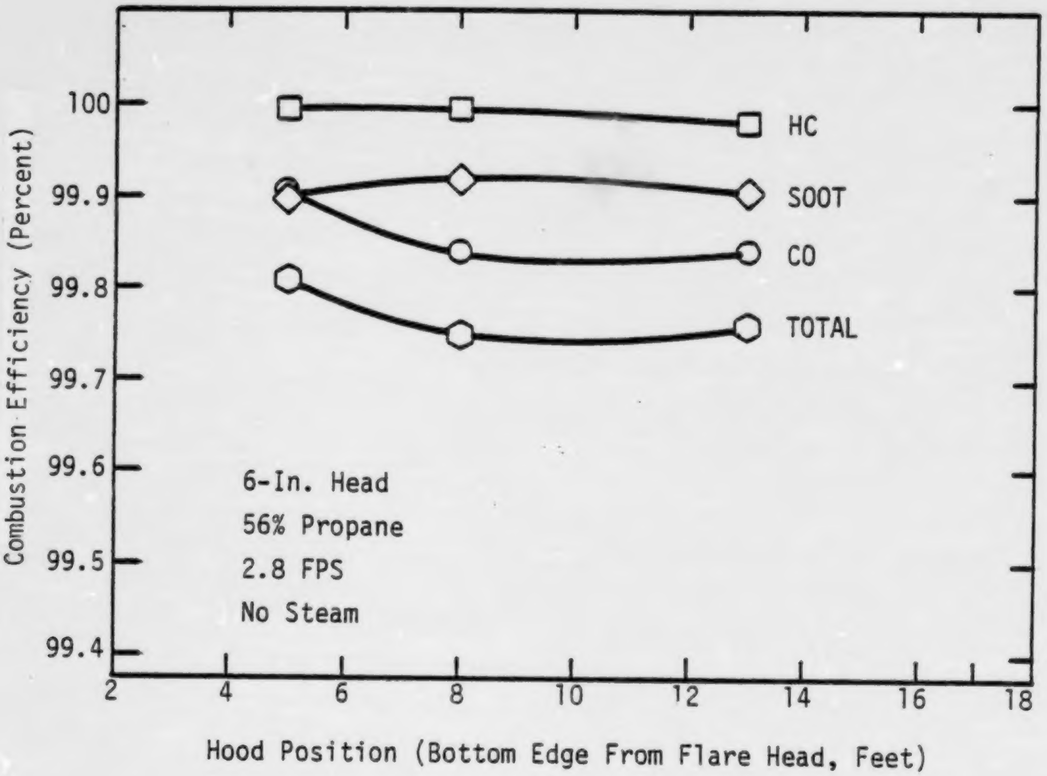

Figure 3-4. Influence of Hood Position on Combustion Efficiency Measured in the Hood.

Carbon monoxide and carbon dioxide are analyzed using non-dispersive infrared analyzers, total hydrocarbons are analyzed as methane using a flame ionization detector, sulfur dioxide is analyzed using absorption in solution followed by titration and by flame photometry. Details of these techniques are described in Appendix A.

Mass Balance

A perceived deficiency with previous studies was the inability to close a mass balance and account for all the carbon. The combustion efficiency in these studies could be lower than implied from the measurements, because the carbon efficiency is calculated based on the amount of unburnt material measured divided by the amount of combustibles fed to the system. This study showed that carbon balances can be attained under some conditions and estimated the importance of closing a material balance. (See Section 5.2)

Two techniques were used to evaluate the influence of mass balance closure on the estimate for the emission of unburned hydrocarbons. In one technique, a hood was used to collect the entire effluent from the flare flame, and the amount of carbon collected in the hood was determined from the mass flow in the hood as calculated from thermocouple measurements and pitot probes, and by analysis of the CO, CO_2 and hydrocarbons in a gas sample withdrawn from the chimney of the hood. Figure 3-5a shows that accurate carbon balances could be attained between mass flow rates of 20- and 40-lbs/hr of propane, while Figure 3-5b shows that mass balances could be closed for many trials using both the 3- and 6-inch flare heads. The discrepancies shown in the figures are thought to be caused by inhomogeneities and measurment inaccuracies at low flow rates and by the loss of material at high flow rates. The loss of material at high flow rates was confirmed by observations of flow patterns in the hood using smoke-tracers. The use of SO_2 as a tracer was inappropriate for tests with the hood. Figure 3-6 shows that carbon mass balances could be closed using a rake probe and SO_2 as a tracer for mass fluxes up to 90 lbs/hr. Carbon mass balances could not be obtained using low flow rates of SO_2 (solid points) because of inaccuracies and limitations of the technique used to measure SO_2 concentrations in the plume.

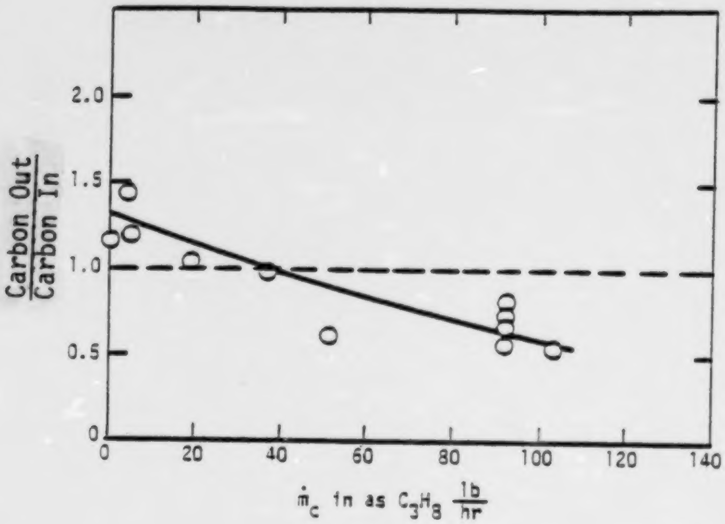

Figure 3-5a. Influence of Mass Flux of Carbon on Closure of a Carbon Balance Using the Mass Flux Measured in the Hood.

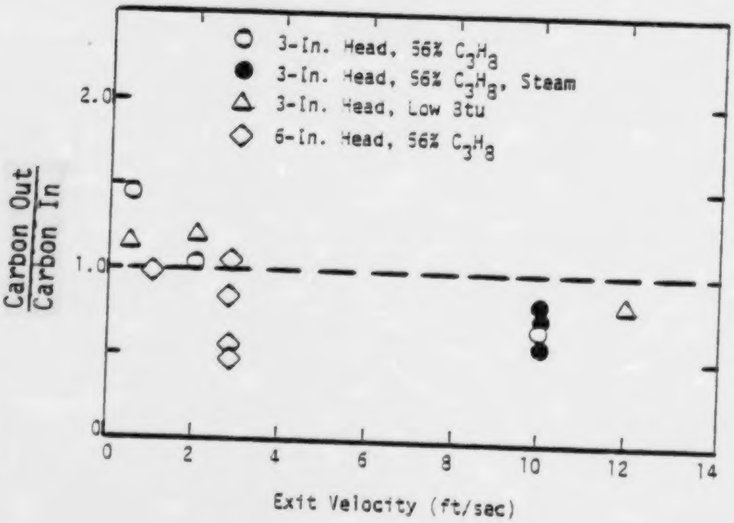

Figure 3-5b. Influence of Velocity on Closure of a Carbon Balance Using Mass Fluxes Measured in a Hood.

Figure 3-5. Verification of Carbon Mass Balance for Hood Measurements.

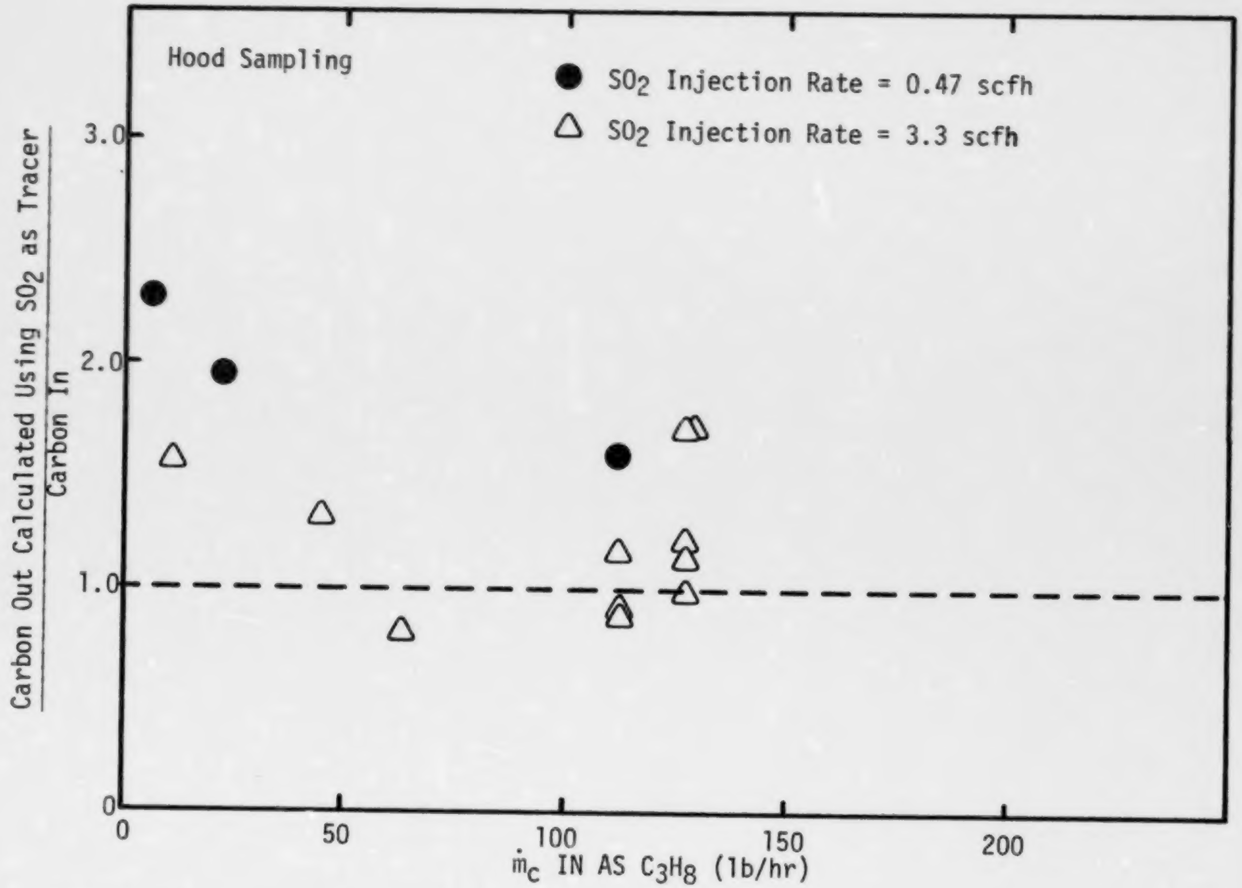

Figure 3-6. Closure of mass balance using SO_2 as a tracer.

3.3 Data Reduction

Reduction of the data requires:

- Correction for background concentrations based on dilution.
- Calculation of local combustion efficiencies and maximum potential errors.
- Integration of local combustion efficiencies to obtain global combustion efficiencies.

The procedures used for these reductions are described below.

Correction For Background

This Section describes the procedures used to calculate the combustion efficiencies at the sample locations and to estimate the maximum potential errors associated with these efficiencies. The procedure requires:

- Assumptions on the nature of the combustion products.
- Correction for concentration of combustion species in the background.
- Estimates of the maximum potential error associated with each local combustion efficiency.

Combustion Products

Knowledge of the completely and incompletely burned combustion products are required to calculate local combustion efficiencies. Calculation of the local combustion efficiencies are based on the incompletely burned carbon. Carbon dioxide is considered the only completely burned carbon species: Carbon monoxide, soot, and hydrocarbons reported as methane equivelents are considered incompletely burned species. Generally, these assumptions are valid.

Dilution Factors and Background Concentrations

The combustion products are mixed with ambient air, which may contain significant levels of the species in the flare plume. The concentrations of incompletely burned species must then be corrected for the amount of material added by the ambient air. This correction is based on the stoichiometric products of combustion and is accomplished through the use of material balances. Simply subtracting the concentration of species in the background from the measured concentrations is incorrect and may lead to errors when concentrations of incompletely burned hydrocarbon in the ambient air and the flame plume are similar. This can occur because of efficient combustion or excessive dilution.

The dilution factor, DF, is defined as the moles of ambient air entrained with one mole of stoichiometric combustion products. The dilution factor is calculated from material balances (see schematic diagram) conserving any of a number of species.

Overall Combustion Efficiencies

An estimate of the total amount of incompletely burned hydrocarbons exiting from flare flames is required to adequately characterize these emissions. The overall emissions were obtained in two ways in this study. First, the entire plume was collected, mixed, and sampled in a hood for flare flames with low flows. This technique was limited to small flows because of the capacity of the hood, fan, and associated duct work. Second, the global efficiencies for flares with large flows were determined by measuring local combustion efficiencies at five locations across the plume and integrating these values to obtain an estimate of the overall efficiency of the flare flame.

Flare flames produced plumes with inhomogeneous combustion efficiencies. Theoretically, a complete map of concentrations and velocities around the flare flame is required to calculate overall combustion efficiencies. In this study, the concentrations are measured at five discrete locations across the plume and the velocity distribution is assumed to take the form calculable from jet theory. The assumptions are:

1. The carbon flux outside the area spanned by the probes is negligible or the combustion efficiency is the same as within the sampling region.
2. Flare flames are axisymmetrical.

3. The flare plume consists of five discrete zones measured by the rake probes inside of which the concentrations and velocities can be approximated by a uniform composition equal to that measured by the probe in the center of the zone.

The combustion efficiencies can be calculated by:

$$\text{Combustion Efficiency} = 1 - \frac{\text{Unburnt Carbon Flow}}{\text{Total Carbon Flow}} \qquad (3\text{-}12)$$

Above the flare flame, the unburnt and total carbons fluxes may be calculated by:

$$\text{Unburnt Carbon Flow} = \sum_i \sum_r C_{i,r} \; V_r \; A_r \qquad (3\text{-}13)$$

$$\text{Total Carbon Flow} = \sum_j \; r \; C_{j,r} \; V_r \; A_r \qquad (3\text{-}14)$$

where C_i is the concentration of carbon species i

V_r is the axial velocity at region r

A_r is the cross section area of region r

i denotes unburnt species CO, HC, soot

j denotes total carbon species: CO, HC, soot, CO_2

r denotes the regions covered by the rake probes

Before the above relationships can be applied to compute combustion efficiencies, the measured species concentrations must be corrected for the influence of background concentration. Also, velocities and areas of flux must be specified.

Background Correction

The concentration of a species at the probe position can be corrected for the concentration of background species by:

$$C_{i,\text{net}} = C_{i,\text{measured}} - \left(\frac{\text{Dilution Factor}}{\text{Dilution Factor} + 1}\right) C_{i,\text{ background}} \qquad (3\text{-}17)$$

where the dilution factor is defined as:

$$DF = \frac{\text{Total Volume Of Gas Which Contains The Stoichiometric Combustion Products}}{\text{Volume of Stoichiometric Combustion Products}} \qquad (3\text{-}18)$$

Locating the Flame Axis

The axis of flare flames occasionally do not correspond to the axis of the flare head. Since the regions along the flame axis have minimum air entrainment, the flame axis is located at the position where the measured dilution is a minimum.

Defining the Sampling Region

The flare flames are assumed to be axisymmetrical. In addition, the species inside the five regions covered by the rake probes are assumed to be homogeneous and identical to that measured by the probe. The boundaries between these regions are selected to be half-way points between adjacent probes.

Velocity Profiles

The velocity profile of the flare plume is assumed to take the form determined by jet theory.

$$V_m = V_o \left(0.16 \left(\frac{X}{d}\right) - 1.5\right) \qquad (3\text{-}15)$$

$$V_{r,X} = V_m \exp\left(- \ 90\left(\frac{r}{X}\right)^2\right) \qquad (3\text{-}16)$$

where X = axial distance from flare head exit

r = radial distance from flame axis

d = diameter of flare head nozzle

V_m = centerline gas velocity

$V_{r,X}$ = local gas velocity at radial distance r and axial distance X

The velocity within each zone is assumed to be uniform and identical to that of the probe position. With the above simplifying assumptions, the relative contribution of each probe sample to the combustion efficiency can be weighed.

The procedure for calculating the combustion efficiencies is recognized to be approximate. However, major errors are eliminated by the procedure used to calculate these efficiencies. The velocity, which is known to be approximate, appears in the numerator and the denominator of the integral equations and, hence, errors introduced by this approximation are partially cancelled. The probes were, in most cases, extended to the maximum radial distances allowed by the geometry of the flare scaffolding. The outside probe usually measured high combustion efficiencies. In some cases, with asymmetrical flames only one outside probe measured high combustion efficiency. These high combustion efficiencies indicate that the amount of incompletely burned hydrocarbons outside the symmetrical probe sampling region can usually be neglected.

Some earlier studies relied on estimating combustion efficiency from a sampling drawn with a single probe positioned on the axis of the flame. These studies argued that rapid motion of the flame and long smapling times would yield the true overall combustion efficiency of the flame. This is true under very restricted conditions but in general may result in inaccurate estimates of the combustion efficiency of the flame. First, a single probe ignores the influence of velocity profiles (variation of mass flux of unburned carbon out of the system at different positions). Second, assuming the probe is sampling at a uniform rate the combustion efficiency determined by a single probe in a fluctuating flame is

$$\eta = 1-\Sigma_j \frac{\dfrac{\Sigma_j C_{iju}}{\Sigma_i C_{ij}} \quad t_j}{T} \qquad (3\text{-}17)$$

where C_{iju} is the unburned carbon and C_{ij} is the total carbon, t_j is the total time sampled at relative flame position j. The fraction of time a flame will be in relative position j is the intermittance factor, Ω_j. Introduction of the intermittance factor at radial position j results in

$$\eta = 1-\Sigma_j \frac{\Sigma_j \; C_{iju}}{\Sigma_j \; Cij} \; \Omega_j \qquad (3\text{-}18)$$

A single probe will then yield the overall combustion of efficiency if the local combustion efficiency $\Sigma_j \frac{C_{iju}}{\Sigma C_j}$ or Ω_j is constant across the flame. Figure 3-7 shows an example of the variation in local combustion efficiency with radial distance. In general, local combustion efficiencies are lower at the edges than on the axises of the flames. Figure 3-8 shows that the intermittence factor, Ω, decrease with increasing radial distance. The net result of these variations is that the overall combustion efficiency measured by a single probe biases the sample towards the higher combustion efficiencies near the axis and could result in overestimation of the overall combustion efficiency.

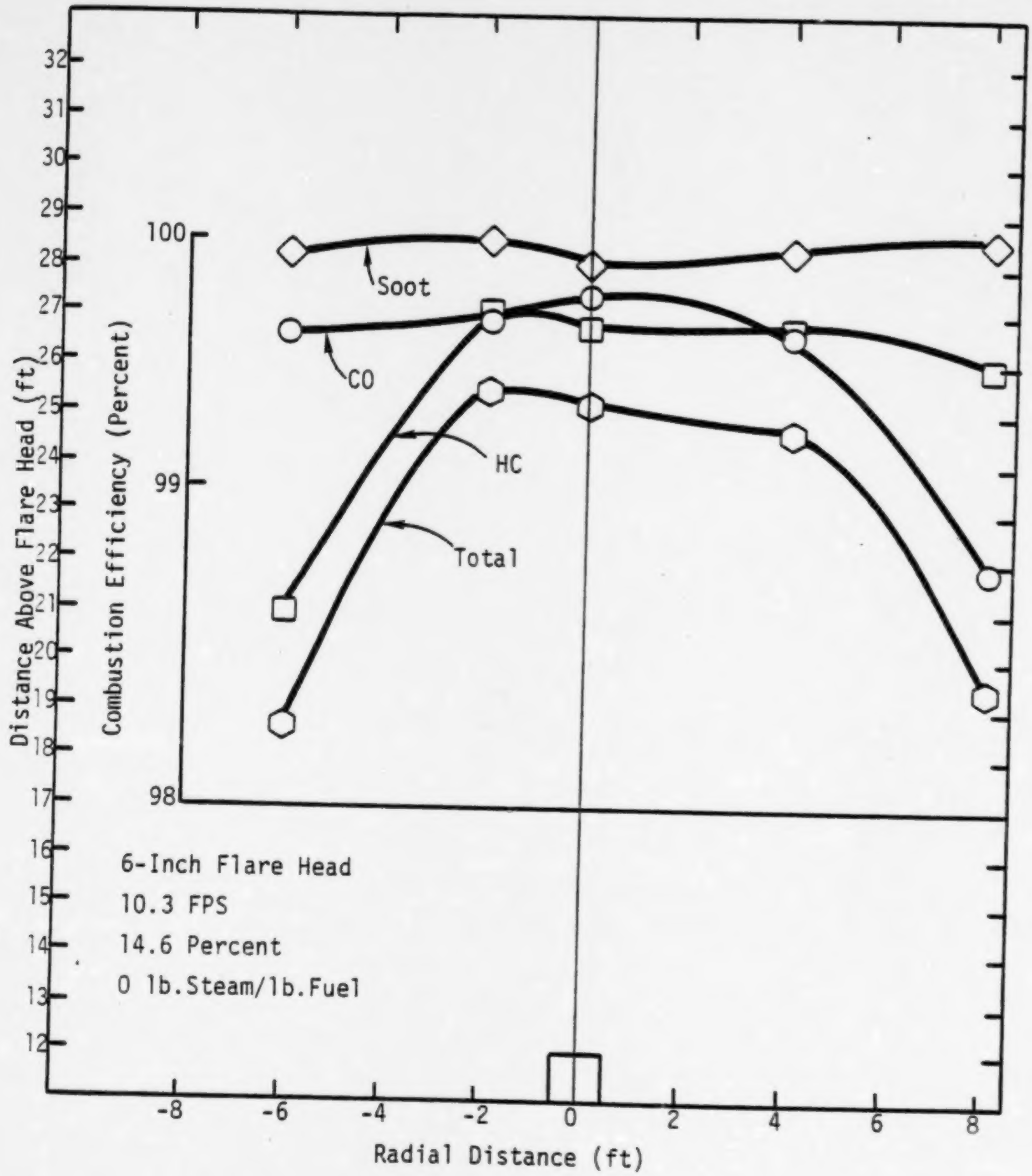

Figure 3-7. Local combustion efficiencies of the 6-inch EER test flare head burning 14.6 percent propane in nitrogen at 10.3 ft/sec with 0.0 lb steam per lb of fuel.

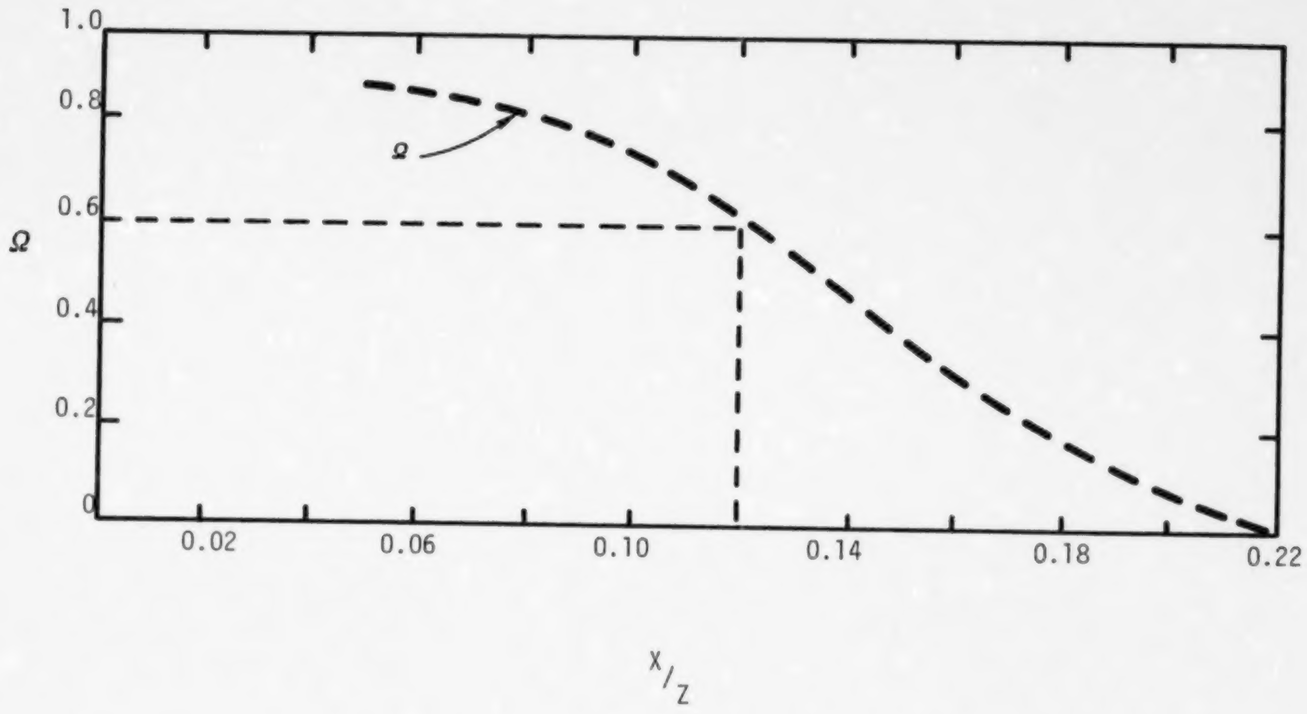

(Re) = 17000 at nozzle

z = axial distance

x = radial distance

d_o = nozzle diameter

Ω = intermittency factor, related to time of presence

Figure 3-8. Distribution of Intermittency Factor, Ω, and Mean Forward Velocity in a Round Free Jet (Corrsin & Kistler, 1954).

REFERENCES

SECTION 3

Corrsin, S., and A. L. Kistler, "The Free-Stream Boundaries of Turbulent Flows," National Advisory Committee for Aeronautics, Technical Note NACA TN 3133 (1954).

4.0 FLAME STRUCTURE

The main purpose of this program was to estimate the combustion efficiency of commercial flares. Currently it is virtually impossible to measure the combustion efficiency of operating flares because of the flame size, elevated location, and lack of spatial stability. As a consequence, this program was designed to measure the combustion efficiency of large, pilot-scale flares.

Extrapolating the results of pilot-scale flares to larger flares requires the knowledge of the scaling laws of combustions and of the mechanisms which lead to inefficiency. Therefore, considerable effort was devoted in this program to defining the operating and design parameters which control the structure of flare flames and determine flare combustion efficiency. In addition, a number of structural features are important to the design and operation of flares:

- Flame volume
- Flame length
- Flame dilution
- Flame liftoff distance
- Flame stability

This program has collected data on large pilot-scale flare flames over a large range of design and operating parameters representative of industrial use. Several measurement techniques were used to investigate the structure of the large pilot-scale flare flames. The characteristics of the flames were observed against a graduated background, visual observations were supplemented with long-exposure and short-exposure photographs, high speed motion pictures, and measurements of gas composition in the plume of the flare flames.

Flame shape (volume and length) is directly related to the rate of combustion and the mechanisms controlling combustion and will influence combustion efficiency as well as the amount and the centroid of radiant emission.

Previously, the length and volume of buoyant transitional and turbulent jets have been studied. Correlations of the flame length have been developed from these studies. These correlations have been suggested and are used to estimate the structure of flare flames. Most of these studies investigated the flame structure of small flames over a limited range of operating conditions. Some of the available correlations were unable to predict the results from this study and are not recommended. The correlation of Zukoski et al (4.1) and of Hottel and Hawthorne (4.2) successfully predicted the results from this study when the coefficients were altered. However, a more accurate correlation for the flame length was developed in this study.

length was developed in this study.

The rate and extent of dilution of the combustion products in a flare flame will influence the temperature, rate of quenching and, hence, combustion efficiency. The dilution factors measured in this study were correlated using a Richardson number approach similar to that of Spaulding and Ricou(4.3). This correlation was unable to adequately account for the influence of diameter on the dilution factor, and a more accurate dimensional correlation was developed.

The liftoff distances of the flame control the extent of entrainment of air prior to combustion and, hence, the rate and extent of combustion. This study showed that detached flames can be stable and operate with high combustion efficiency. The liftoff distances of this study were correlated by assuming dilution of the combustion products followed measurements made in simple jets, and the criteria that the flame speed must equal the imposed velocity for stable combustion. Efficient combustion can only take place when the flare flame is maintained. Inefficient combustion often occurs near the limits of flame stability. The stability limits of flames in this study were correlated using results from simple jet theory, measured flame speeds and measured flammability

from simple jet theory, measured flame speeds and measured flammability

limits. Calculations based upon accepted theories were unsuccessful in predicting the performance of flare flames (liftoff distance, shape, combustion efficiency), but correlations were developed with special constants based upon the theoretical equations.

4.1 Test Conditions

The operating conditions of the flares tested in this program covered the range of parameters of commercial flares. This section will discuss the design of the test matrices, explain any modifications to the test matrices, and compare the conditions tested versus those of commercial flares.

Test Matrices

Three test matrices were developed initially and modified as the program progressed. The first test matrix was designed to develop scaling principles for flare flames. The second was designed to test commercial flare heads at conditions comparable with those of the first test matrix. The third was designed to test combustion efficiencies of flare flames at high velocities.

The original test matrix was designed to develop scaling laws for the structure and emission of flare flames. As such, the matrix was designed to test four scaling criteria over three small, but commercial size, flare heads. The scaling principles were:

- Constant velocity, u
- Constant residence time, d/u
- Constant Reynolds number, $\frac{\rho d u}{\mu}$
- Constant Richardson number, gd/u^2

where u and d are the exit velocity and diameter, ρ and μ are the exit gas density and viscosity, and g is the gravitational constant. The sizes of the flare heads were 3-, 6-, and 12-inches in diameter. The matrix was also designed to test the influence of steam injection on combustion efficiency. The original test matrix as modified in the program is shown in Table 4-1. The conditions of this matrix, denoted by an "X", were tested one or more times.

A second test matrix was designed to compare the flame structure and emissions of commercial flare heads with those of the prototype head designed by EER. The matrix for testing of commercial flare heads is shown in Table 4-2. This test matrix was completed with minor exceptions. The combustion efficiency at one probe position for the Industrial Flare Head B was not measured; however, a complete stability curve was obtained for this head and time did not permit determining combustion efficiency at the last probe position. This omission was thought to be of minor importance since the combustion efficiency was determined at two other rake positions for the same

TABLE 4-1. FLARE TEST CONDITIONS

Flare Head Size Inches			Velocity ft/sec			Heating Value Btu/ft^3		Steam/Fuel Ratios					Smoke-less	Wind		Sampling Rake Position			
3	6	12	Low	Med	High	1300	300	0.15	0.30	0.50	0.75	1.0		Low	Natural	Hood	1	2	3
X			0.5			X								X		X	X	X	X
X				2.0		X								X		X	X	X	X
X					10	X								X		X	X	X	X
X					10	X							X	X		X			
X			0.5				X							X		X			
X				2.0			X							X		X	X	X	X
X					10		X							X		X			
X					10	X		X	X	X		X		X		X			
	X		1.0			X								X		X			
	X			2.8		X								X		X	X	X	X
	X				10	X								X					X
	X		1.0			X							X	X					X
	X			2.8		X							X	X		X			
	X				10	X							X	X					
	X		1.0				X							X		X			
	X			2.8			X							X		X	X	X	X
	X				10		X							X					X
	X				10	X									X				
		X	0.2			X								X					X
		X		2.0										X					X
		X			4	X								X			X	X	X
		X	0.2				X							X					X
		X		2.0			X							X					X
		X			4		X							X			X	X	X
		X			4	X							X						X

X = Tests conducted

TABLE 4-2. MATRIX FOR TESTING COMMERCIAL FLARE HEADS

				Measurement of Combustion Efficiency		
	Velocity	Gas Btu/ft^3	Steam	Rake 1	Probe 2	Position 3
Industrial Flare Head A	0.2	1300	No			X
	2	1300	No			X
	4	1300	No	X	X	X
	4	1300	Yes			X
	4	286	No			X
	Optional Stability Curve		No			Ⓧ
Industrial Flare Head B	0.2	1300	No			X
	2	1300	No			X
	4	1300	No	Ⓧ	X	X
	4	1300	Yes			X
	4	286	No			X
	Optional Stability Curve		No			X
Industrial Flare Head C	0.2	1300	No			X
	2	1300	No			X
	4	1300	No	X	X	X
	4	1300	Yes			X
	4	286	No			X
	Optional Stability Curve		No			X

Ⓧ = Test not conducted

flare flame conditions. Time did not permit completion of the optional stability curve for the Industrial Flare Head A, however one point of the stability curve was determined.

A third test matrix, Table 4-3, was developed to test the influence of high velocities on the combustion efficiency of flare flames.

Operating Conditions

The range of conditions tested in this study covered the majority of the operating conditions which are common practice commercially. Figure 4-1 shows the range of flare diameters, exit velocities, residence times, Reynolds numbers and Richardson numbers tested in this study. The range of commercially operated flare is similar but includes larger diameter flare heads.

4.2 Mechanism of Combustion

As described above, flares have a wide range of operating conditions and these conditions result in different mechanisms controlling combustion. Combustion is controlled in all flare flames by the rate of mixing of the flame gas with oxygen from the air. Mixing in the flare flame is dictated by:

- Buoyancy forces
- Molecular difdfusion
- Jet mixing.

This section described correlations developed for the flame length, entrainment, liftoff distance and flame stability with operating parameters of the flare. These correlations were developed for propane-nitrogen mixtures and applicability to other gases has not been demonstrated.

Mixing Mechanism

Two classical descriptions of flame structure are available. Hottel and Hawthorne [(4.2)] described the length of flames as a function of velocity, and Ricou and Spaulding [(4.3)] described the entrainment of ambient gases into flames as a function of the Froude number (ratio of inertial forces to buoyancy forces; it is the reciprocal of the Richardson number).

TABLE 4-3. TEST CONDITIONS FOR HIGH-VELOCITY FLARES

Test Flames	Flare	Btu/ft^3	Steam	Velocity Low	 Medium	 High
1	Open	1300	30 lb/hr or Soot Suppression	X	X	X
2	Ring	1300	30 lb/hr or Soot Suppression	X	X	X
3	Ring	Minimum	Soot Suppression	X	X	X
4	Ring	600	Soot Suppression	X	X	X
5	Ring	1300	Soot Suppression	X	X	X
6	Ring	2350	Soot Suppression	X	X	X

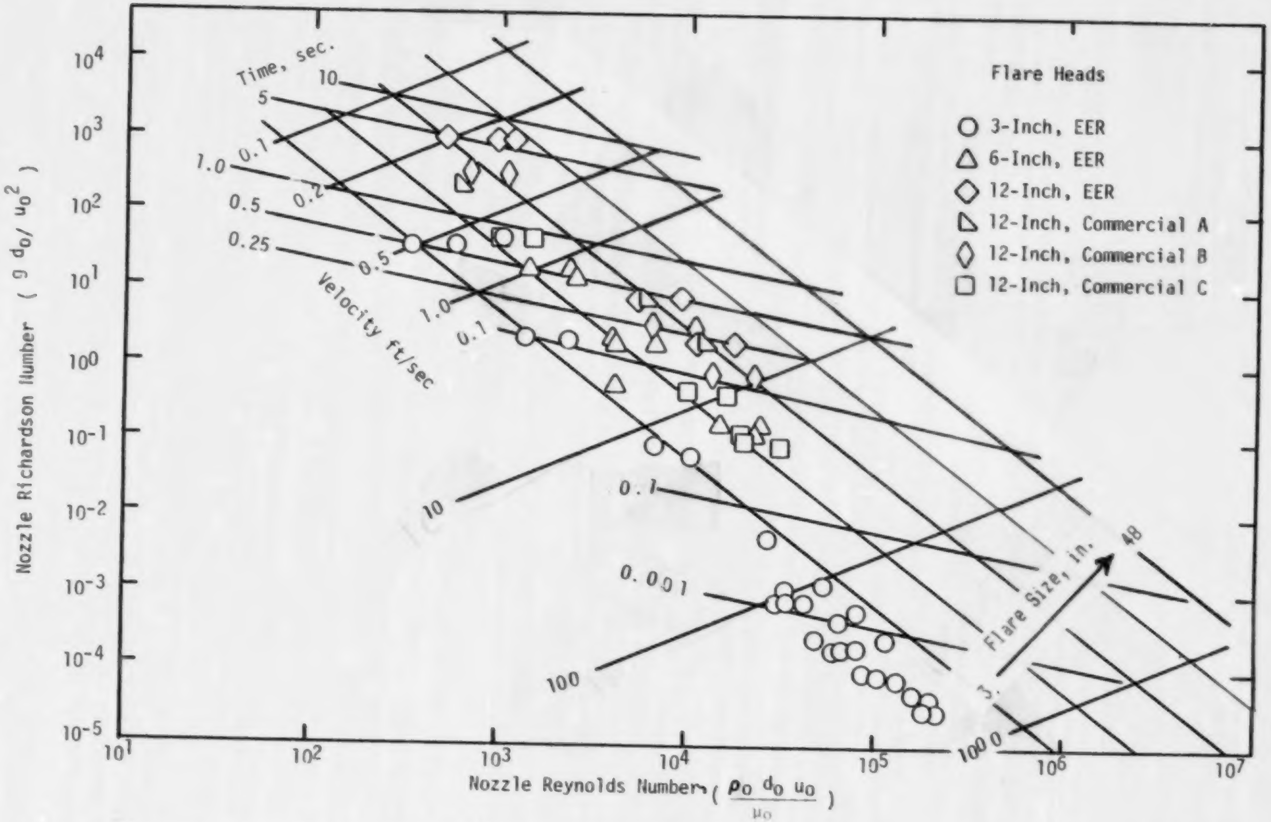

Figure 4-1. Comparison of the Range of Conditions Tested in This Study and Those of Commercial Flare Flames.

The flames of this study had Reynolds numbers below $2x10^5$ and based on the flame length criteria of Hottel and Hawthorne (4.2), they were not fully developed turbulently. Figure 4-2 shows the length of flames measured in this study on a plot similar to that suggested by Hottel and Hawthorne. The plot indicates that the length of the flames in this study continued to increase as the Reynolds number increased. The line in Figure 4-2 corresponds to flames burning 56 percent propane in nitrogen. The length and structure of fully turbulently developed flames no longer depends on Reynolds number. Since the flames of this study were independent of Reynolds number, mixing is partially controlled by molecular diffusion and buoyancy forces. Figure 4-2 also shows that smaller nozzles and higher amounts of combustibles yielded longer flames, while addition of steam slightly reduced the length of the flame.

Similarly, the Richardson number for the flames studied varied from 3x10-5 to $8x10^2$, indicating that most flames were controlled by buoyancy-dominated mixing. The Richardson number is the ratio of buoyance forces to inertia forces: values greater than one indicate predominance of buoyancy forces, while values less than one indicate a predominance of inertial forces. Entrainment as a function of Richardson number will be shown later on a plot similar to that suggested by Ricou and Spaulding(4.3).

Rate of Surface Combustion

Control of mixing by molecular diffusion to the flame would yield flames with constant-heat-release-per-unit-surface. Figure 4-3 shows that the surface heat release rate increases with heat release rate from 10,000 to almost 200,000 $Btu/ft^2/hr$. Therefore, mixing of material on the flame surface does not strongly contribute to control of the combustion rate for flare flames of this study.

Volumetric Combustion Rate

Volumetric control of combustion could be the result of control by two mechanisms. The first can occur when gases are completely mixed at the molecular level and the combustion rate is controlled by kinetics. Kinetic control is unlikely for those flames with slow mixing and rapid combustion. The second can occur when mixing is controlled within a volume. This can occur when the flame envelope includes pockets of air and combustible gases which are not mixed on the molecular level. Figure 4-4 shows that constant volumetric combustion is approximated for all the flames of this study. A

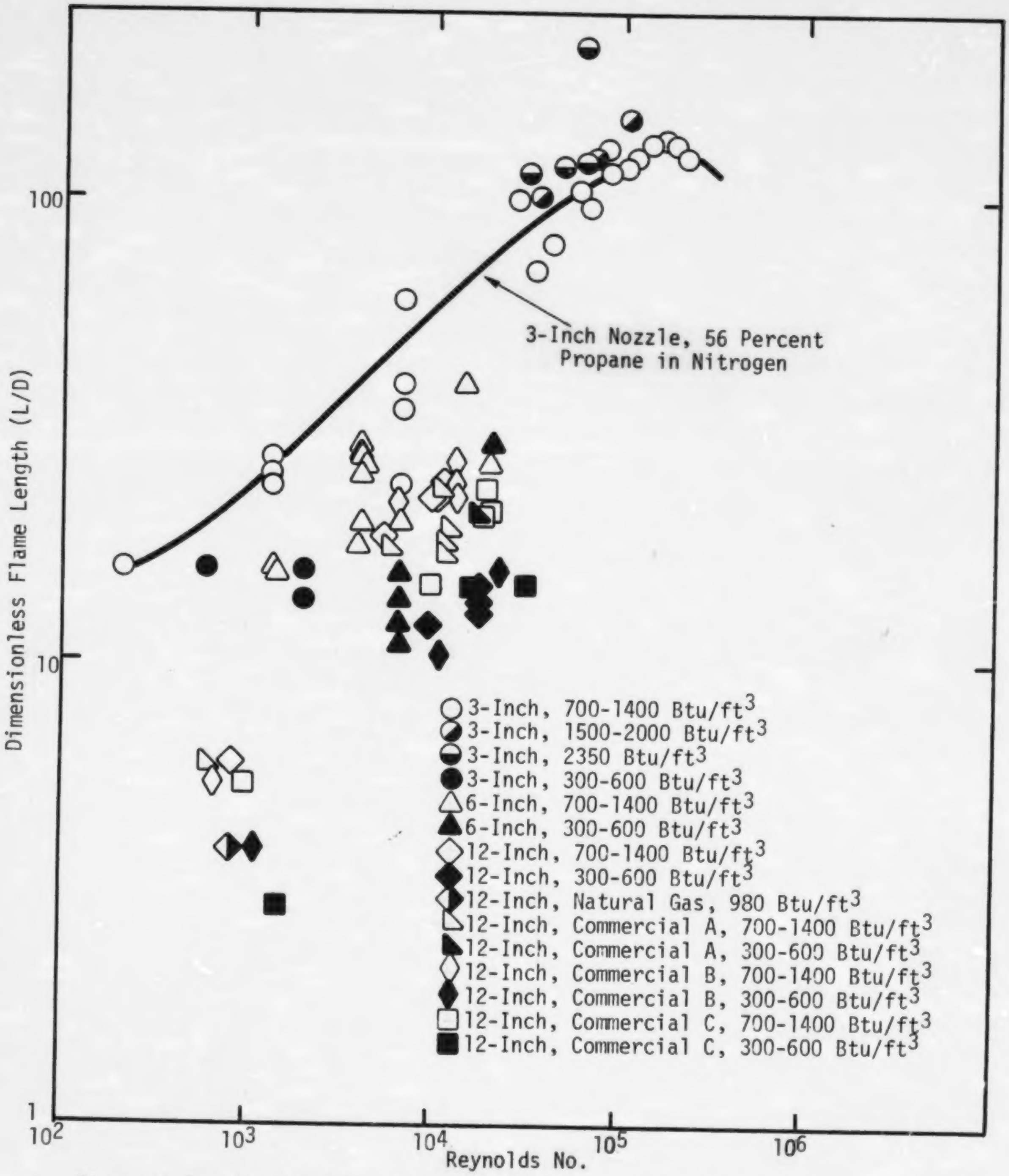

Figure 4-2. Correlation of Lengths of Flames Studied with Reynolds Number.

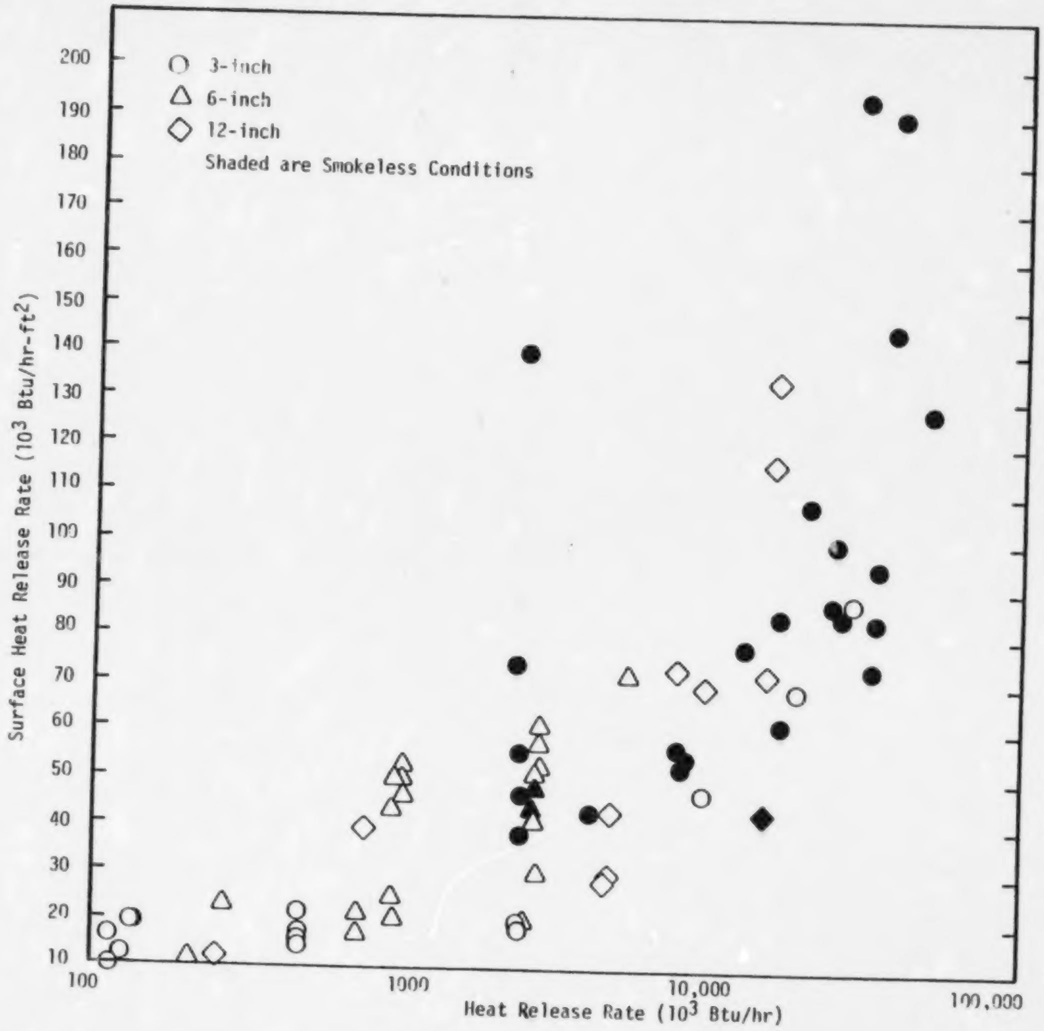

Figure 4-3. Surface Rate of Combustion of Flare Flames.

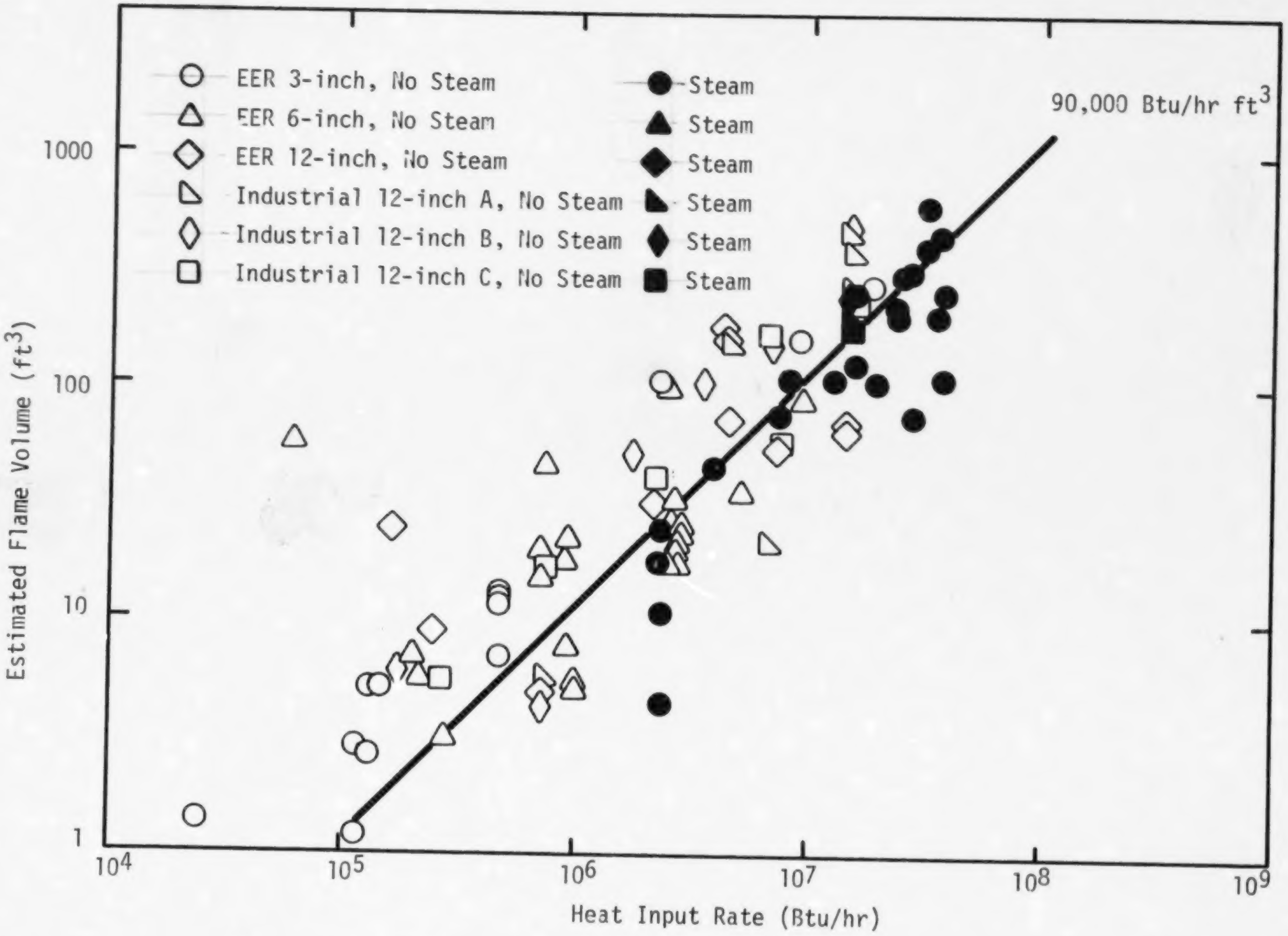

Figure 4-4. Volumetric Combustion Intensity of Flare Flames.

A least square regression analysis would yield:

$$\text{Flame Volume} = 1.21 \times 10^{-5} (\text{firing rate, Btu/hr})^{0.85} \quad (4\text{-}1)$$

However, the data does not support such an accurate equation and the simple relation that the volumetric heat release of flare flames is constant at 90,000 Btu/hr/ft^3 is preferred. This value is supported by evidence on pool flames(4.5) and from industrial experience(4.6).

The volumetric heat release of the flare with steam injection is typically increased (lower volume of the flame for a given heat-release rate). This confirms conventional thinking that steam increases the induction of air into the root of the flame and increases mixing inside the flame envelope. The reduction of the flame volume by steam injection is not large, but observations and measurements show that this difference is sufficient to completely suppress soot production.

The above evidence supports ideas of combustion by volumetric mixing in flare flames. Volumetric mixing will be important in flames into which air is induced by gross mixing mechanisms. This can occur when the buoyancy-dominated flame engulfs large amounts of air into the apparent flame volume. Combustible materials are not molecularly mixed inside this volume, but are congregated into pockets of air which are mixing with pockets of fuel. The mixing of these pockets controls the burning rate. This view is supported by short-exposure photographs and high-speed motion pictures taken during this study and is consistent with the view of coherent structures(4.7-4.9).

4.3 Flame Length

Calculations of the length of flare flames are needed to estimate radiation from the flames to the ground, and as an indication of the combustion mechanism of the flames. At the start of this work, a number of empirical relationships for flame lengths existed. Some of these were particularly complex(4.10-4.11), and some were recommended for predicting the length of flare flames(4.11). The conditions under which these expressions for flame length were derived are listed in Table 4-4. Many of the correlations were derived under conditions different from those of flare flames. Table 4-4 shows that the major differences between this and previous studies is the use of large nozzles and extension to high Richardson numbers (i.e., buoyancy-dominated flames).

TABLE 4-4. CONDITIONS UNDER WHICH CORRELATIONS FOR FLAMES WERE DERIVED

INVESTIGATIONS	NOZZLE SIZES (INCHES)	FUEL OR INJECTED GAS	NOZZLE GAS VELOCITY (FT/SEC)	REYNOLDS NUMBER	RICHARDSON NUMBER
This Work	3, 6, 12	Propane-Nitrogen Mixtures, Natural Gas	0.2 to 428	337 to 217,000	2.9×10^{-5} to 8.04×10^{2}
Hottel & Hawthorne (4.2)	0.25, 0.1875, 0.125	H_2, CO, City Gas	To 258	1910 to 16,700	Greater than 1.0×10^{-5}
Ricou & Spaulding (4.3)	0.0625 to 1.25	Air, Hydrogen Propane, CO_2	80 to 250	2500 to 80,000	2.68×10^{-6} to 5.24×10^{-4}
Becker & Liang (4.10)	0.1, 0.18	Commercial Propane	11.5 to 260	1310 to 48,200	0.91×10^{-5} to 4.43×10^{-3}
Brzustowski (4.11)	0.197		41	15,823	3.14×10^{-4}
Zukoski (4.1)	2.54, 7.48 19.69	City Gas	0.0427 to 0.984	160 to 2500	2.33 to 6.4×10^{4}

Most of the existing models were unable to predict the flame lengths observed in this study. Figure 4-5 shows that estimates by Becker and Liang(4.10) and Brzustowski(4.11) could predict neither the absolute value nor the trends in flame length. However, while the expression of Hottel and Hawthorne(4.2) could not predict the absolute value of the flame length, the expression predicted the trends.

The expression of Hottel and Hawthorne was derived for laminar diffusion flames and contained two constants. Adjustment of these constants resulted in a simple expression which reasonably fits the data of this study (Figure 4-6). The success of the Hottel and Hawthorne correlations suggests that, to some extent, the amount of fuel fed to the flare partially controls the rate of mixing and, hence, the flame length. Correlations of flame length for pool fires were also available. These correlations were obtained assuming the buoyant force is dominant. The result of one such correlation is shown in Figure 4-7. The correlation of flame length with buoyancy forces is quite reasonable for short flames which were minimally influenced by velocity. However, the relationship under-predicted the length of long flames which were partially controlled by inertial effects.

Finally, a correlation was derived which predicted the lengths of all the flames of this study. The correlation is based on the Richardson number corrected for the temperature rise of the plume. The Richardson number contains both the influence of inertial and buoyancy forces. The correlation:

$$L/D = 7.41 \left(\frac{Q \times F}{C_{p\infty} T_{\infty} (1 + 26 x)} \right)^{0.60} R_i^{-0.216} \qquad (4\text{-}2)$$

is shown in Figure 4-8, and is capable of predicting the flame length of this study within about 20 percent. The terms are defined as:

L = Flame length, ft

D = Nozzle diameter, ft

Q = Heat release of fuel, Btu

X = The fraction of propane in the propane-nitrogen mixture

26 = A factor to account for stoichiometric combustion of propane with air and will change for other fuels

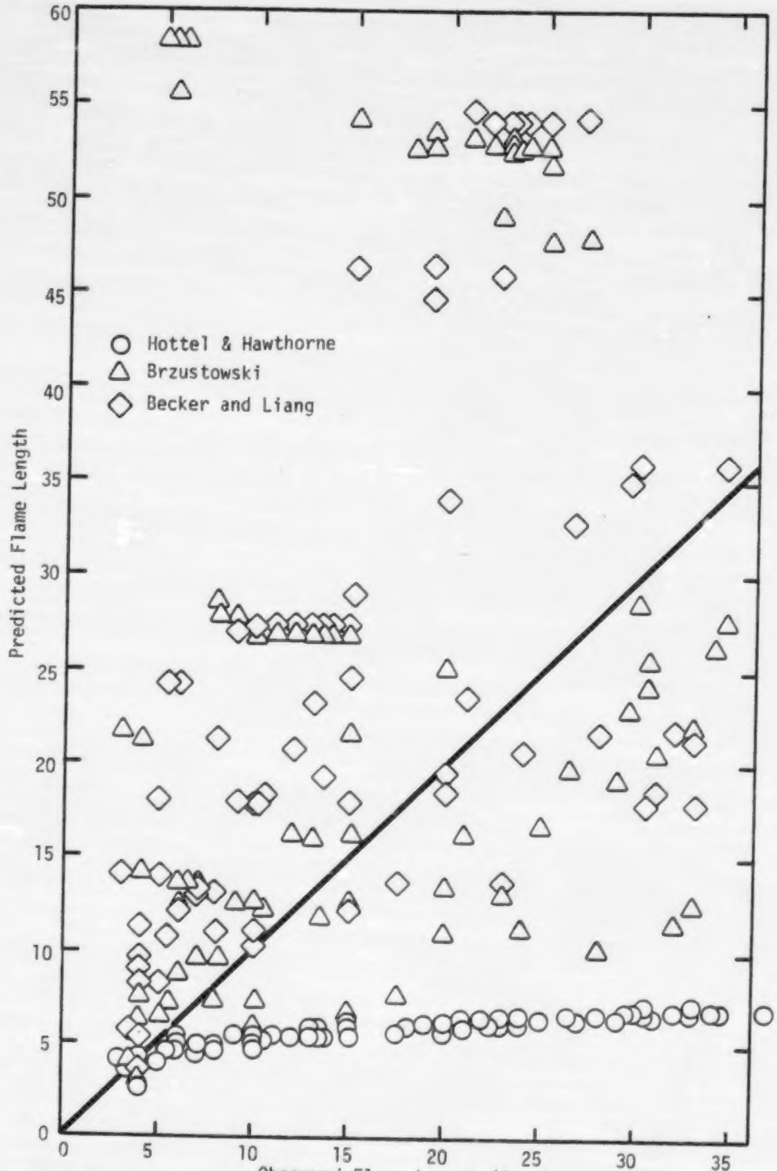

Figure 4-5. Comparison of Flame Lengths Predicted by Available Studies With Those Observed in This Study.

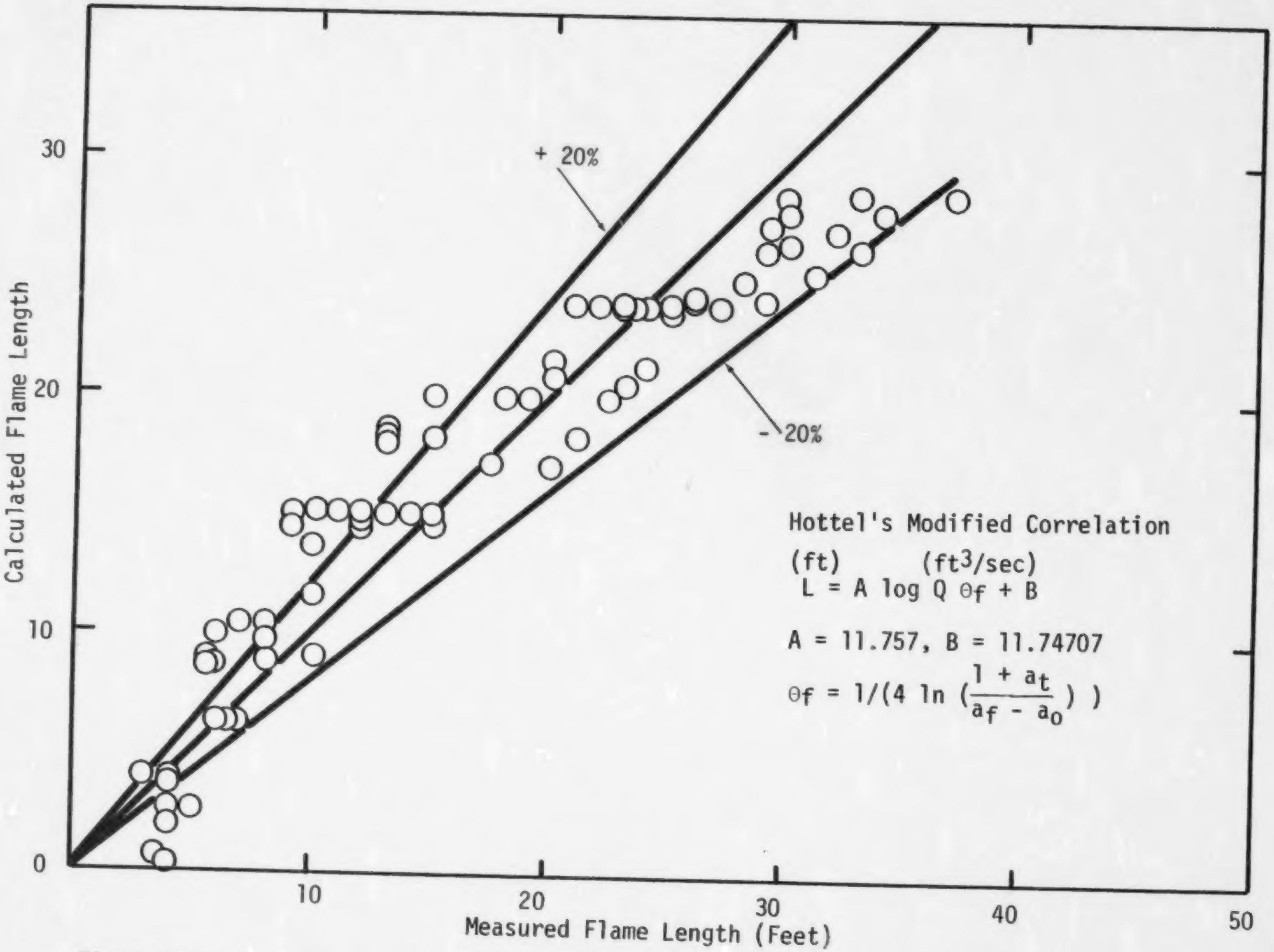

Figure 4-6. Comparison of a Hottel and Hawthorne Correlation with the Flame Length of This Study.

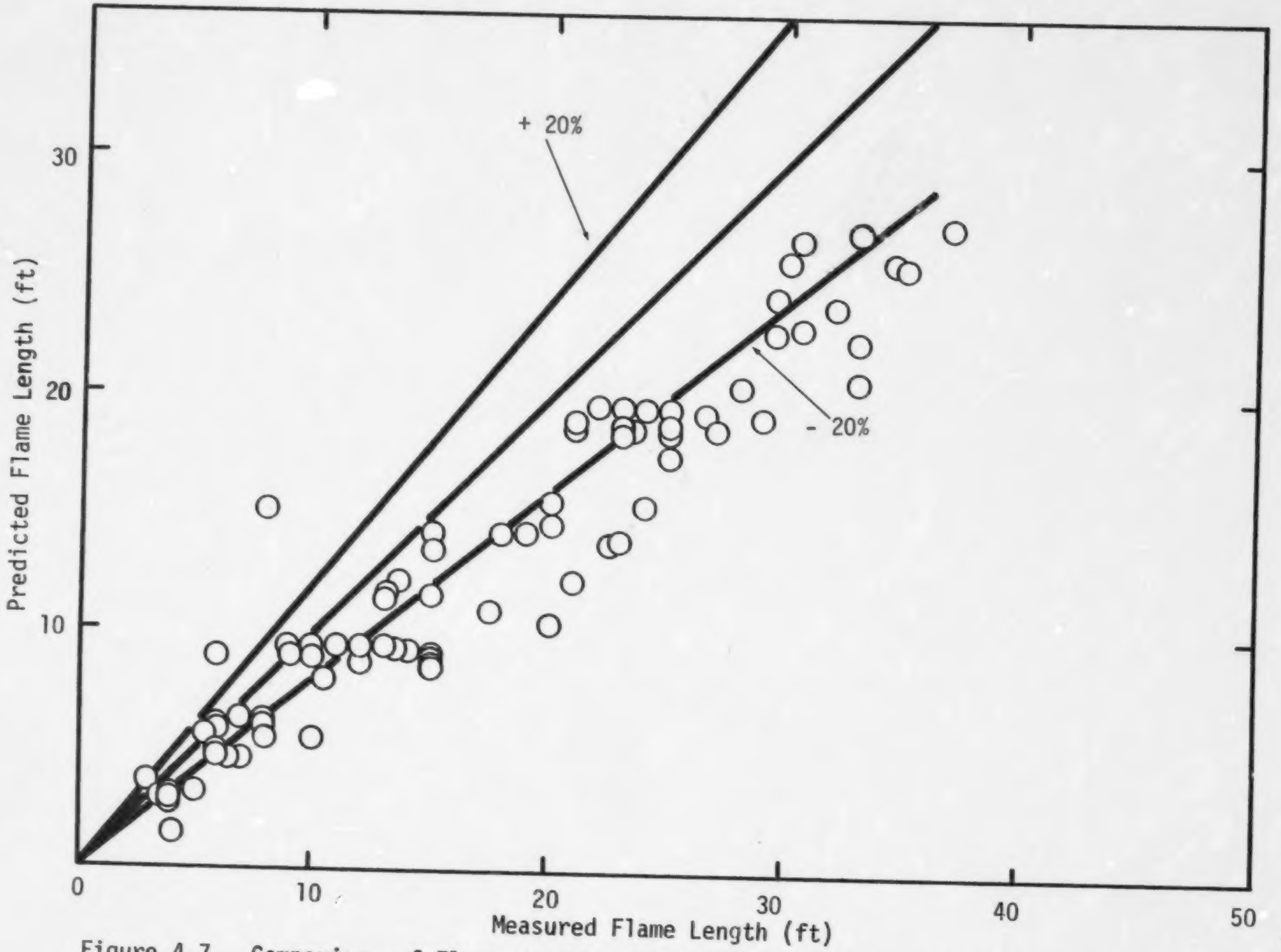

Figure 4-7. Comparison of Flame Lengths Predicted by a Buoyance Correlation with Observed Flame Lengths of This Study.

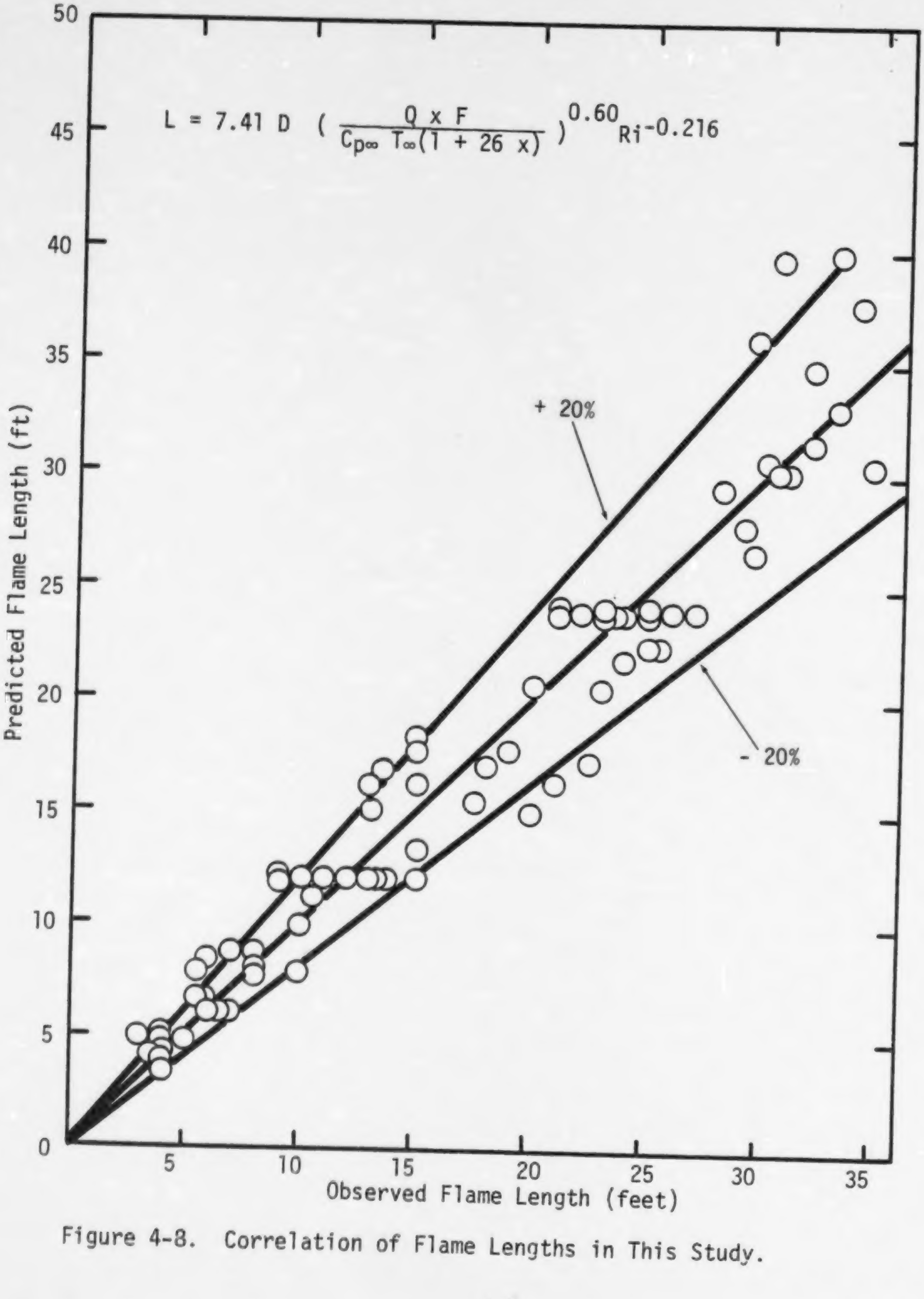

Figure 4-8. Correlation of Flame Lengths in This Study.

$C_{p\infty}$ = Heat capacity of ambient air, Btu/lb mole °F

T_∞ = Temperature of ambient air, °F

F = Fraction of heat radiated from the flame (empirically derived)

R_i = Richardson number = gd/u^2

The fraction of heat release emitted from the flame was derived from a single set of data at a Richardson number of 2.0, as shown in Figure 4-9. The fraction of heat of a pure propane flame was assumed to be that value necessary to predict the flame lengths. The factors determined are a function of only gas composition and are shown in Figure 4-9. These values were then successfully correlated with all the flame lengths of this study. The derived factors agree with visual observation of flames burning different amounts of propane. The amount of propane does not affect the flame structure or apparent radiation above 60 percent propane. Below that value, the radiation of the flame decreases with decreasing concentration of propane.

4.4 Entrainment

The rate of air entrainment has some influence on the rate of combustion and flame length, but has a large influence on flame liftoff and stability. The flames of this study had Richardson numbers varying from 3×10^{-5} (momentum-dominated flames), to 8×10^{2} (buoyancy-dominated flames) (see Figure 4-1). Ricou and Spaulding(4.3) have successfully correlated the rate of entrainment for momentum-dominated jets and flames. The correlation involves the Froude number (the reciprocal of the Richardson number); however, this term appeared on both sides of the expression and cancelled from the final correlation.

Entrainment in the flare flames of these studies was much faster than predicted by jet theory. Figure 4-10 shows that entrainment in this study was grouped into two regimes. The first regime is for flames with low velocities. Entrainment in this regime was two-to-three orders-of-magnitude faster than that predicted by jet theory, depended inversely on velocity, but did not strongly depend on nozzle size or the heating value of the gases. The entrainment for high-velocity flames fell into the second regime. Here

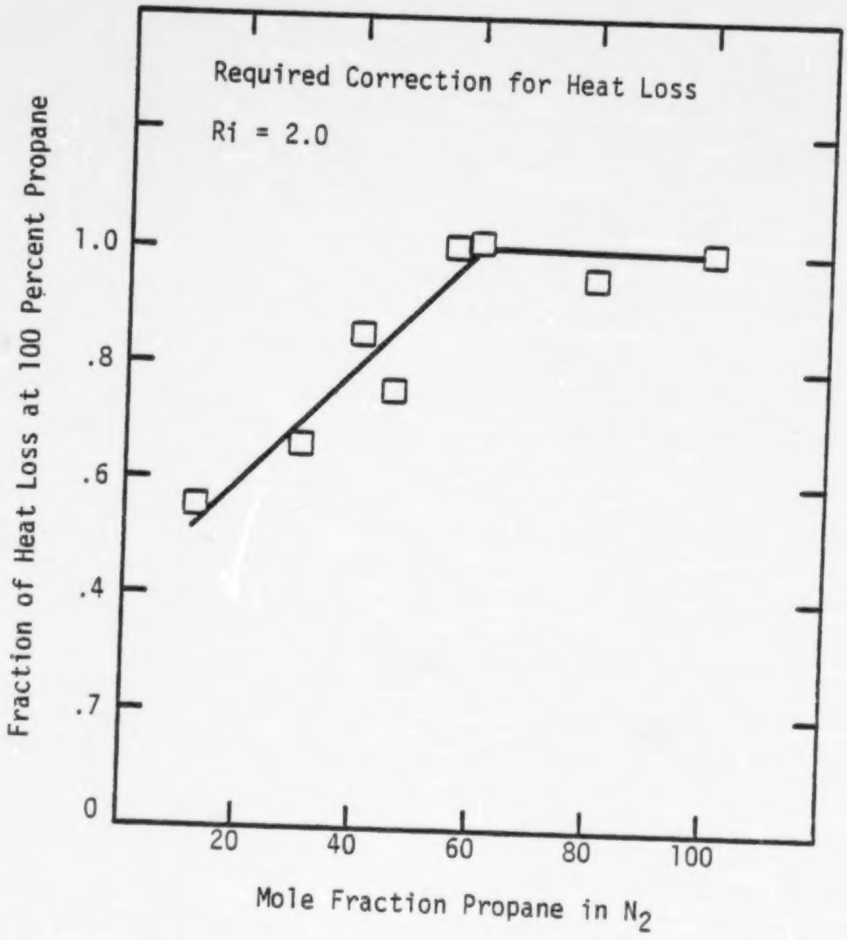

Figure 4-9. Empirical Correction for Radiation Loss from Flare Flames.

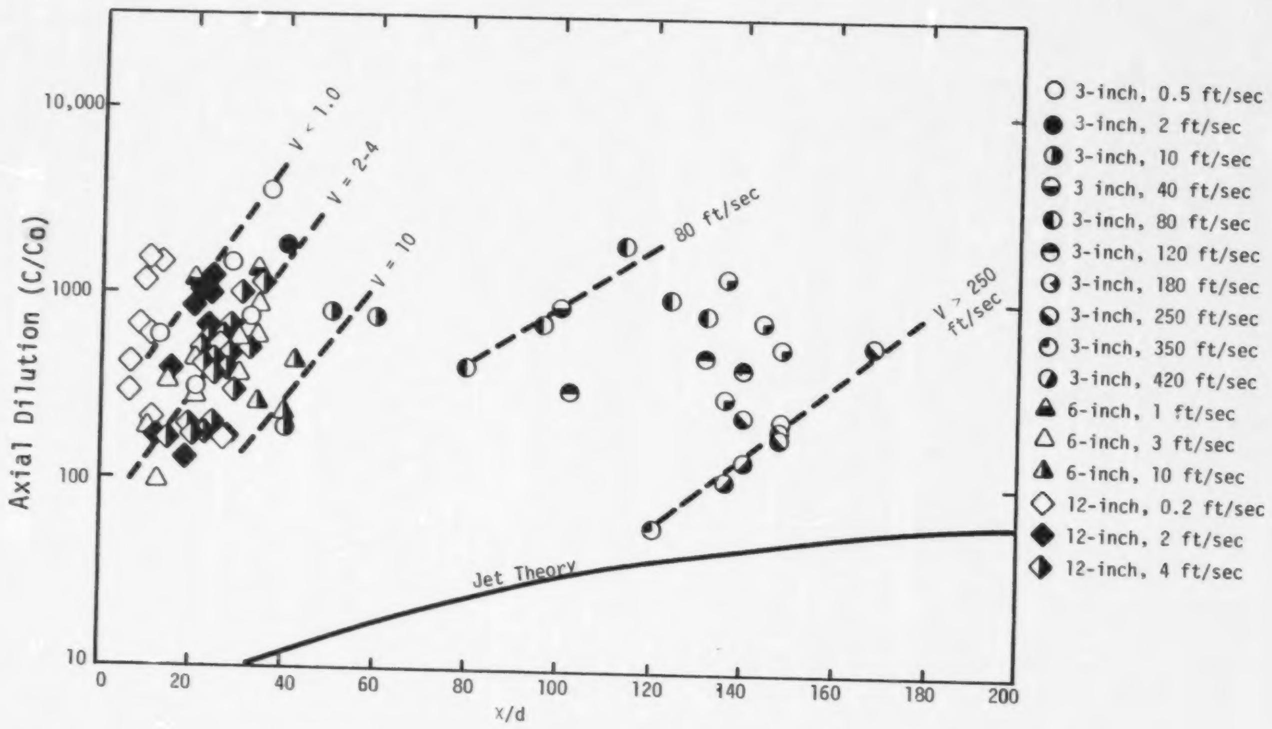

Figure 4-10. Entrainment Air into Flare Flames.

the entrainment was closer to that predicted by jet theory for the higher velocity jets in this study.

Attempts to correlate the entrainment rate using the dimensionless distance and the Richardson number were only partially successful. The high rate of entrainment apparently caused by engulfing fluid in a buoyant plume, and the inverse relationship between entrainment and velocity, suggest that the Richardson number should aid in correlating the entrainment rate for flare flames. Likewise, the increase in entrainment with distance above the flare head suggests that the dimensionless distance, X/d, should aid in correlating entrainment. Correlations of the entrainment rate with the product of X/d and the Richardson number were developed and are shown in Figure 4-11, but were of only medium strength. Development of strong correlations was hampered because of the strong dependence on nozzle diameter and the fact that this was reduced by inclusion of the Richardson number which also contained the nozzle diameter.

F4-11

A dimensional correlation was developed which reasonably correlated the data. This correlation involved the dimensionless distance and the reciprocal of velocity. The correlation shown in Figure 4-12 successfully collapsed all the data of Figure 4-10. This data included 3-, 6-, and 12-inch nozzles, variation in heating value from 300- to 2350-Btu/ft^3, and nozzle velocities from 0.2 to 430 ft/sec. This correlation can be used to roughly estimate the entrainment of ambient fluids into large flare flames operating in the region between buoyant- and momentum-domination.

F4-12

4.5 Flame Liftoff

The liftoff distance of a flame can, in theory, be estimated by simple combustion theory. The liftoff distance will be the distance required to induce sufficient air to reduce the jet velocity at least in one location, to the flame velocity. The flame velocity will pass through a maximum near the stoichiometric mixture as air is mixed with fuel. Once the flame is stabilized at a location, the propagation of an ignition source must extend to all regions of the flared gas to achieve efficient combustion. Aerodynamic devices or pilot flames can create regions of ignition which will propagate and stabilize a flame under conditions where the flame would

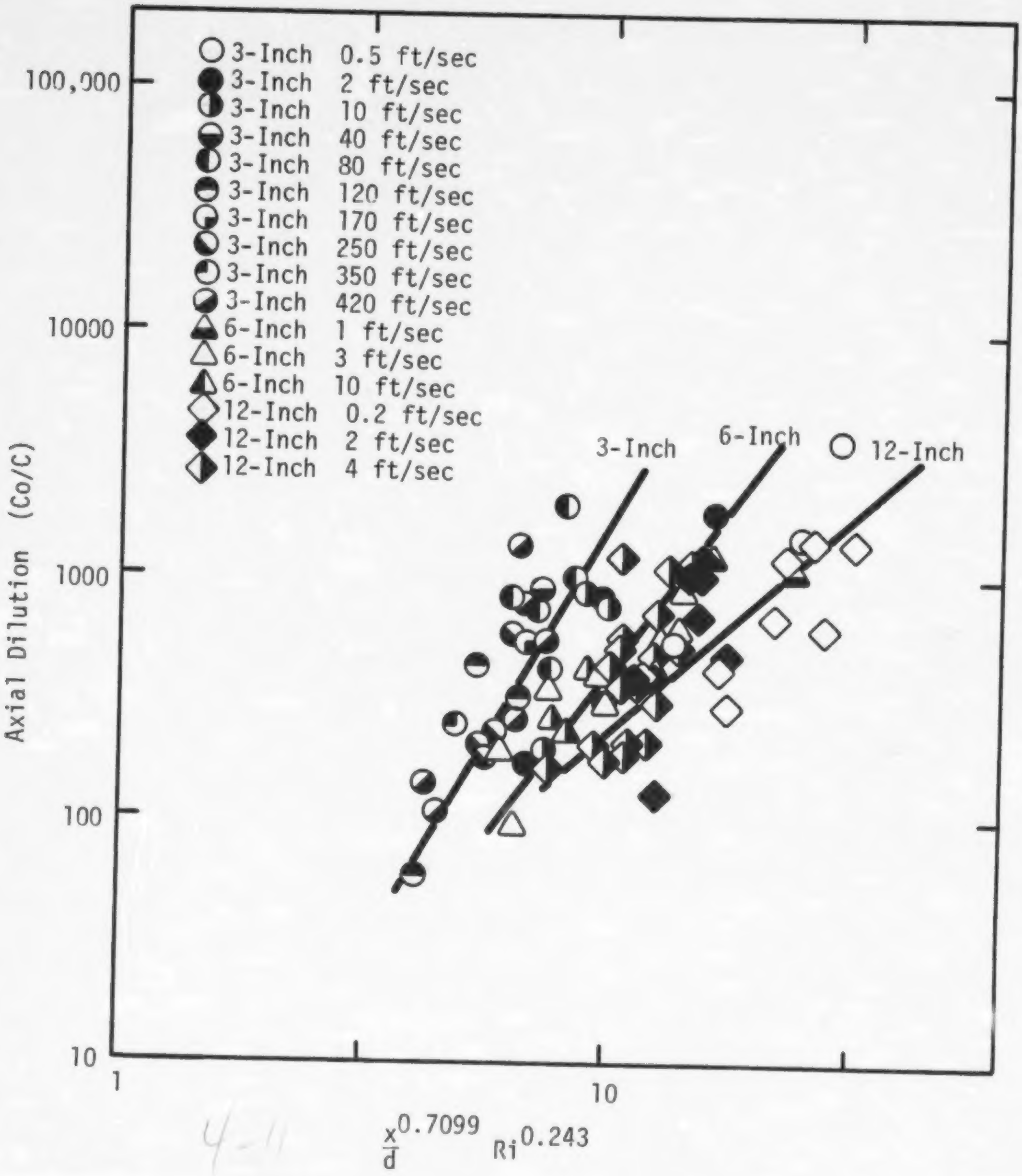

4-11

Figure 4-11. Correlation of entrainment rate for flare flames.

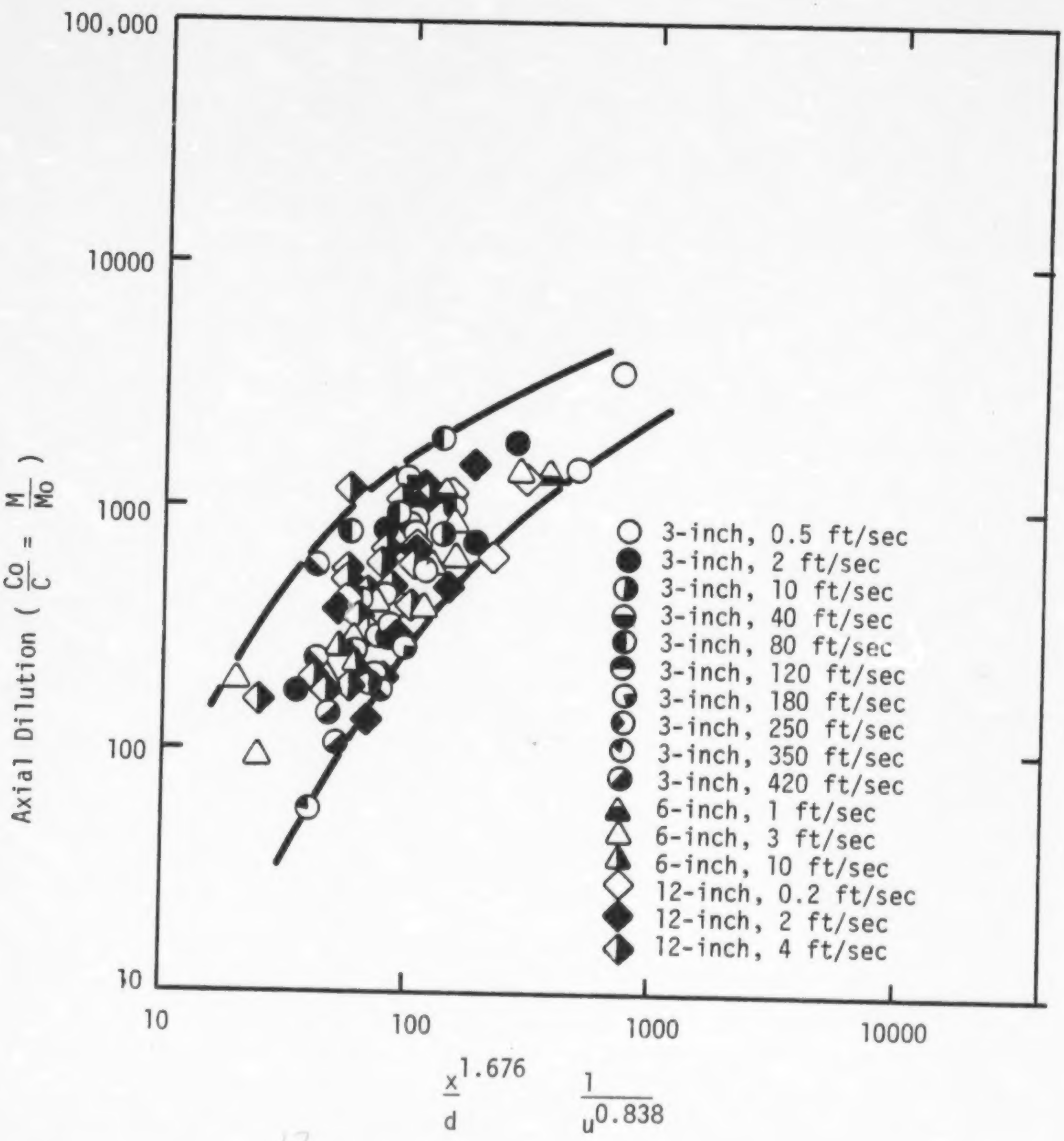

Figure 4-12. Correlation of entrainment rate for flare flames.

normally be unstable.

F4-13

The liftoff distances measured in this study are shown in Figure 4-13. A reasonable curve of liftoff distance versus velocity is defined for gases with heating values between 700- and 1400-Btu/ft^3. Gases with higher heating values have slightly smaller liftoff distances at equivalent velocities. The liftoff distances for low-Btu gases do not correlate as well. This is ascribed to the extreme sensitivity of the stable flame location for low-Btu gases to ambient perturbations.

Attempts to calculate the liftoff distances using jet theory and flame speeds were unsuccessful. Jet theory is strictly applicable to fully developed jets outside of the core region. The flare flames studied here are not developed turbulently, and the liftoff distance typically is within the core region and is difficult to characterize. Some success was achieved in estimating liftoff distances using jet theory modified to the conditions of the flames of this study. However the stability, and hence the liftoff distances of the flames, was found to be extremely sensitive to the velocity profiles and few useful results could be obtained using modified jet theory to estimate liftoff distances.

F4-14

A successful correlation of liftoff distances was, however, developed using the above principles. Figure 4-14 shows the liftoff distances measured in this study correlated with the product of the ratio of nozzle velocity to maximum flame velocity, and the ratio of concentration at the maximum flame speed to the concentration of gas in the nozzle. The correlation is very good. However, sensitivity of flames burning low-Btu gases to perturbations results in uncertainties in the measurements as it did in the calculations.

4.6 Flame Stability

The stability of the flame will influence the combustion efficiencies. Flames operating near the region of stability (as defined in Section 2) may result in incompletely burned hydrocarbons when slightly disturbed. A flame will be unstable when the vectorial jet velocity is greater than the flame velocity. The flame may adjust itself to a position where the two are equal. However, the jet velocity is reduced in flare flames by induction of air. This lowers the mixing strength of the fuel and the flame

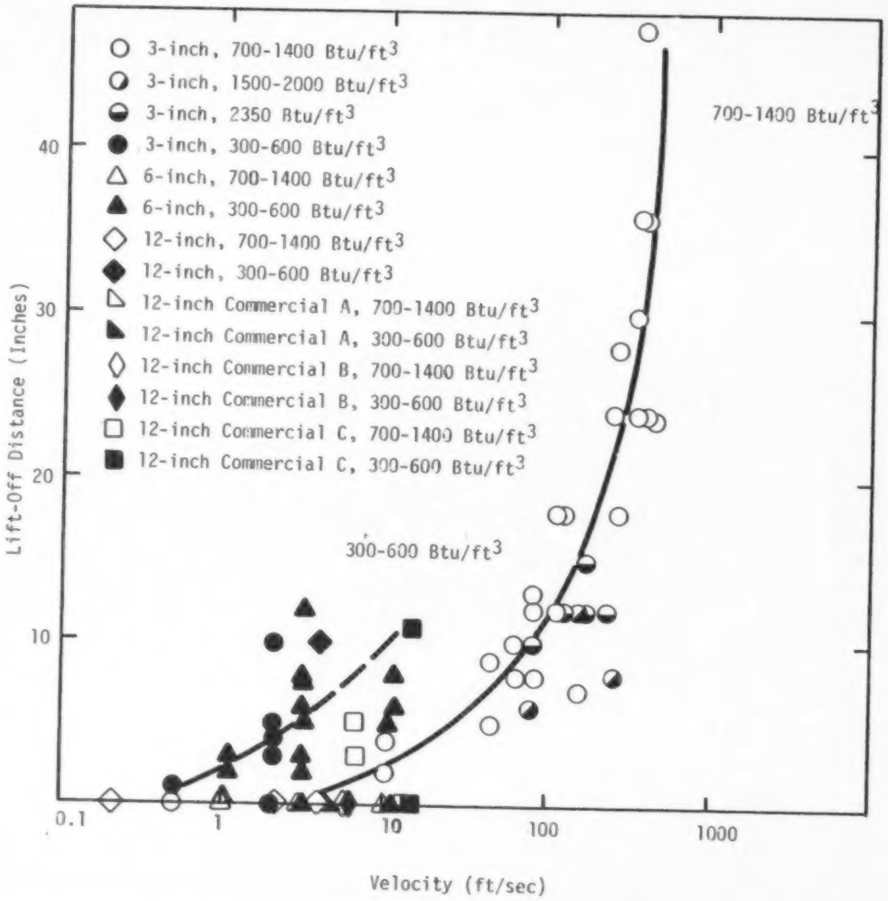

Figure 4-13. Liftoff of flare flames without pilot flames.

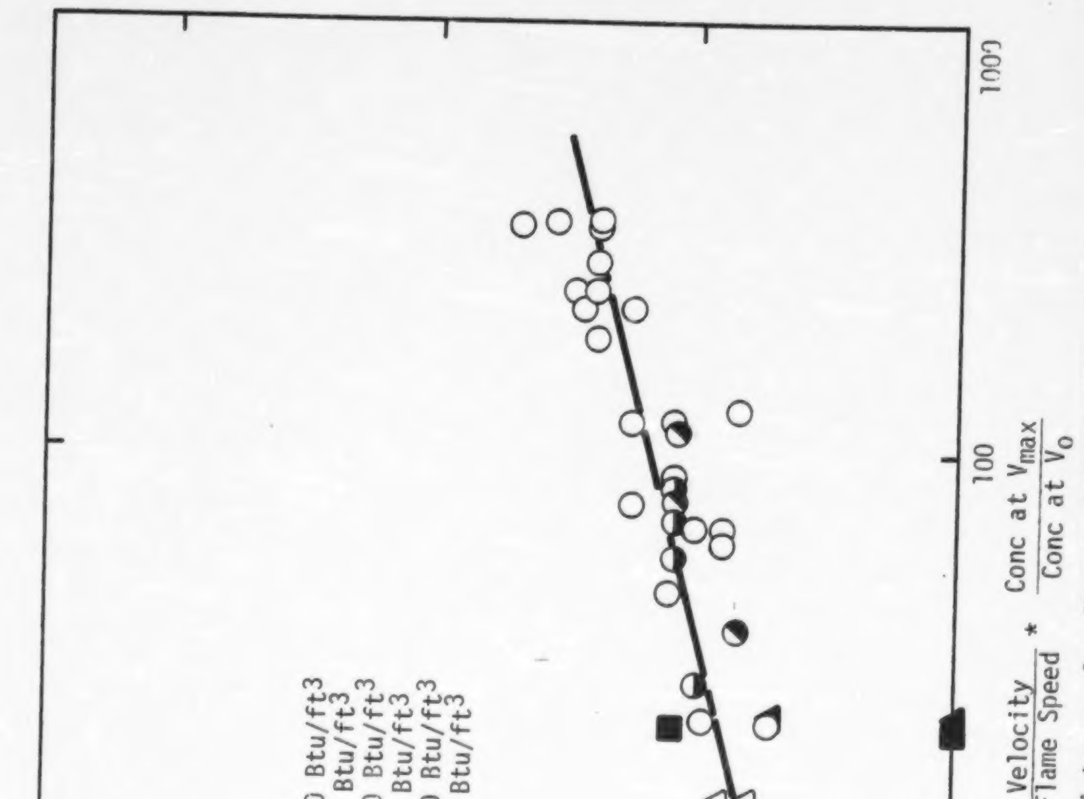

Figure 4-14. Correlation of liftoff distances for flames without pilot flames.

speed when the mixture strength is on the lean side of stoichiometry. A flame cannot be maintained under conditions where the vectorial jet velocity cannot be reduced to the flame speed before the mixture strength of the fuel is outside the limits of flammability. The result is that low-calorific gases flared at high velocities have narrow regions of stability, operate close to the limits of stability, and are subject to perturbations and may result in poor combustion efficiency.

The minimum heating value of propane-nitrogen mixtures required to maintain a stable flame with a given nozzle velocity was determined in this study. Figure 4-15 shows that at low velocities, stable flames could be obtained with gases of heating values of approximately 300 Btu/ft^3. However, high heating values of the gases were required to stabilize the flames at higher velocities.

Most of the data was obtained for flare heads without special means of stabilizing the flame. None of the flames were retained with a pilot flame. A convergent and a divergent ring were used on the 3-inch flare flames but this did not improve flame stability. Some commercial flare heads employed proprietary devices to aerodynamically stabilize the flame. These devices resulted in some differences in stability between the EER prototype flare head and the commercial flare heads.

In theory, the stability curve shown in Figure 4-14 may be generalized using other fuels by plotting the log of velocity versus a reciprocal flame temperature. Figure 4-16 shows that many normal hydrocarbons follow this relationship. This relationship assumes that the flame velocity is a function of reactions with similar Arrehenius parameters. As evidence from Figure 4-16, this is not true for compounds of widely different structures. However, Figure 4-17 shows this relationship to hold for the propane data of this study. In this plot, the flame temperature is approximated by:

$$\text{Flame Temp} = C_{p\infty} \frac{(1 + 26\ X)}{QX}$$

where $C_{p\infty}$ is the heat capacity of ambient air, X is the volume fraction of propane in the fuel, 26 is the number of moles of products for stoichiometric

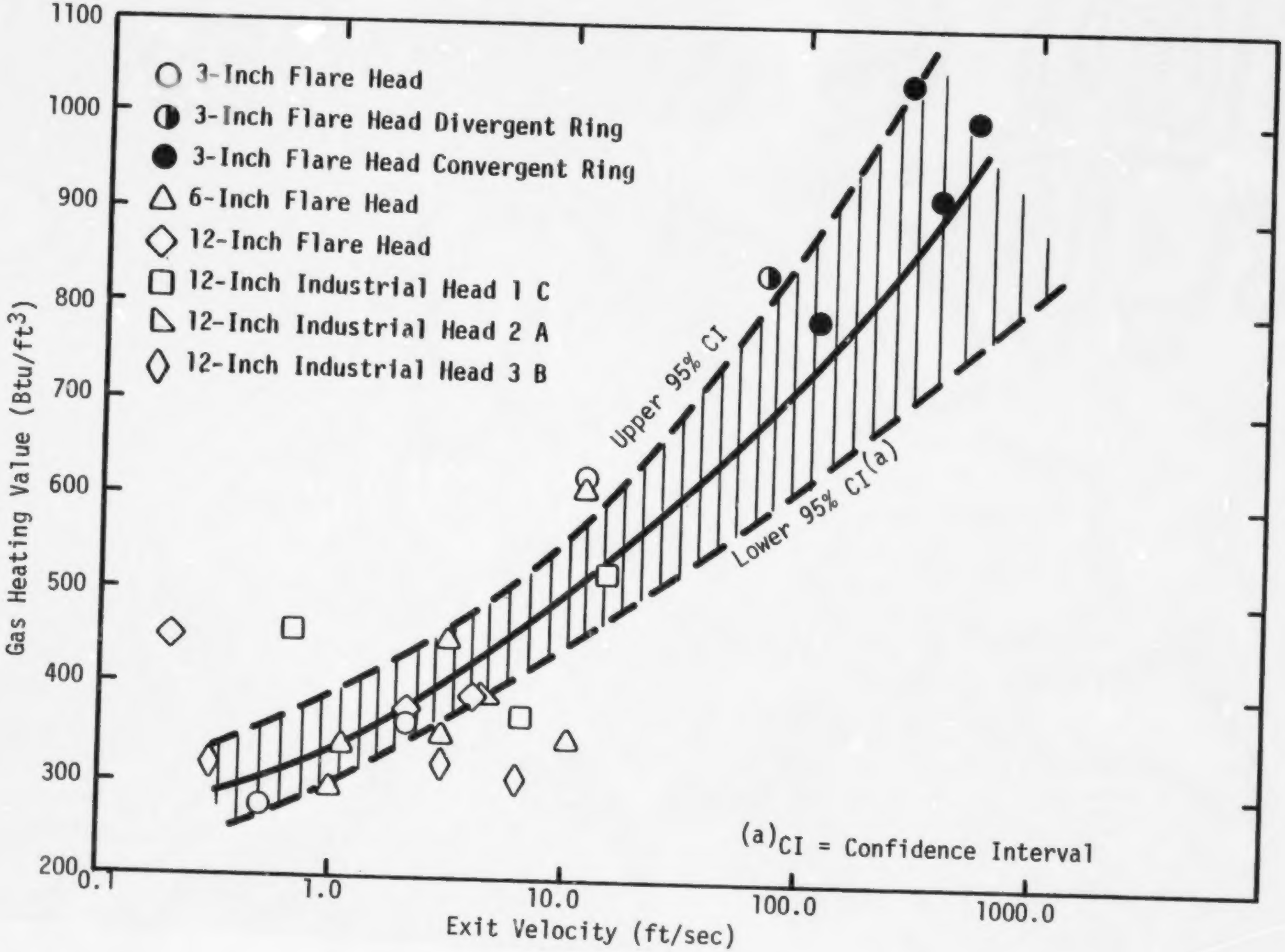

Figure 4-15. Region of flame instability.[b]

(b) Based on flares burning propane/nitrogen mixtures with no pilot flame.

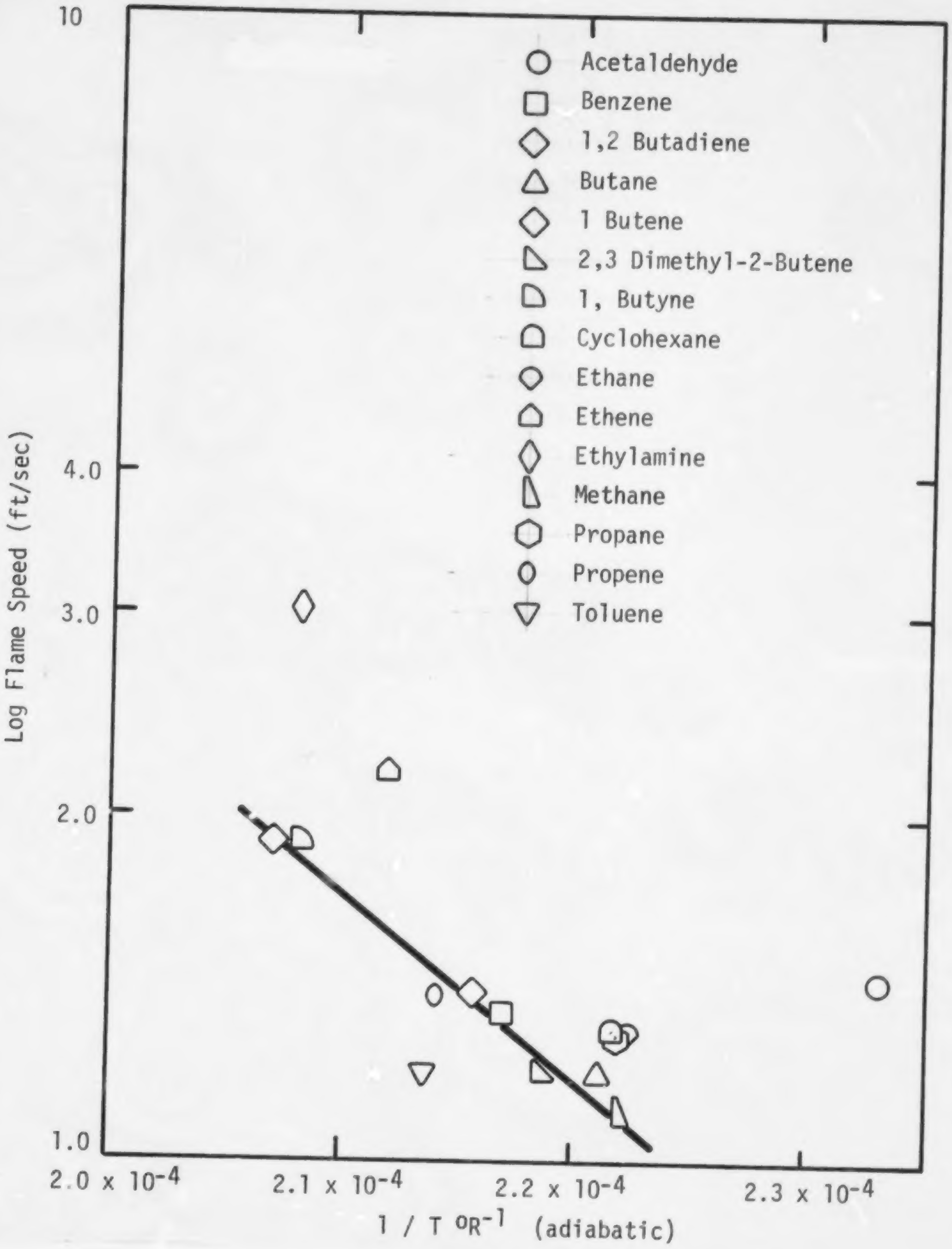

Figure 4-16. Flame speeds of hydrocarbons.

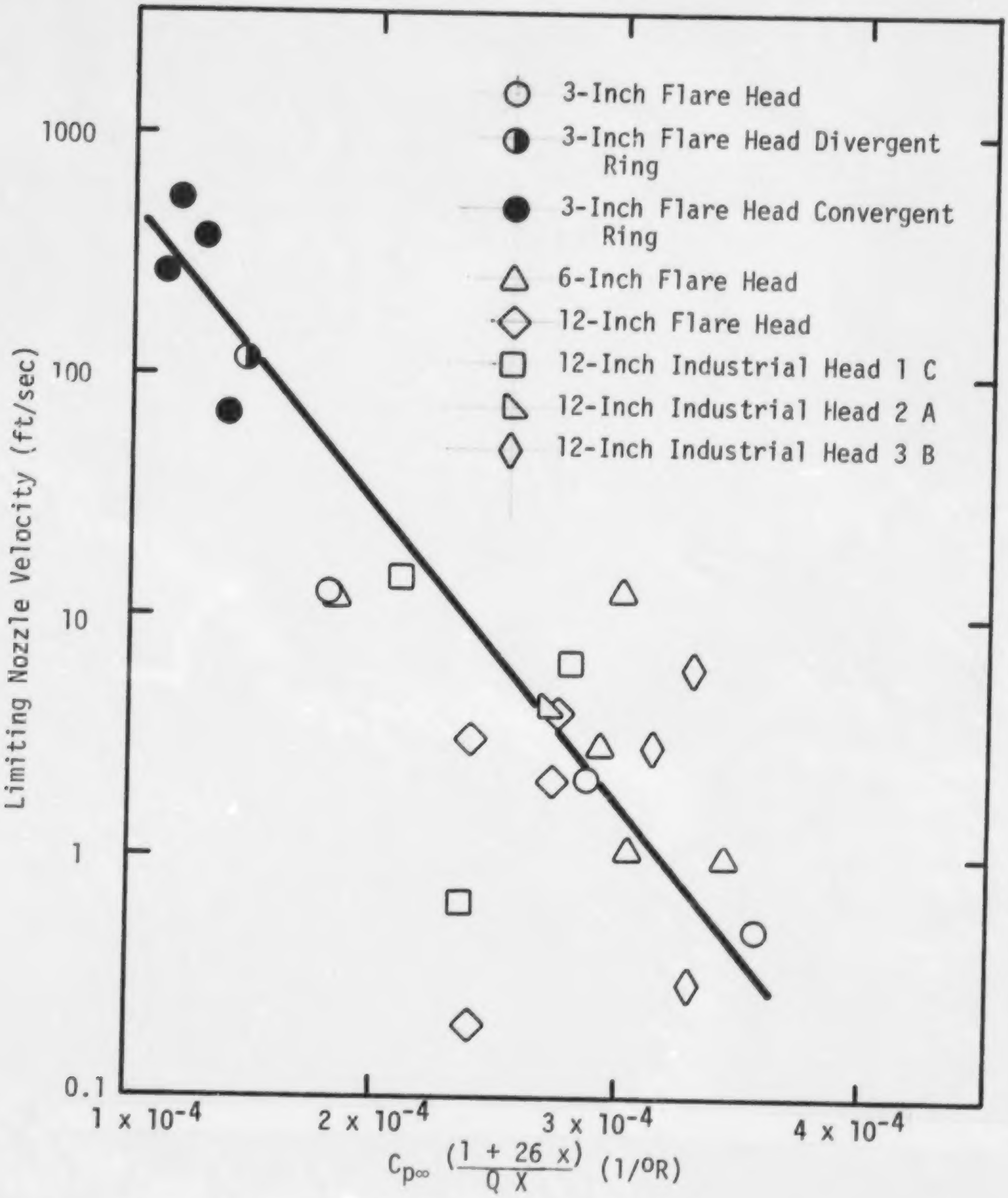

Figure 4-17. Limits of flame stability as a function of estimated temperature.

combustion of propane with air, and Q is the low heating value of pure propane.

REFERENCES

SECTION 4.0

4.1 Zukowski, E., T. Kubota and B. Cetegen, "Entrainment in Fire Plumes." *Fire Safety Journal*, Vol. 3, pp. 107-121 (1980/1981).

4.2 Hottel, H. C., and W. R. Hawthorne, "Diffusion in Laminary Flame Jets." Third Symposium on Combustion, Flame and Explosion Phenomena, pp. 254-266 (1949).

4.3 Ricou, F. P., and D. B. Spaulding, "Measurements of Entrainment Axisymmetrical Turbulent Jets." *J. Fluid Mech.*, Vol. 2, pp. 21-32 (1961).

4.4 Seebold, J. G., Private Communication, Standard Oil Company of California, San Francisco, California (1982).

4.5 Orloff, L., and J. de Ris, "Froude Modeling of Pool Fires." Nineteenth Symposium (International) on Combustion, pp. 885-895 (1982).

4.6 Shore, D., Private Communication, Flare Gas Corporation, Spring Valley, New York (1983).

4.7 Roshko, A., "Progress and Problems in Understanding Turbulent Shear Flows" in S.N.G. Monthly, ed., *Turbulent Mixing in Nonreacting and Reactive Flows*, pp. 295-311, Plenum (1975).

4.8 Broadwell, P. E., and P. E. Dimotakis. Contractor Coordination Meeting, Fundamental Combustion Research, U.S. EPA Contract No. 68-02-2631, Newport Beach, California (1980).

4.9 Marble, F. E., and J. E. Broadwell, "A Theoretical Analysis of Nitric Oxide Production in a Methane-Air Turbulent Diffusion Flame." EPA Contract No. 68-02-2613, April 1979.

4.10 Becker, H. A., and D. Liang, "Visible Length of Vertical-Free Turbulent Diffusion Flames." *Combustion and Flame*, Vol. 32, pp. 215-237 (1978).

4.11 Brzustowski, T. A., "Flaring in the Energy Industry." *Progress in Energy and Combustion Science*, Vol. 2, pp. 129-161 (1976).

5.0 COMBUSTION EFFICIENCIES IN FLARES

The main objective of this study was to develop methods to characterize the combustion efficiency of commercial flares. This section reports the characteristics and combustion efficiency of the flames of this investigation, compares the results of this study with those of other studies, and correlates the combustion efficiency with operating parameters of the flare. This section reports the results of tests which developed techniques to scale the emission of incompletely burned hydrocarbons from flare flames, tests of commercial flare heads, tests of flares at high exit velocities, and tests on the influence of steam injection on the emission of incompletely burned hydrocarbon from flare flames.

5.1 Study Conditions

Appendix C provides a complete list of all tests conducted. Tables 2-1 through 2-7 summarize these conditions and eliminate duplicate conditions, samples withdrawn from the same flare and the rake probe at different positions, and samples taken within the flame. Conditions studied include:

- Flare Head
  - 3-inch EER prototype
  - 6-inch EER prototype
  - 12-inch EER prototype
  - 3-inch EER prototype with convergent ring
  - 3-inch EER prototype with divergent ring
  - 12-inch commercial; 3 manufacturers
- Gases
  - Mostly propane diluted with nitrogen
  - One data point using methane
- Gas Heating Value from 286 - 2350 Btu/ft^3
- Gas Exit Velocity from 0.2 to 428 ft/sec
- Steam Injection from 0 to 1.0 lb steam/lb fuel

The combustion efficiencies of these trials are reported in the following sections.

5.2 Comparison with Other Studies

This study set out to remove some of the uncertainty of previous studies. The major uncertainties were:

- Ability to close a mass balance;
- Measurement of soot concentration;
- Assumption that the local combustion efficiency measured at one point is representative of the global combustion efficiency;
- Development of a scaling methodology.

Mass Balance

This study was able to close a mass balance using both the hood and SO_2 as a tracer (see Section 3). The results indicate that flare combustion efficiencies can usually be determined without strict closure of a mass balance. This implies that material which is lost form the sampling region is negligible or of similar composition to that in the sampling regime. Therefore, the inability to close a mass balance does not preclude use of the data from previous studies.

Soot Concentration

Most previous studies failed to measure the concentration of carbon as soot for a large number of samples. The combustion efficiency measured in such studies would be higher by the amount of unmeasured soot which escapes the flame. Data from this study (see Appendix D) indicate that soot rarely accounts for more than 0.5 percent of combustion inefficiency and can be completely eliminated by injection of steam. Measurement of the soot concentration is usually unimportant for the determination of combustion efficiency.

Axial Combustion Efficiency

Measurements of local combustion efficiency at a single axial position may not be representative of the combustion efficiency of flares as discussed in section 3.3. Graphs of dilution factors at various distances from the plume center line (see Appendix F) show that velocity profiles must be combined with concentration profiles and integrated across the flame to obtain overall combustion efficiencies. Thus, the single probe technique for estimating combustion efficiencies may not be as accurate as the multiple probe technique used the study.

Scaling Methodology

Scaling methodologies were developed for all the important characteristics of flare flames in this study. Volumetric combustion was found to be a constant, 90,000 Btu/ft^3-hr, for the flames of this study. However, the nozzle size and operating conditions were required to scale the following characteristics of flame structure:

- Flame Length
- Flame Lift-off
- Flame Dilution

The limits of flame stability could be correlated with the properties of the gases irrespective of size of the flare head. These correlations are discussed in detail in Section 4.0.

The combustion efficiency could also be correlated using only the properties of the gases for the flares of this study. However, the combustion efficiency is correlated with the stability limit of the flame which could be changed by addition of proprietary stabilizers and pilot lights or different gases.

5.3 Correlations

The goal of the correlations was to determine if the test data was scalable over the range of variables examined. The combustion efficiency of the large pilot-scale and commercial flare flames was found to be independent of the diameter of the flare head within the size range tested.

The combustion efficiencies estimated in this study did depend on the exit velocity and the heating value of the gas. The velocities studied were in the range of velocities for commercial flare heads. However, only mixtures of propane and nitrogen were tested. The results may be different for other gases, but are expected to correlate with the same parameters as propane.

F5-1

Figure 5-1 shows the conditions (dark symbols) which resulted in combustion efficiencies lower than 98 percent. The line is a least-square fit to the stability curve of Figures 2-2 and 4-15. Most of the conditions which result in combustion efficiencies less than 98 percent are below the region

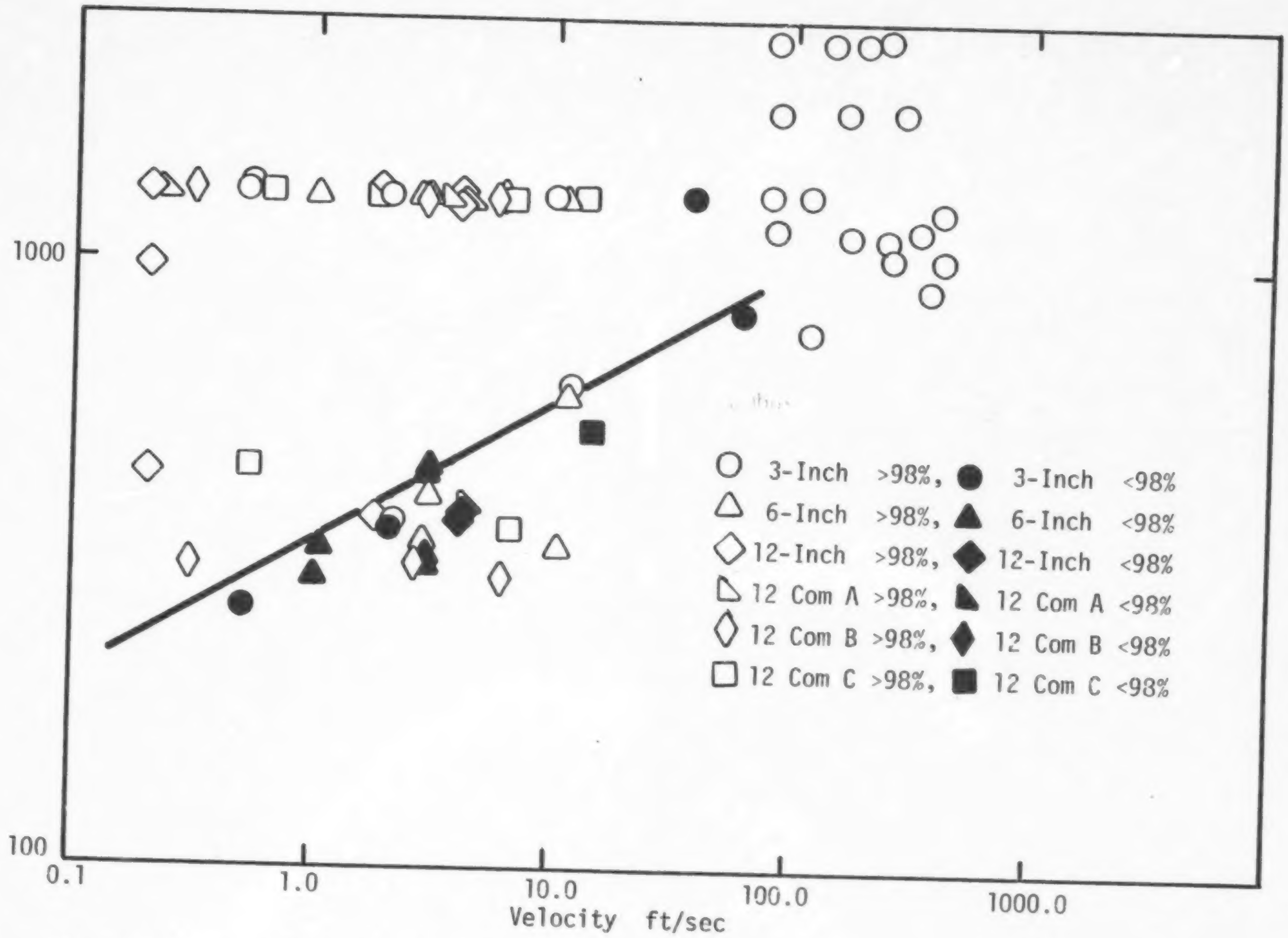

Figure 5-1. Conditions to Obtain 98-Percent Combustion Efficiency for Mixtures of Propane and Nitrogen.[a]

[a] No pilot flame.

of stability. Some flames at similar conditions resulted in combustion efficiency greater than 98 percent. However, all these conditions are near the limits of flame stability. At these conditions, slight perturbations will cause a flame operating with high combustion efficiency to become unstable with a resultant decrease in combustion efficiency.

The influence of flame stability is more clearly shown when the graph is plotted in dimensionless form. Figure 5-2 shows the plot of combustion efficiency versus the ratio of the heating value of the flame to the minimum heating value necessary to sustain a flame at that velocity. The heating values at the stability limit were determined from the lower region of stability shown in Figure 4-15. Some flares operating below the minimum heating value required to maintain a flame have high combustion efficiencies. However, all conditions which caused low combustion efficiency were firing gases within 10 percent of the minmum heating value required for a stable flame. Only one flame firing a gas with a ratio greater than 10 percent above the value required for a stable flame resulted in low-combustion efficiency; the reason for this is unknown, and the data point is considered an anomoly. Those flares firing gases with heating values near the stability limits are susceptible to perturbations and poor combustion efficiency.

These results are limited to the conditions and gas mixtures of this study. However, the form of the correlation is expected to be generally valid for many gases and for flare heads which rely on external mixing. Future studies evaluating the effects of other gases and the influence of pilot flames and aerodynamic devices on flame stability will provide additional information.

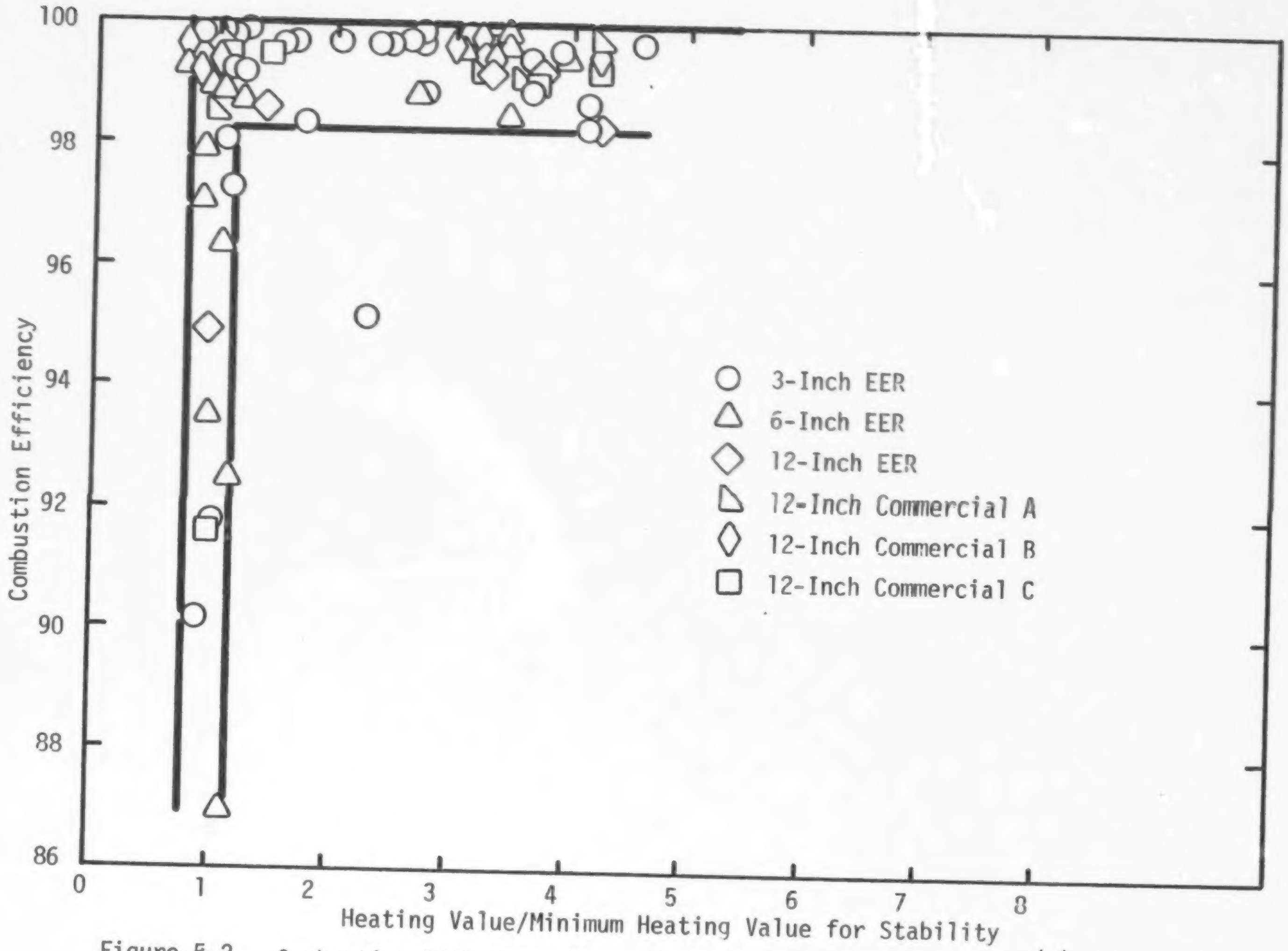

Figure 5-2. Combustion Efficiency Near the Limits of Flame Stability.(a)

(a) Based on flares burning propane/nitrogen mixtures with no pilot flame.

5.4 Commercial Flare Heads

Three commercial flare heads were loaned to the program by manufacturers and tested. The manufacturers were requested to supply a standard 12-inch flare head as described in Section 3.0. The geometry of the heads differed and all velocities reported here are based on the open area of the head.

The flare heads showed small differences in combustion efficiency when burning 56 percent propane. Tables 2-5, 2-6, and 2-7 show combustion efficiencies for the different heads ranging from 98.3 to 99.7 percent.

When burning the minimum heating value gas required to sustain a flame, larger differences in combustion efficiencies were observed. (See "Low Btu Tests" on Tables 2-4 through 2-7.) At low velocities the performance of the heads was similar. However, the performance of the EER prototype head, which had no flame retention device, and flame head C, were poorer at higher velocities.

5.5 High Velocity

Tests were conducted to determine the influence of high velocity on the combustion efficiency of flare flames. Propane-nitrogen mixtures were burned on the 3-inch flare head at velocities up to 428 ft/sec. All the flames in these tests were lifted. Results are shown in Figure 5-1. Only two conditions at intermediate velocity resulted in a low combustion efficiency. The combustion efficiency at all other conditions was greater than 99 percent. From this we concluded that, provided the heating value of the gas is not close to the minimum value to maintain a flame, high velocities may slightly improve the combustion efficiency of flare flames.

5.6 Steam

The influence of steam injection on cumbustion efficiency was also determined during these trials. Figure 5-3 shows that steam injected into the flares of this study had effects similar to those expected in commercial practice. That is, steam completely suppressed soot. However, steam injection at normal rates had a minor influence on overall combustion efficiency because the amount of soot is small. Optimum levels of steam injection for combustion efficiency were found to be 0.3 to 0.5 lb steam/lb fuel suppressed the soot, but reduced the overall combustion efficiency by quenching combustion of CO and hydrocarbons.

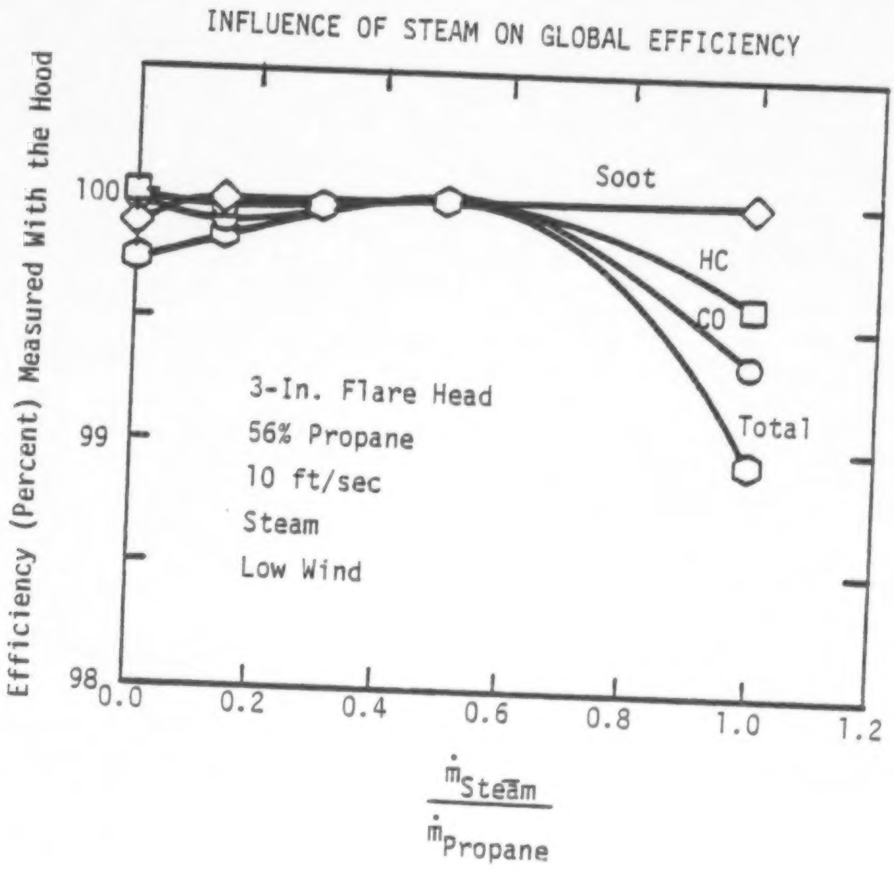

Figure 5-3. Influence of Steam on Combustion Efficiency.

APPENDIX A

EPA FLARE TEST FACILITY AT EER

ABSTRACT

The design of the Environmental Protection Agency's (EPA) Flare Test Facility (FTF) at Energy and Environmental Research Corporation is described. The criteria for the design, construction, calibration and operation of the FTF are reported. Details of construction and operation are given of the:

- Test Site
- Fuel System
- Tracer System
- Steam System
- Flare Head
- Sampling System
- Visual Monitors
- Ambient Monitors
- Support Structure
- Data Recording

The FTF is used in EPA programs to determine the combustion efficiency of flares, and is available by arrangement for testing of design, construction, operation and use of commercial flare heads.

TABLE OF CONTENTS

Section Page

1.0 OVERVIEW

1.1 Objective . . . . .A 1-1
1.2 Design Guidelines . . . . .A 1-1

2.0 FACILITY SITE . . . . .A 2-1

2.1 Topography . . . . .A 2-1
2.2 Facility Layout . . . . .A 2-1
2.3 Control Room . . . . .A 2-1
2.4 Utilities . . . . .A 2-5

3.0 FUEL SYSTEM . . . . .A 3-1

3.1 Fuel Supply . . . . .A 3-1
3.2 Flow Control Metering . . . . .A 3-1
3.3 Specification Performance . . . . .A 3-4

4.0 TRACER SYSTEM . . . . .A 4-1

4.1 Tracer Supply . . . . .A 4-1
4.2 Tracer Flow Control Metering . . . . .A 4-1

5.0 STEAM SYSTEM . . . . .A 5-1

5.1 Steam Supply . . . . .A 5-1
5.2 Flow Control and Metering . . . . .A 5-1
5.3 Performance . . . . .A 5-4

6.0 DESIGN OF FLARE HEADS . . . . .A 6-1

6.1 Flare Head Support Base . . . . .A 6-1
6.2 Flare Tip . . . . .A 6-1
6.3 Steam Ring and Nozzles . . . . .A 6-1
6.4 Pilot . . . . .A 6-5
6.5 Flame Arrestor . . . . .A 6-5
6.6 Flame Retention Ring .A 6-6

Section Page

7.0 EXTRACTIVE SAMPLE SYSTEM . . . . A 7-1

- 7.1 Sample Points . . . . A 7-1
- 7.2 Hood Design . . . . A 7-1
- 7.3 Multiple Point Sampling . . . . A 7-3
- 7.4 Sampling Conditioning . . . . A 7-5
- 7.5 Analysis . . . . A 7-8

8.0 VISUAL MONITORS . . . . A 8-1

- 8.1 Video System . . . . A 8-1
- 8.2 Photography . . . . A 8-1
- 8.3 High-Speed Cinematography . . . . A 8-1

9.0 AMBIENT MONITORS AND CONTROLS . . . . A 9-1

- 9.1 Wind Screens . . . . A 9-1
- 9.2 Monitors . . . . A 9-1

10.0 SUPPORT STRUCTURE . . . . A 10-1

- 10.1 Overall Structures . . . . A 10-1
- 10.2 Hood Support . . . . A 10-1
- 10.3 Rake Probe Support . . . . A 10-1
- 10.4 Windscreen Support . . . . A 10-1

11.0 DATA RECORDING SYSTEMS . . . . A 11-1

- 11.1 Data System . . . . A 11-1
- 11.2 Strip Recorder . . . . A 11-1

12.0 ORIFICE CALIBRATION . . . . A 12-1

FIGURES

Figure		Page
1-1	EPA flare test facility at EER	A1-2
2-1	Terrain around flare test facility	A2-2
2-2	Flare test facility site plan	A2-3
2-3	Flare test control room	A2-4
3-1	Fuel flow control and metering system schematic	A3-2
4-1	SO_2 vaporizer	A4-2
4-2	SO_2 flow control and metering system schematic	A4-3
5-1	Steam flow control and metering system schematic	A5-2
5-2	Calibration of steam flow	A5-5
5-3	Calibration of steam flow	A5-6
5-4	Calibration of steam flow	A5-7
5-5	Calibration of steam flow	A5-8
6-1	Flare head support structure	A6-2
6-2	Flare head design	A6-3
7-1	Sampling hood assembly	A7-2
7-2	Filter probe design	A7-4
7-3	Hood and probe rake positioning mechanism	A7-6
7-4	Flare sample system	A7-7
8-1	Camera platform	A8-2
9-1	Perforated plate windscreen	A9-2
10-1	Support structure for sampling hood and rake probes	A10-2

TABLES

Table		Page
3-1	Pilot-scale flare test conditions	A3-3
3-2	Fuel system components	A3-5
4-1	Tracer flow system component specification	A4-4
5-1	Steam metering system components	A5-3
6-1	Flare head specifications	A6-4
7-1	Analytical methods and accuracies	A7-9
A-1	Calibration constants of laminar flowmeters	A12-2
A-2	Orifice flowmeters calibration constants	A12-4

1.0 OVERVIEW

A test facility (Figure 1-1) has been designed and constructed at Energy and Environmental Research Corporation (EER) to test large pilot-scale flares under U.S. EPA Contract 68-02-3661. This report describes the following:

- Facility site
- Flare gas delivery system
- Tracer delivery system
- Steam delivery system
- Design of the flare heads
- Extractive sampling systems
- Visual monitors
- Ambient monitors and controls
- Support structures
- Data recording systems

1.1 Objective

The pilot-scale facility has been designed to determine the combustion efficiency of small flares. In particular, the facility is designed to answer the following questions:

- What are the combustion efficiencies of pilot and small commercial flares?
- How are these efficiencies influenced by operating parameters, flare design, fuel composition and size?
- What mechanisms control these influences?

1.2 Design Guidelines

The criteria for designing the pilot-scale facility were established by consultation with the Technical Advisory Panel, composed of flare

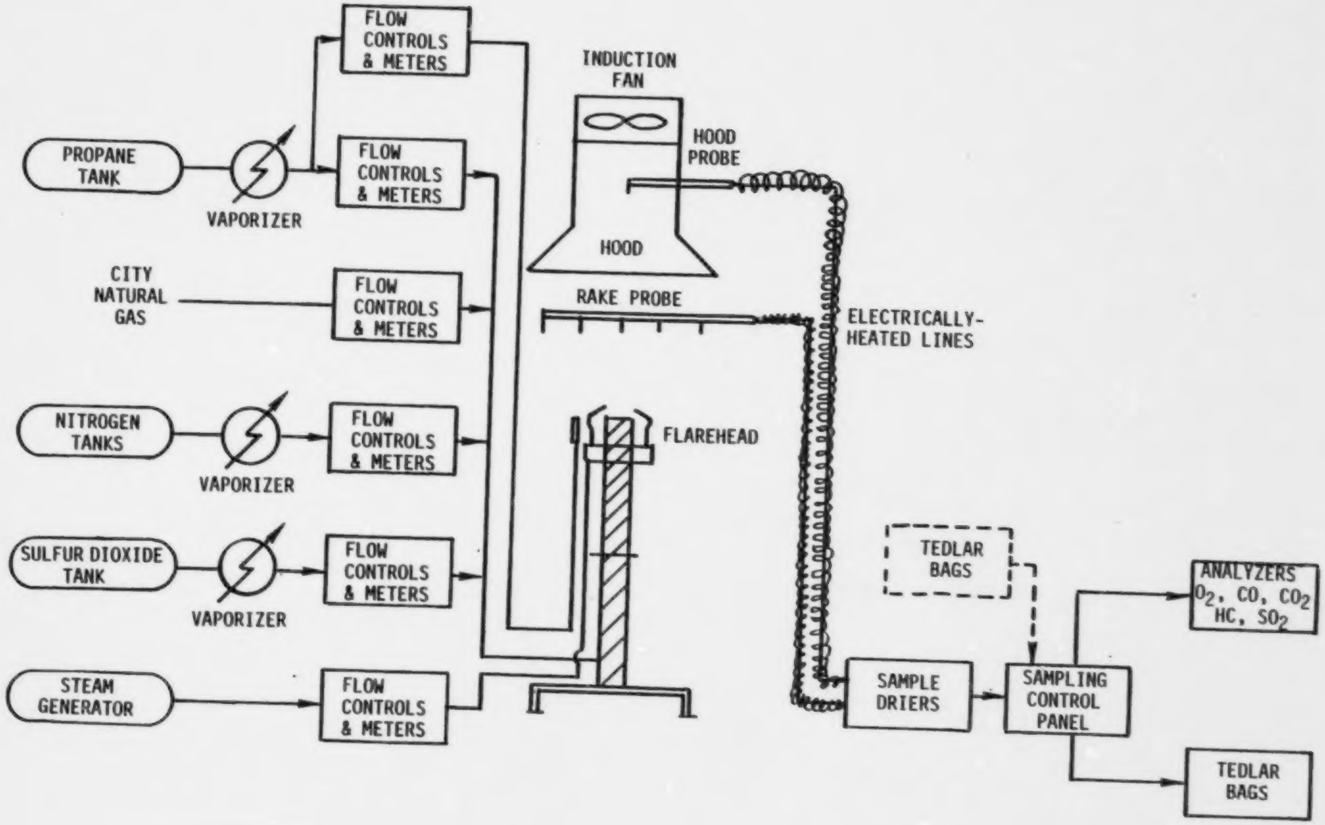
FLOW CONTROLS & METERS
INDUCTION FAN
PROPANE TANK
VAPORIZER
FLOW CONTROLS & METERS
HOOD PROBE
HOOD
CITY NATURAL GAS
FLOW CONTROLS & METERS
RAKE PROBE
ELECTRICALLY-HEATED LINES
NITROGEN TANKS
VAPORIZER
FLOW CONTROLS & METERS
FLAREHEAD
SULFUR DIOXIDE TANK
VAPORIZER
FLOW CONTROLS & METERS
TEDLAR BAGS
ANALYZERS O_2, CO, CO_2 HC, SO_2
STEAM GENERATOR
FLOW CONTROLS & METERS
SAMPLE DRIERS
SAMPLING CONTROL PANEL
TEDLAR BAGS

Figure 1-1. EPA flare test facility at EER.

NP

manufacturers and users, and are summarized in EPA Report No. 600/2-83-070.

- Flare head size - 3, 6, and 12 inches in diameter
- Fuel gas - Propane is the base fuel. Nitrogen is used to dilute the fuel to the appropriate heating value.
- Gas velocity - Maximum of 10 ft/sec for all sizes.(1)
  Minimum of about 0.5 ft/sec.
- Steam rates - Maximum of 1 lb steam/lb of fuel.
- Wind condition - Natural calm condition (< 5 mph)

The flames from this facility are characterized for structure and emissions of incompletely burned hydrocarbons.

Visual Characterization

Visual characterization is used to establish flame form and structure and to identify sources of emissions and means of scaling the phenomena which results in incomplete combustion. Visual characterization consists of still photographs and high-speed movies.

Still photography is used to record the average and instantaneous geometry and structure of the flare flames. The fluctuating nature of flare flames requires that the average flame structure be recorded on film using long exposure times and that the instantaneous structure of the flame be recorded on film using exposure times on the order of one millisecond. The results will establish maximum, minimum and average flame geometry and provide limited information of flame structure.

High-speed movies are used to record the evolution of the flame structure. Tests have shown that a speed of 200 frames/second can satisfactorily record the evolution of turbulent luminous pockets in the flames. The high-speed movies are used to evaluate the generation, size and history of these luminous structures.

---

(1) This design criterion was subsequently changed to provide for exit velocities in excess of 400 ft/sec.

Concentration Measurements

The efficiency of flares is determined from gas concentrations of samples collected in a hood or probes at several points above the flame. Species concentrations of O_2, CO, CO_2, soot and SO_2 are obtained using both techniques. Compositions obtained from flares operated at different conditions are used to establish the combustion efficiency.

2.0 FACILITY SITE

The site for the flare test facility was selected to provide:

- predictable wind conditions;
- low background levels of SO_2, CO, CO_2, soot and hydrocarbons;
- isolation from heat-sensitive equipment.

The flare test facility was built in a canyon which provides suitable topography; room for facility layout, including the control room, and access to necessary utilities.

2.1 Topography

The topography of the test site can minimize the difficult problem of isolating the flare from the ambient conditions. Figure 2-1 shows the terrain around the test site. The canyon wall is about 70 feet high and surrounds the flare facility on three sides. Wind blows predominantly along the direction of the canyon. The flare facility is on a flat clearing about 200 feet long and 100 feet wide.

2.2 Facility Layout

Figure 2-2 shows the plan of the facility site. A chain-link fence topped with barbed wire surrounds the area to prevent unauthorized entry. Access to the test site is through an eleven-foot wide swing gate. The major installations include the control room, the hood and sampling support structure, the steam boiler, fuel tanks and vaporizer, the liquid nitrogen supply and vaporizer, the flow controls and the flowmeters.

2.3 Control Room

The control room is directly opposite and provides view and access to the flare head. It houses the gas flow control panels, the electric control panels, the sample flow control panels, the gas analyzers, and data recording equipment. Figure 2-3 shows the arrangement of the control room. A window provides a complete view of the flare head, sample hood, and probes. Gas flow rates and electrical power are controlled inside and can be turned off rapidly during emergencies.

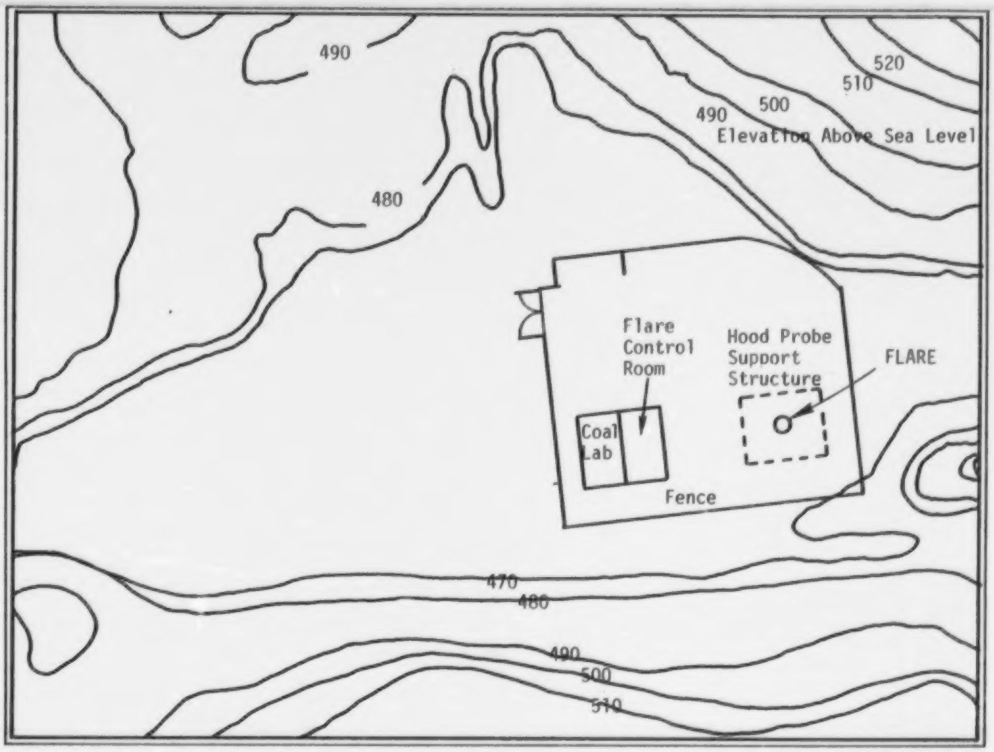
490
520
510
500
490
Elevation Above Sea Level
480
Flare Control Room
Hood Probe Support Structure
FLARE
Coal Lab
Fence
470
480
490
500
510

Figure 2-1. Terrain around flare test facility.

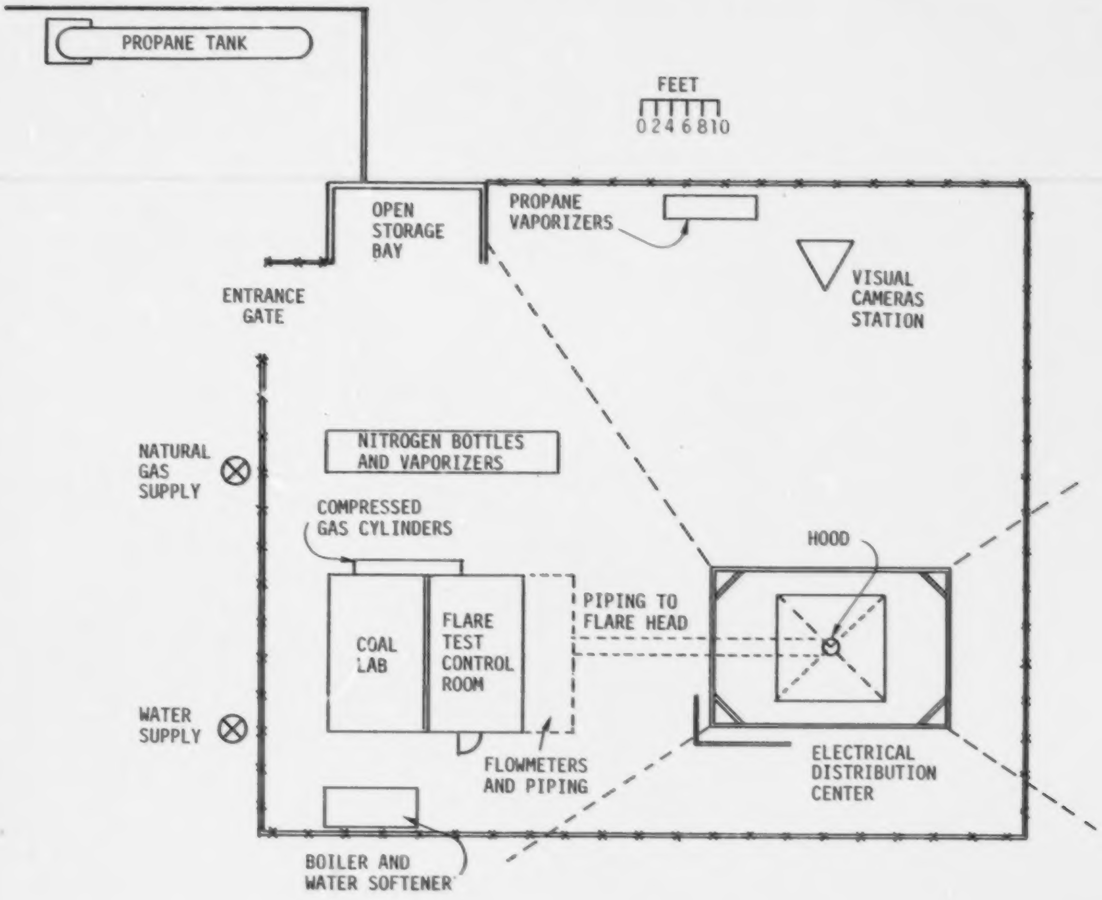
PROPANE TANK
FEET
0 2 4 6 8 10
OPEN STORAGE BAY
PROPANE VAPORIZERS
VISUAL CAMERAS STATION
ENTRANCE GATE
NATURAL GAS SUPPLY
NITROGEN BOTTLES AND VAPORIZERS
COMPRESSED GAS CYLINDERS
HOOD
COAL LAB
FLARE TEST CONTROL ROOM
PIPING TO FLARE HEAD
WATER SUPPLY
FLOWMETERS AND PIPING
ELECTRICAL DISTRIBUTION CENTER
BOILER AND WATER SOFTENER

Figure 2-2. Flare test facility site plan.

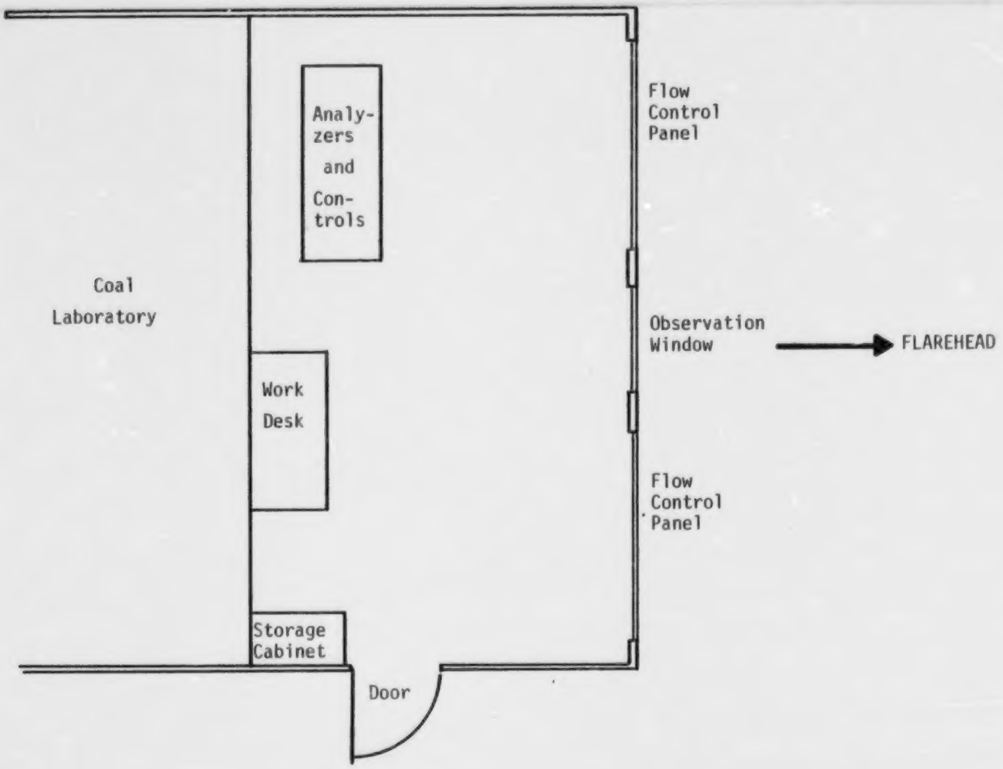
Analy-
zers
and
Con-
trols
Flow
Control
Panel
Coal
Laboratory
Observation
Window
FLAREHEAD
Work
Desk
Flow
Control
Panel
Storage
Cabinet
Door

Figure 2-3. Flare test control room.

2.4 Utilities

Water, compressed air, natural gas, and electricity are available at the test site. Water is supplied through a 6 in. pipe at 70 psig. Natural gas is supplied at 15 psig through a 2 in. pipe. Compressed air is supplied by a shop compressor at 100 psig through a 1 in. pipe. Electricity is delivered to the test site at 440 V three-phase and 110 V and 220 V are obtained through a transformer. The available electrical capacity is 300 KVA.

3.0 FUEL SYSTEM

The fuel system includes the supply and flow control and metering equipment for the fuel and diluent gases. The experiments reported herein used propane and natural gas as fuels. These gases have H/C ratios of 2.67 and 4, and heating values of 2450 and 985 Btu/ft^3, respectively. Nitrogen was used to dilute the fuel gases to the desired heating values. All gases were metered to control the gas exit velocity at the flare head. Figure 3-1 illustrates the control system for the fuel system.

3.1 Fuel Supply

Table 3-1 lists the planned experimental conditions and the flow requirements. The total flow rates range from 11 to more than 28,000 cu ft/hr. Propane is stored as a liquid in a 2100 gallon tank. Natural vaporization of the liquid provides sufficient propane gas for low-flow experiments. At high demand rates, three propane-fired vaporizers, each capable of 2900 cu ft/hr supply the needed gas. The tank will last about 11 hours at the highest flow rate anticipated.

Natural gas is supplied at 15 psig from the gas utility company through a 2 in. pipe. The capacity is expected to be about 7000 cu ft/hr which is sufficient for testing the 6-inch flare at 10 ft/sec and the 12-inch flare at slightly more than 2 ft/sec.

Nitrogen is used to dilute the fuel gases to the desired heat content. A manifold accepts the liquid nitrogen from twelve 3500 scf bottles of gas. Three atmospheric convective vaporizers (Cosmodyne Model SV-2x4) each capable of vaporizing 3000 cu ft/hr supply the gaseous nitrogen.

3.2 Flow Control Metering

The very wide range of flow rates (2570:1) cannot be controlled and measured by a single valve and flowmeter. Valves and flowmeters typically have maximum usable ranges of less than 10:1. Hence, parallel systems with four valves and flowmeters are used to control the propane, methane, and nitrogen flow rates.

Figure 3-1 shows the common design of the flow systems. The gas supply pressure is regulated to less than 45 psig by an air-loaded pressure reducing

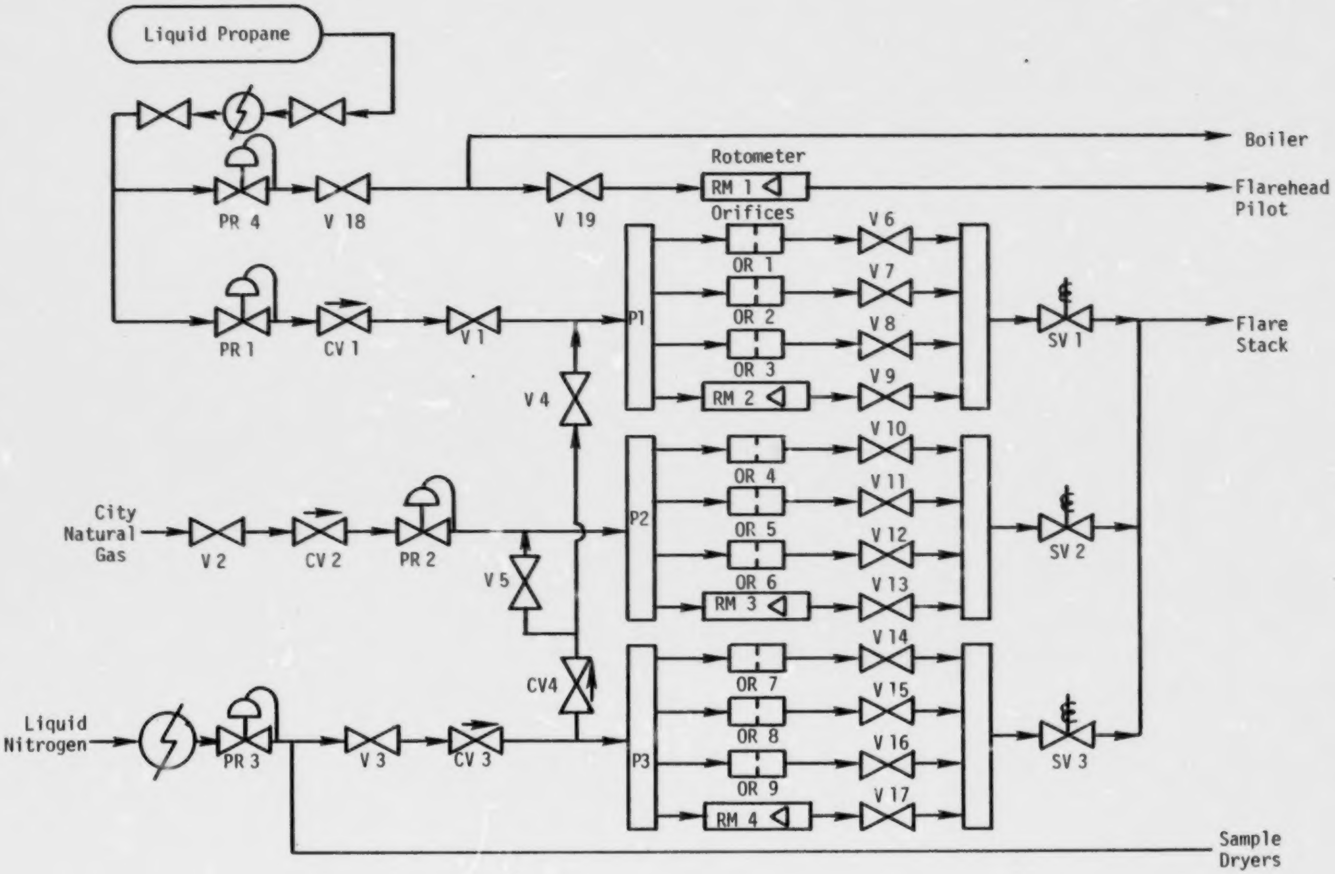
Liquid Propane
Boiler
Rotometer
RM 1
Flarehead
Pilot
PR 4
V 18
V 19
Orifices
V 6
OR 1
V 7
PR 1
CV 1
V 1
P1
OR 2
V 8
Flare
Stack
SV 1
OR 3
V 9
RM 2
V 4
V 10
OR 4
V 11
City
Natural
Gas
V 2
CV 2
PR 2
P2
OR 5
V 12
SV 2
V 5
OR 6
V 13
RM 3
V 14
CV4
OR 7
V 15
Liquid
Nitrogen
PR 3
V 3
CV 3
P3
OR 8
V 16
SV 3
OR 9
V 17
RM 4
Sample
Dryers

Figure 3-1. Fuel flow control and metering system schematic.

TABLE 3-1. PILOT-SCALE FLARE TEST CONDITIONS*

Dia. In.	Case	Velocity (ft/sec)	Flow Rate (CFH)	$\tau = \frac{do}{Vo}$ (msec)	Reynolds Number (d)	$g \frac{d}{uo^2}$ Richardson Number	Propane Flow Rate (lb/hr)(a)	Propane Cost ($/hr)	Methane Flow Rate (lb/hr)(b)	Methane Cost ($/hr)	Nitrogen Flow Rate (lb/hr)(c)	Nitrogen Cost ($/hr)
3.0	1	0.5	88	500	334	32.20	5.6	1.0	3.64	0.6	5.5	1.13
	2	2.0	353	125	1337	2.013	23	4.1	14.6	2.4	22.1	4.63
	3	10.0	1767	25	6687	0.081	113	20.0	73.0	12.0	110.6	23.22
6.0	4	1.0	707	500	1337	16.1	45	8.0	29.2	4.8	44.3	9.3
	5	2.83	2000	177	3785	2.013	128	22.6	82.6	13.5	125.2	26.2
	6	10.0	7069	50	13373	0.161	451	79.8	292.1	47.9	442.4	92.8
12.0	7	0.2	566	5000	535	805	36	6.4	23.4	3.9	35.4	7.4
	8	2.0	5655	500	5349	8.05	361	63.8	233.7	38.8	354	74.2
	9	4.0	11310	250	10699	2.013	722	127.7	467.7	76.6	708	148.5

(a) Propane diluted to 1350 Btu/ft^3 (56 volume %)
(b) Methane fired without dilution
(c) Nitrogen used to dilute propane to 300 Btu/ft^3 (87.5 volume %)
(d) Reynolds number based on 56% propane, 44% nitrogen mixture

* Based on original test matrix; see section 4-1 for additional test conditions.

valve which is remotely activated at the control panel. The flow rate is controlled by manually adjusting one of four valves and is measured with one of four calibrated square-edge orifice plates. The differential pressure signal increases with the flow rate and is indicated with a Dwyer Manometer (Model 422-23). The metered gases are combined in a header which is plumbed to the flare stack.

3.3 Specification, Performance

T3-2

Table 3-2 lists the valves and orifice bore sizes for the three gases. The orifice plates have been calibrated using air as the flow medium and referenced to one of two Meriam laminar flowmeters. The calibration arrangement and procedure is described at the end of this Appendix. The applicability of the air-calibrations to propane, methane and nitrogen was verified using the smallest bore orifice plates and a liquid displacement technique.

The calibration data indicate that the flow rates can be calculated according to the following general equation:

$$q = 932.22 \times K \times \frac{1}{\sqrt{MW}} \times \sqrt{h_{H_2O}} \times \sqrt{\frac{P + 14.7}{T + 460}}$$

where

q is flow rate, SCFM

K is orifice flow factor derived from calibration data

MW is molecular weight of gas

h_{H_2O} is pressure drop, feet of water column

P is pressure upstream of orifice, psig

T is temperature upstream of orifice, °F

The calculated flow rated agreed to within 3 percent of the calibrated flow rates.

The accuracy of the metering system depends on the condition of the orifice plates and the differential pressure sensing system. Absolute accuracy is 3 percent and repeatability is better than 3 percent. Flow rates through the fuel system are stable and unaffected by variations in wind and combustion conditions.

TABLE 3-2. FUEL SYSTEM COMPONENTS

COMPONENT	DESCRIPTION	MODEL	SIZE OR CAPACITY
PR1	Propane Pressure Regulator	Leslie GPAK-4	1" NPT
PR3	Nitrogen Pressure Regulator	Leslie GPAK-4	1" NPT
PR2	Natural Gas Pressure Regulator	Leslie GPAK-4	3/4" NPT
V1	Propane Shut-Off Valve	Worcester 5811-R	2" NPT
V2	Nitrogen Shut-Off Valve	Worcester 5811-R	2" NPT
V3	Natural Gas Shut-Off Valve	Lunkenheimer 708-HST	2" NPT
V6, V10, V14	Flow Control Valve (propane, nitrogen, n. gas)	Lunkenheimer 72-PS	1-1/2" NPT
V7, V11, V15	Flow Control Valve (propane, nitrogen, n. gas)	Lunkenheimer 907-BS	3/4" NPT
V8, V12, V16	Flow Control Valve (propane, nitrogen, n. gas)	Lunkenheimer 907-SS	1/2" NPT
V9, V13, V17	Flow Control Valve (propane, nitrogen, n. gas)	Lunkenheimer 907-SS	1/8" NPT
ORF 1 to 9	Orifice Flanges (propane, nitrogen, n. gas)	Daniels 30-RT	2-1/2", 1-1/2", 1/2" NPT
ORF 1 to 9	Orifice Plates (propane, nitrogen, n. gas)	Custom	See Appendix Table A-2
P1, P2, P3	Pressure Gauges (propane, nitrogne, n. gas)	Marsh Quality Gauge	0-60 psig 6" Dial
MN1, MN2	Manometer	Dwyer 422-23	0-23" W.C.
SV1, SV2, SV3	Solenoid Emergency Shut-Off (propane, nitrogen, n. gas)	ASCO 8215-B81	2" NPT
PR4	Ancillary Propane Pressure Regulator	REGU 1586 YN	3/4" NPT
RM1	Pilot Propane Rotometer	Dwyer RMB	1-10 SCFH
RM2 to RM4	Fuel Rotameters (propane, nitrogen, n. gas)	Brooks R-2-15-AAA	1-10 SCHF
V18	Ancillary Propane, Shut-off	Worcester 5811-R	3/4" NPT
V19	Pilot Program Flow Control Valve	Whitey SS-2RS4	CV = 0.15

4.0 TRACER SYSTEM

Measured amounts of sulfur dioxide will be added to the fuel gases as a tracer to determine dilution factors and verify material balances. The actual SO_2 addition rate will be determined during experimentation. However, it is estimated that one volume percent SO_x in the fuel will be sufficient to produce about 1.0 ppm in the combustion product. The rate of SO_2 anticipated ranges from 0.11 to 283 SCFH.

4.1 Tracer Supply

The SO_2 is purchased from Union Carbide as a liquid compressed gas cylinders containing 900 SCF. A dip tube draws liquid and passes it through two steam-heated shell and tube vaporizers shown in Figure 4-1. After vaporization the SO_2 is controlled and meter-delivered to the flare head. Figure 4-2 shows the flow schematic of the SO_2 system.

4.2 Tracer Flow Control and Metering

The wide range of flow rates (2570:1) requires using multiple valves and flow meters. The SO_2 pressure (34 psig) from the vaporizer is regulated to 15 psig with a stainless steel regulator (Union Carbide Model CRC-15). Depending on the use rate, the SO_2 is controlled by a sized needle valve and metered with a rotometer. Table 4-1 lists the component specifications of the valves and flow meters.

4.3 Performance

The performance of the system mixing and delivering the SO_2 tracer has been verified by measuring SO_2 profiles at the base of the flare stack.

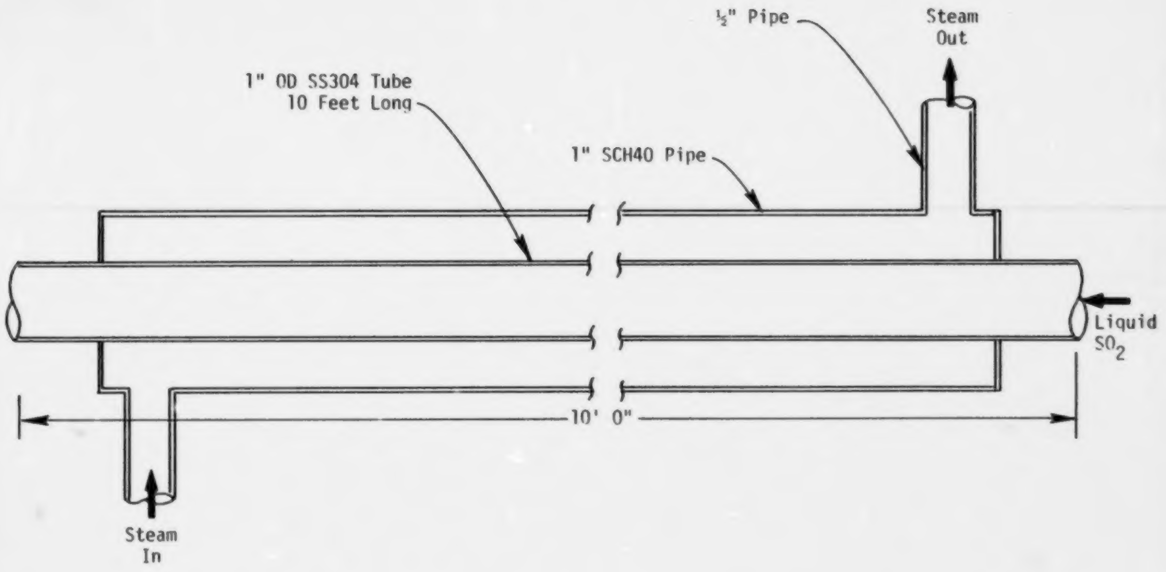
½" Pipe
Steam
Out
1" OD SS304 Tube
10 Feet Long
1" SCH40 Pipe
Liquid
SO_2
10' 0"
Steam
In

Figure 4-1. SO_2 vaporizer.

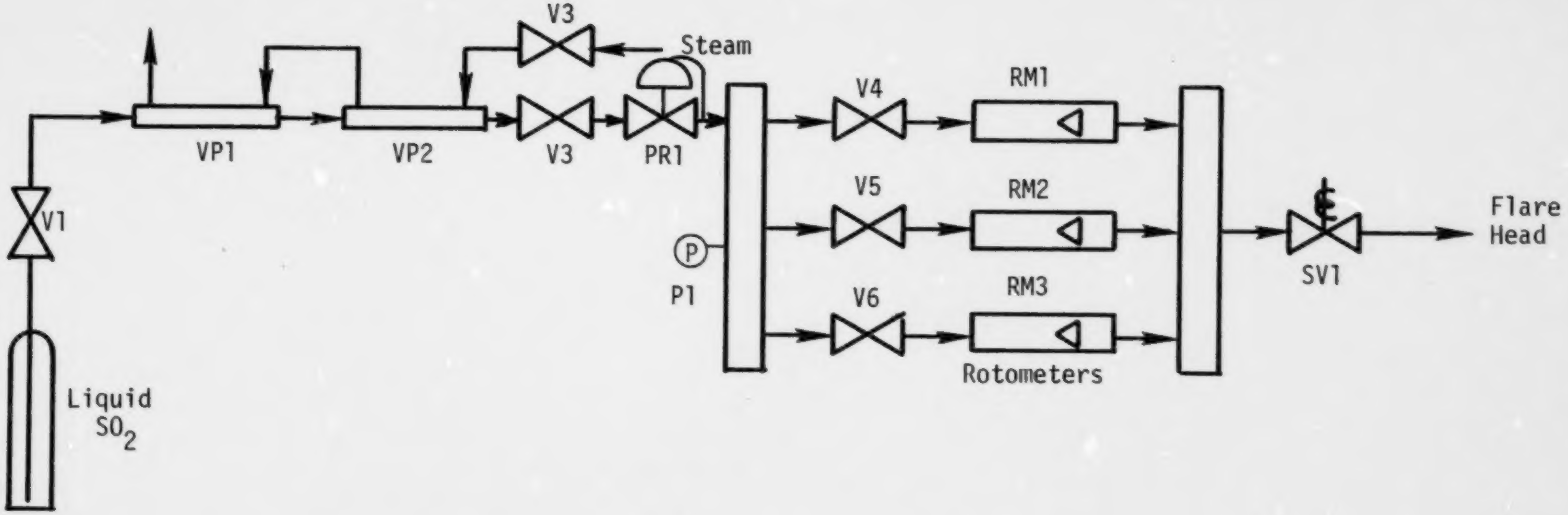
V3
Steam
VP1
VP2
V3
PR1
V4
RM1
V5
RM2
V6
RM3
V1
P
P1
Rotometers
SV1
Flare Head
Liquid SO_2

Figure 4-2. SO_2 flow control and metering system schematic.

TABLE 4-1. TRACER FLOW SYSTEM COMPONENT SPECIFICATION

COMPONENT NO.	DESCRIPTION	MODEL NO.	SIZE OR CAPACITY	REMARKS
VP1, VP2	Vaporizer	Custom	10 CFH	Steam Heated
V1	Bottle Shut-off	-	-	On Bottle
V2	Ball Valve, Stainless Steel	Worcester	1" NPT	Main Shut-off
PR1	Pressure Regulator	Union Carbide CRC-15	1/4" NPT 10.1-15 psig	
PR1	Pressure Gauge	Marsh Type 100-3	6" Dial 0-60 psig	Stainless Steel
RM1	Rotameter	Brooks 1110-09H3B1A	0-727 CFH	
RM2	Rotameter	Dwyer, RMB	0-20 CFH	
RM3	Rotameter	Dwyer, RMB	0-5 CFH	
V4	Control Valve	Whitey, SS-4RS6	CV = 0.51	
V5	Control Valve	Whitey, SS-2RS4	CV = 0.15	
V6	Control Valve	Whitey, SS-21RS4	CV = 0.007	
SV1	Solenoid Valve	ASCO, 8211C87	1/8"	Fast Shut-off

5.0 STEAM SYSTEM

Steam is required at the flare facility for simulating steam-assisted flares and for auxiliary heating. Steam is injected into the flame at the flare head to increase air entrainment and combustion intensity and reduce luminousity. Typical injection rates are from 0 to 1 pound of steam for each pound of combustible gas. Steam is also used at the flare facility to vaporize SO_2 for use as a tracer and to heat sample lines to avoid condensation which would cause loss of sulfur and hydrocarbons in the lines.

5.1 Steam Supply

Steam is supplied to the flare test facility by a 15 hp boiler. The boiler, which can fire propane or natural gas, supplies 400 pounds of saturated steam per hour at 100 psig.

The feedwater to the boiler is filtered and the calcium and magnesium ions are removed by a resin-bed ion-exchange water softener. The water softener has a one-cubic-foot bed and can process 10 gallons of water per minute. The resin bed is automatically regenerated by salt solution.

5.2 Flow Control and Metering

Metering of steam is difficult because of the wide range of flow rates and the problem of metering a gas which may condense at the metering temperature. Figure 5-1 illustrates the steam-flow control and metering system. All lines are insulated to minimize heat losses. The boiler produces saturated steam at 100 psig (348°F). The steam flows through a pressure-reducing valve (Leslie Model GPK-1½") which controls the steam pressure between 10 to 60 psig. Expansion produces dry superheated steam. Condensation formed downstream of the pressure-reducing valve is removed by a steam trap at the manifold and the "dry" steam flows through one of four orifice meters and is controlled by manual valves. The flow rate is indicated by the pressure drop across the orifice meter measured by a differential pressure transducer (Validyne Model P305D). Special precautions are used to read the differential pressure in the steam line. Bleed-valves clear the pressure sensing lines of liquid before each reading. The manifold pressure and temperature are measured on dial gauges. Table 5-1 lists the specifications of the metering system.

(5-1

T 5-1

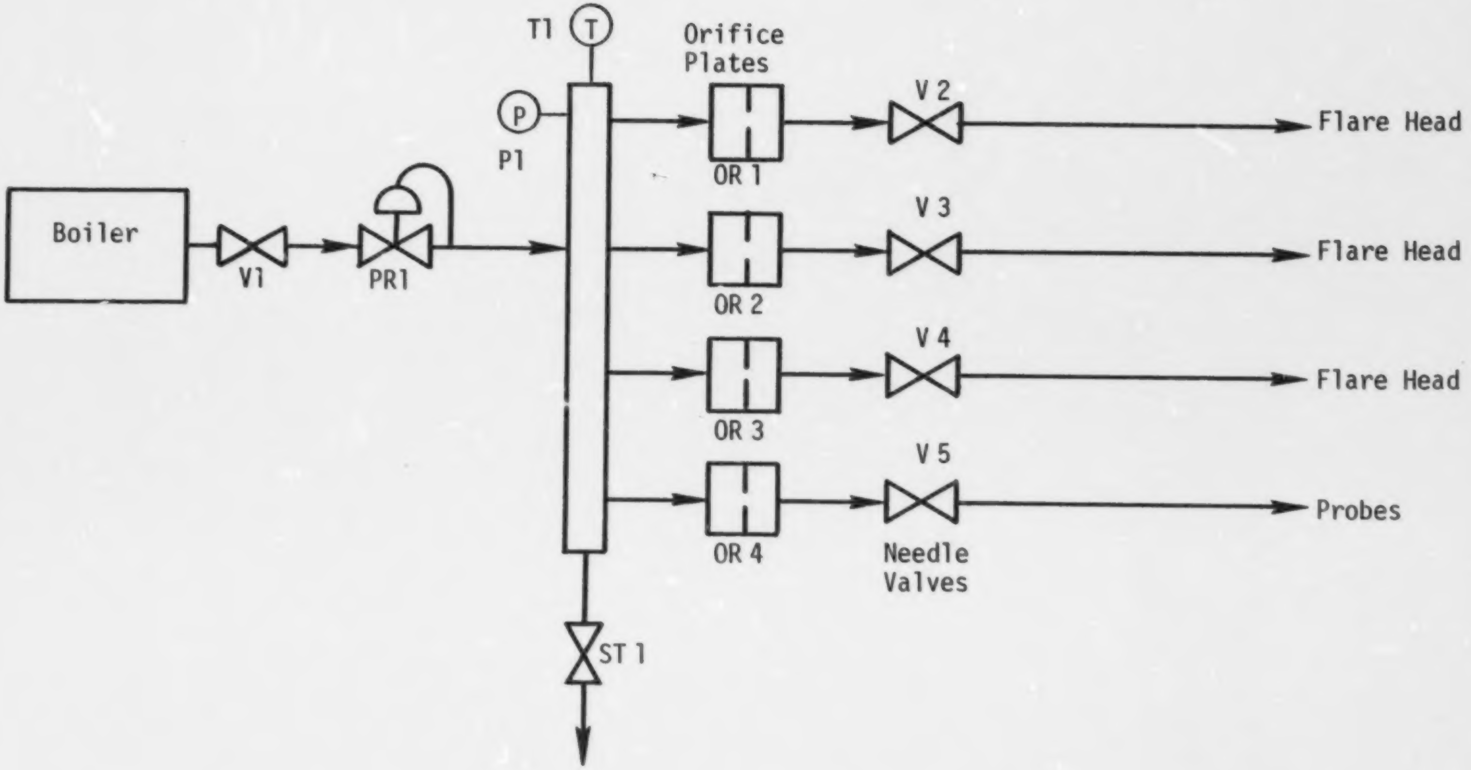
T1
T
Orifice Plates
P
P1
Boiler
V1
PR1
OR 1
OR 2
OR 3
OR 4
V 2
V 3
V 4
V 5
Needle Valves
Flare Head
Flare Head
Flare Head
Probes
ST 1

Figure 5-1. Steam flow control and metering system schematic.

TABLE 5-1. STEAM METERING SYSTEM COMPONENTS

COMPONENT NO.	MODEL NO.	DESCRIPTION	SIZE OR CAPACITY	REMARKS
V1	Lunkenheimer LQ-602	Gate Valve	2"	Shut Off
PR1	Leslie GPK-2	Pressure Reducing Valve	2"	
ST1	Flexitrap	Steam Trap	1/2"	
P1	Marsh Master Gauge	Pressure Gauge	6" Dial 0-200 psig	
ORF 1	Daniels 30-RT	Orifice Flange	2-1/2" NPT	
ORF 2	Daniels	Orifice Flange	3/4" NPT	
ORF 3	Daniels 30-RT	Orifice Flange	1-1/2" NPT	
ORF 1	Custom	Orifice Plate	0.987" Bore	
ORF 2	Custom	Orifice Plate	0.459" Bore	
ORF 3	Custom	Orifice Plate	0.205" Bore	
ORF 4	Custom	Orifice Plate	0.095" Bore	
V1	Powell	Control Valve	1-1/2" NPT	
V2	Lunkenheimer 907-BS	Control Valve	1" NPT	
V3	Lunkenheimer 907-BS	Control Valve	3/4" NPT	
V4	Lunkenheimer 907-BS	Control Valve	1/4" NPT	
PT1	Validyne P305D	Differential Pressure Transducer	0-5 psid	
T1	Trend	Temperature Gauge	3" Dial 50-500 °F	
VM1	Newport	Transducer Output Voltage Readout	0-19.99 VDC	0.01 VDC Resolution

5.3 Performance

The steam system operates satisfactorily. Figures 5-2 through 5-5 show the calibration curves of the orifice meters. Flows were calibrated by condensing the steam downstream of the control valve and weighing the collected condensate over a timed interval.

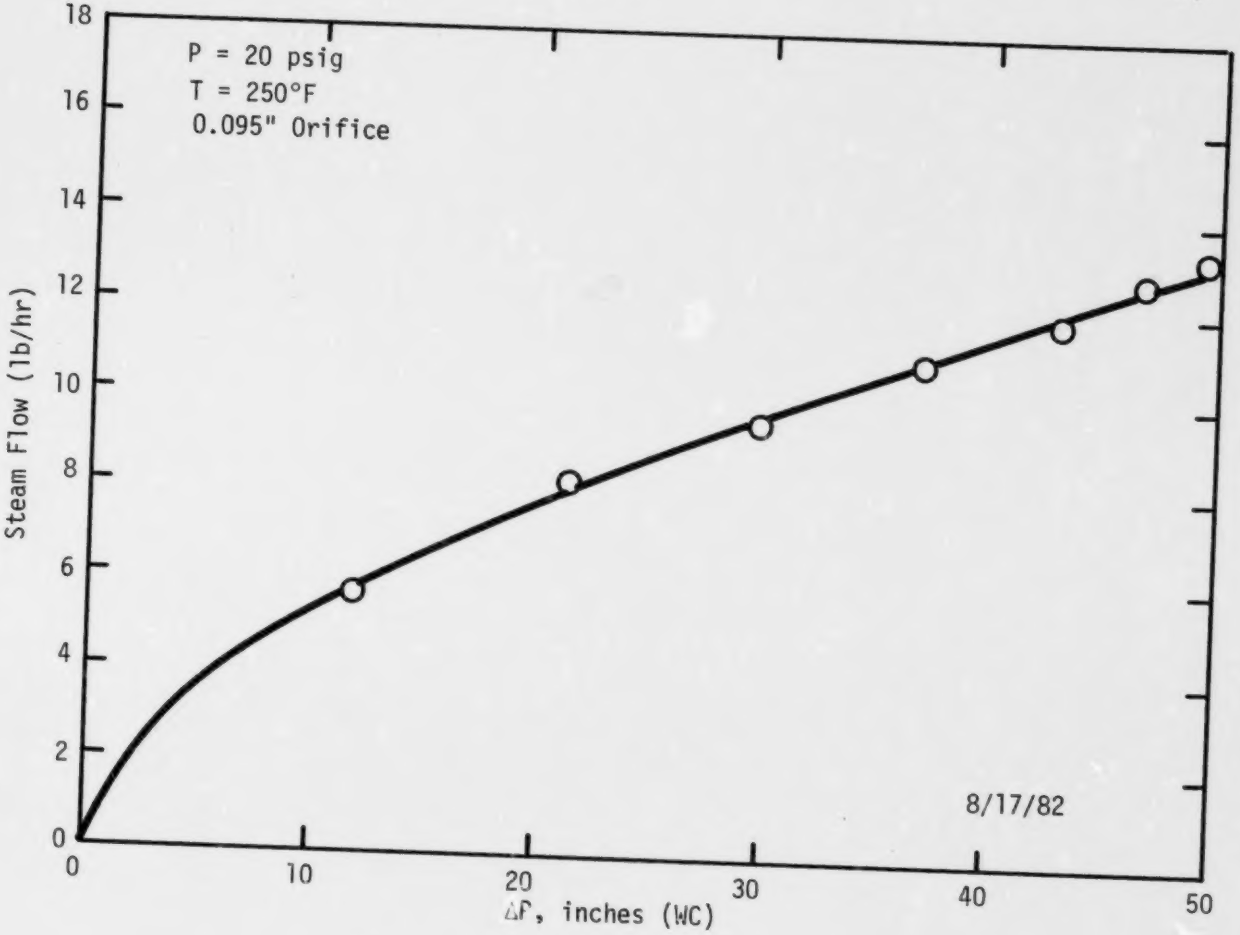

Figure 5-2. Calibration of steam flow.

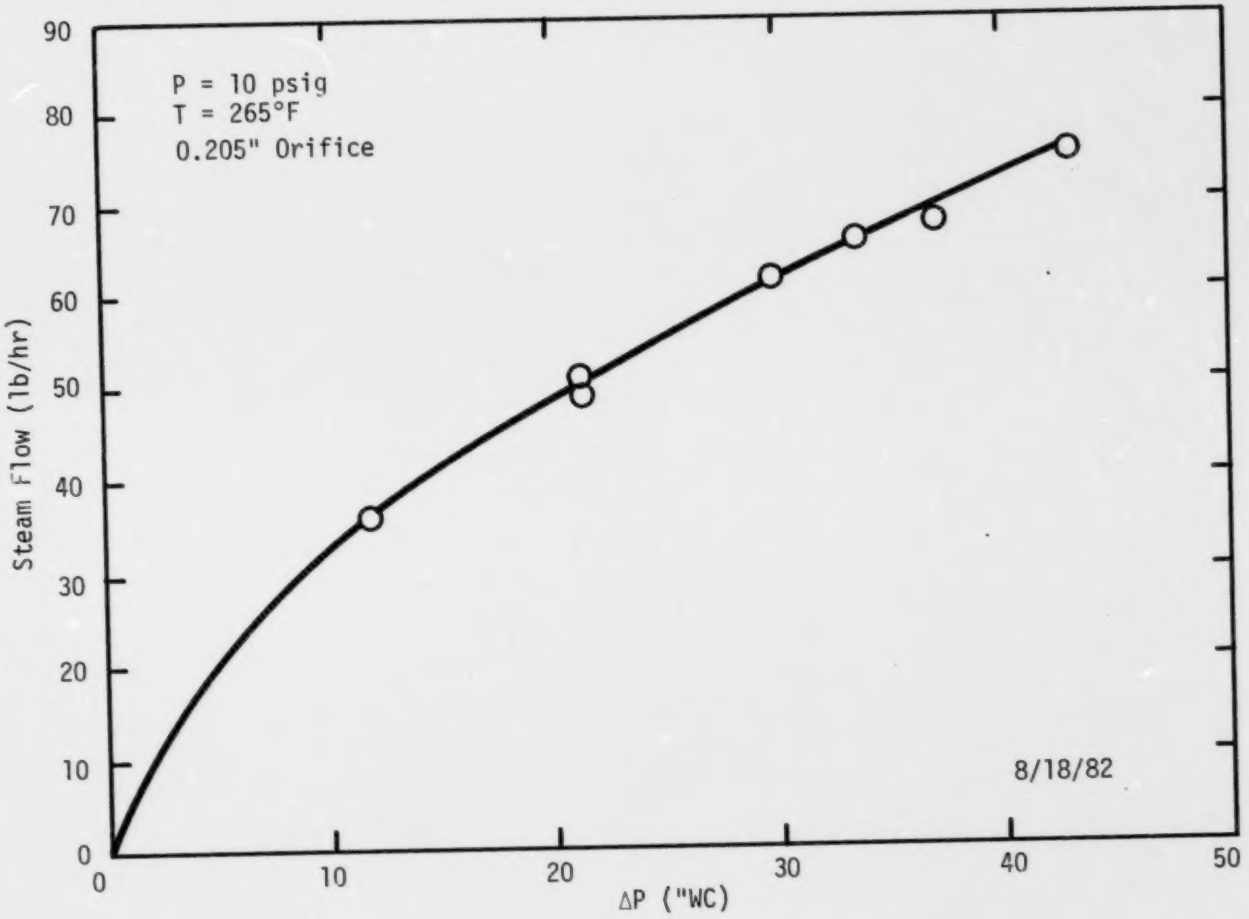

Figure 5-3. Calibration of steam flow.

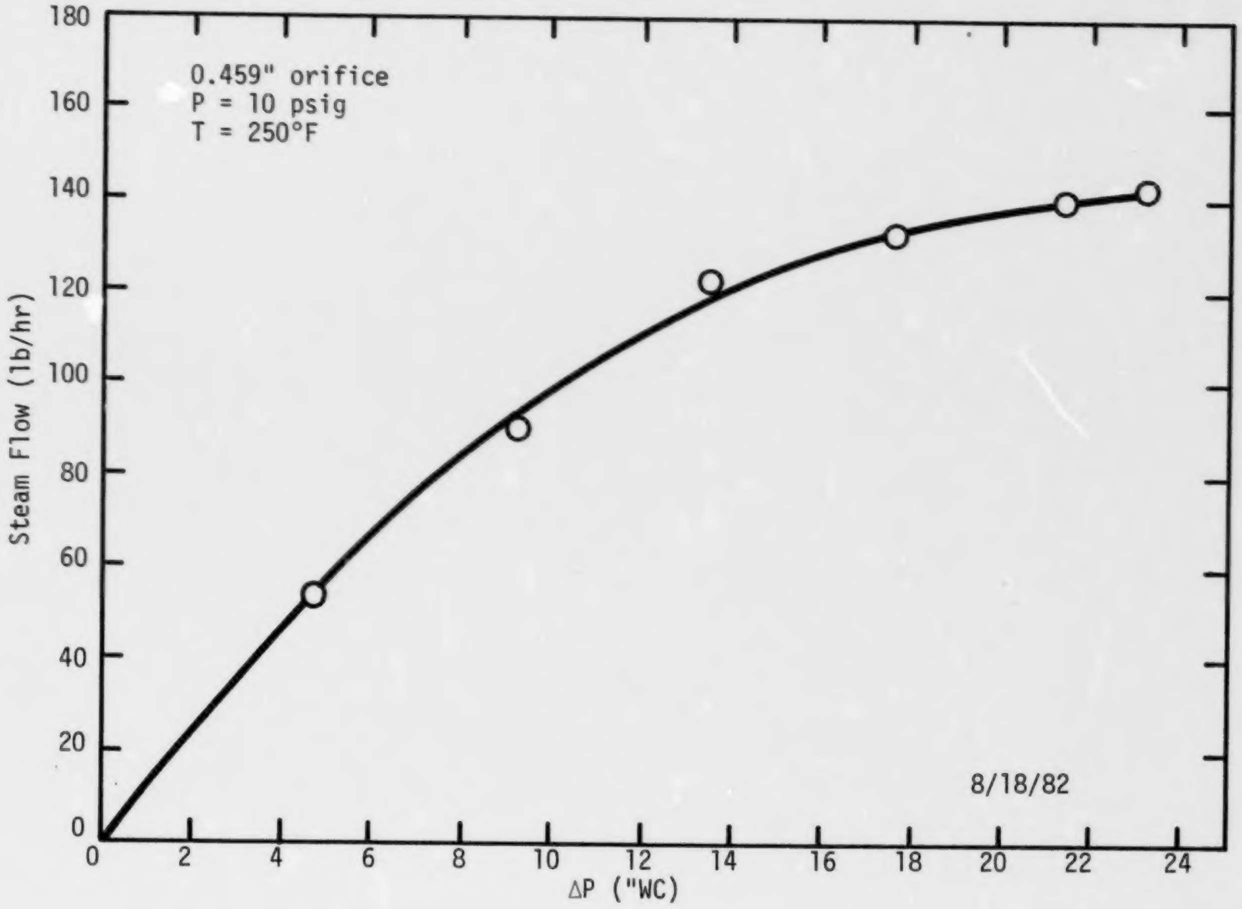

Figure 5-4. Calibration of steam flow.

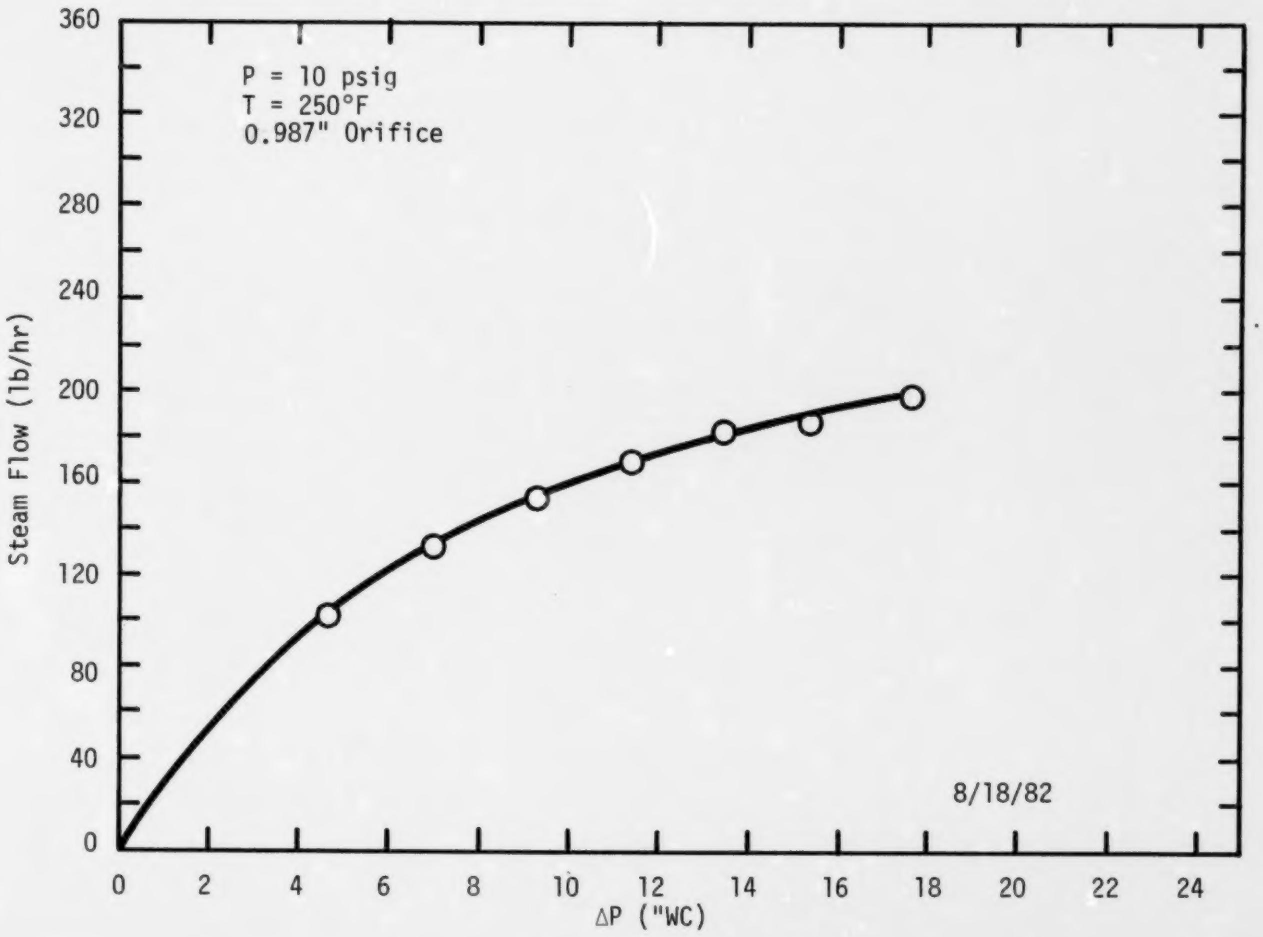

Figure 5-5. Calibrated steam flow.

6.0 DESIGN OF FLARE HEADS

The flare heads should:

- be geometrically simple to allow a scientific interpretation of the results;
- simulate the important features of commercial flare heads;
- produce flare flames representative of commercial flare flames;
- be consistently scaled.

A straight pipe was used for the flare heads on the advice of the Technical Advisory Committee. They concluded that flame arrestors, retention rings, and other proprietary features of commercial flare heads were unnecessary and undesirable for the flare test facility. The head was provided with a simple steam-ring and steam-nozzles for injecting steam to suppress soot.

6.1 Flare Head Support Base

F6-1

Different flare heads can be mounted on the flare base shown in Figure 6-1. The base is a 6-foot long, 6-inch diameter pipe welded to a platform composed of a ½-inch thick steel plate and four legs. The gas inlet is a 2-inch pipe ending with a standard 150 pound flange. The mount for the four flare heads is a standard 150-pound, 6-inch pipe flange. The top of the flare head support base is 7 feet above ground level.

6.2 Flare Tip

The flare heads are nominally 3, 6 and 12 inches in diameter and each is 8-feet long. An illustration is shown in Figure 6-2, and the dimensions are listed in Table 6-1.

F6-2
T6-1

6.3 Steam Ring and Nozzles

A key feature of commercial flare heads is the steam ring and injection nozzles. These are designed to induce air entrainment and turbulence at the base of the flare flame. The design principles employed in commercial flare heads are proprietary and unavailable. Hence, the design of the steam injection nozzle assembly for the test flare was based on empirical information reported in the literature. The basic assumptions applied to the steam

A	6" Weld Flange Raised Face, 150#
B	6" SCH 40 Pipe 6' Long
C	2"x 2" H-Beam to 4 Corners
D	2" Weld Flange Raised Face, 150#
E	2" Black Pipe SCH 40
F	1/2" Thick Plate 3'x 3'
G	2" Pipe Leg 1' Long
H	Footing Plate 1/2" Thick 4"x 4"

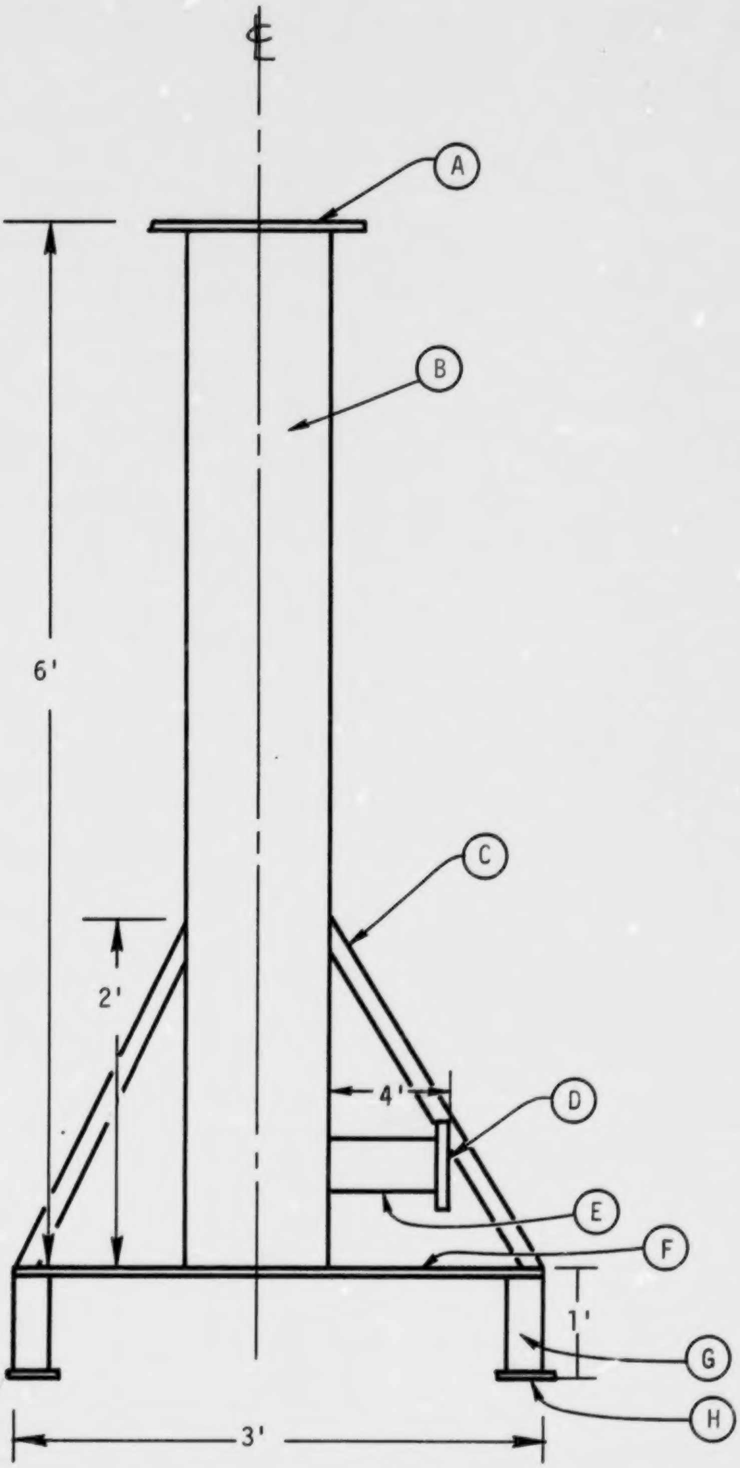

Figure 6-1. Flare head support structure.

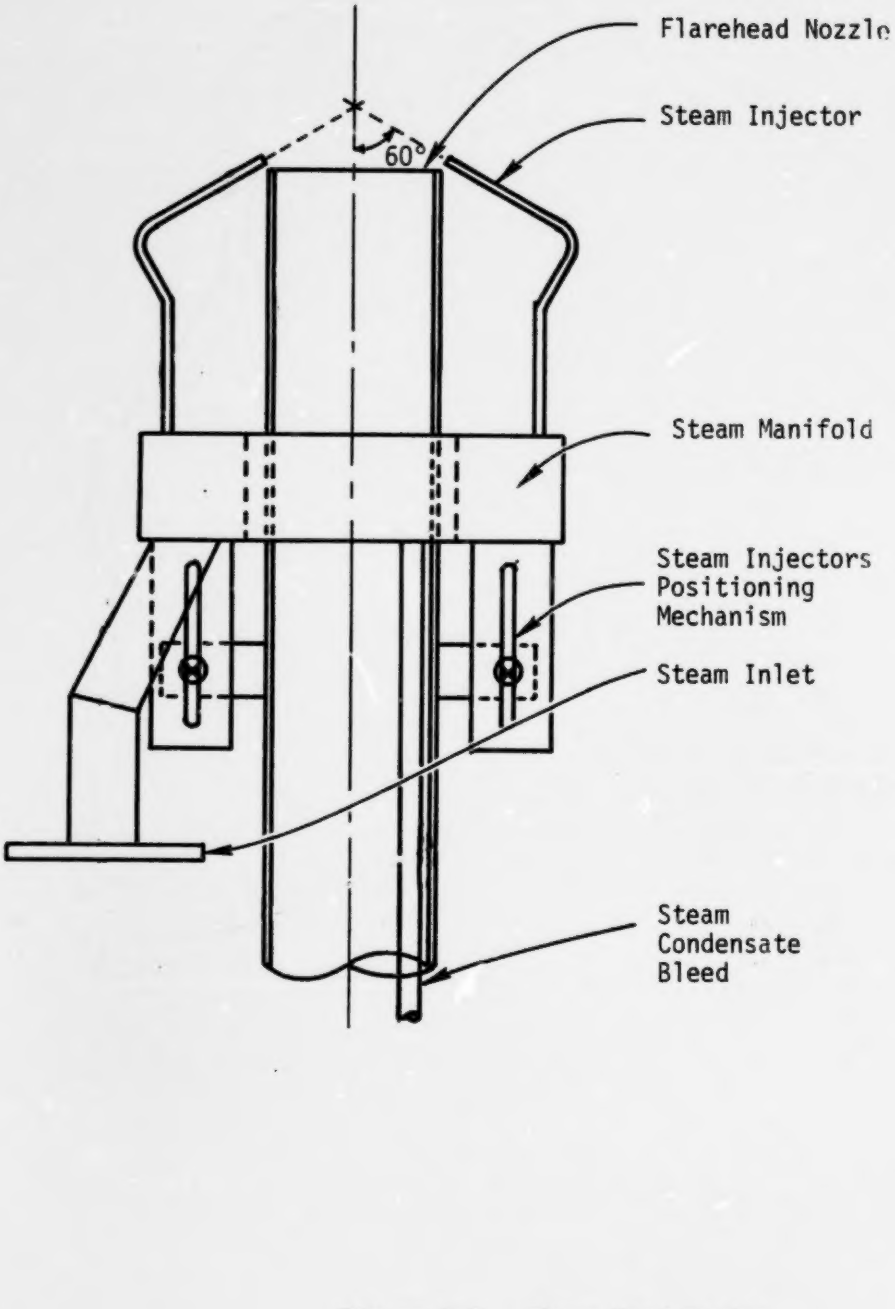
Flarehead Nozzle
Steam Injector
60°
Steam Manifold
Steam Injectors Positioning Mechanism
Steam Inlet
Steam Condensate Bleed

Figure 6-2. Flare Head Design

TABLE 6-1. FLARE HEAD SPECIFICATIONS

PARAMETER	Nominal Size (inch)		
	3	6	12
Inside Diameter (inch)	3.06	6.3	12.3
Outside Diameter (inch)	3.5	6.6	12.8
Flow Area (in^2)	7.35	31.2	118.8
Manifold Flow Area (in^2)	3.06	14.1	33.1
Number of Nozzles	4	8	16
Nozzle ID (inch)	0.263	0.37	0.525
Nozzle OD (inch)	0.375	0.50	0.625
Length of Nozzle (inch)	3	5	7
Vertical Position (inches from tip of flarehead)	0.5-4.5	-1 to 5	0 to 6
Total Flow Area (in^2)	0.217	0.860	3.464
Overall Height (feet from ground)	15	15	15

nozzle design are:

- Commercial flares have smokeless capacity of about 20 percent of the maximum gas capacity. This yields a smokeless exit velocity of about 120 ft/sec.
- Flared gases have densities of 0.0637 pounds of hydrocarbon per cubic foot.
- Smokeless operation requires 0.27 pounds of steam per pound of hydrocarbon.

From these assumptions the steam flow capacities are computed and the steam ring and nozzles sized. To simplify the analysis of steam jet entrainment, straight stainless steel tubes with large length-to-diameter ratios are used for the steam nozzles. Figure 6-2 shows the flareheads with the steam ring and Table 6-1 lists the specifications of the flarehead, steam rings and nozzles. Some steam condenses in the steam ring in spite of line insulation. The steam ring is drained through blow-down valves prior to tests with steam injection to eliminate the injection of water into the flame.

6.4 Pilot

The pilot is required to ignite the fuel gases at the flarehead. Typically, the fuel gases will remain lit unless the exit velocity is too high, the wind is too strong or the gas heating value is too low. Under such conditions the pilot will provide a reliable continuous source of ignition.

Commercial flares burn about 125-200 scfh of natural gas continuously as pilot flames. This is similar to the fuel flow for the main flare for many of the tests. In these cases, use of a continuous pilot flame would obscure the major objective of this program which is to determine the combustion efficiency of the main flare. Therefore, a small hand-held torch which uses less than one scfh of gas was used to ignite the flare flames.

6.5 Flame Arrestors

Commercial flare heads are equipped with air or liquid seals or flame arrestors to minimize the potential of flash-back which can occur when air enters the stack and forms a combustible mixture of gas. The Technical Advisory Committee suggested a flame arrestor not be used on the flare test facility. The arrestor was unnecessary because the head is purged with nitrogen before and after each test and it would distort the velocity profile at the exit of the flare head.

6.6 Flame Retention Ring

Retention rings are used on flare tips to stabilize flare flames at high velocities. The rings are usually of special proprietary design and are not required for small flares with low exit velocities. Therefore, the Technical Advisory Committee recommended the pilot-scale flares be operated without a retention ring. (Note that in subsequent tests at high velocities, retention rings were used.)

7.0 EXTRACTIVE SAMPLE SYSTEM

In order to determine the combustion efficiency of flares, samples are extracted from the flame plume and analyzed for O_2, CO, CO_2, sulfur, hydrocarbon and particulates.

7.1 Sample Points

The locations for sample withdrawal must be determined experimentally. A hood placed above the flare flame collects the entire plume and a five-probe rake withdraws samples at selected locations above the flare flame.

7.2 Hood Sampling

The hood collects the flame plume into a chimney and homogenizes the combustion products. If this method is successful, it is a quick way to determine overall flame combustion efficiencies for small flames.

Hood Design

Figure 7-1 shows the sampling hood assembly. The hood design was improved several times during the program in order to better meet the program objectives:

- To collect the entire flare-flame plumes from the 3" flare head and the plumes from a flame at 2.8 ft/sec gas exit velocity for the 6" flare-head.
- To homogenize the plume to a mixture with uniform species concentrations.
- To provide means to measure material balances through the hood.
- To minimize disturbances to the flare flames.

The hood assembly consists of two hood sections, an axial duct booster fan, a mixing chamber, a flow straightener, a measurement chamber and a flow damper. The two hood sections are constructed of 12-gauge carbon steel and cover areas 8 feet square and 13 feet 8 inches square, respectively.

The hood converges to a 2-foot diameter chimney. The 2 hp axial flow booster fan at the entrance to the chimney can draw 8200 CFM of air at static pressure of 1/4-inch water column. This flow rate is about 250 times the

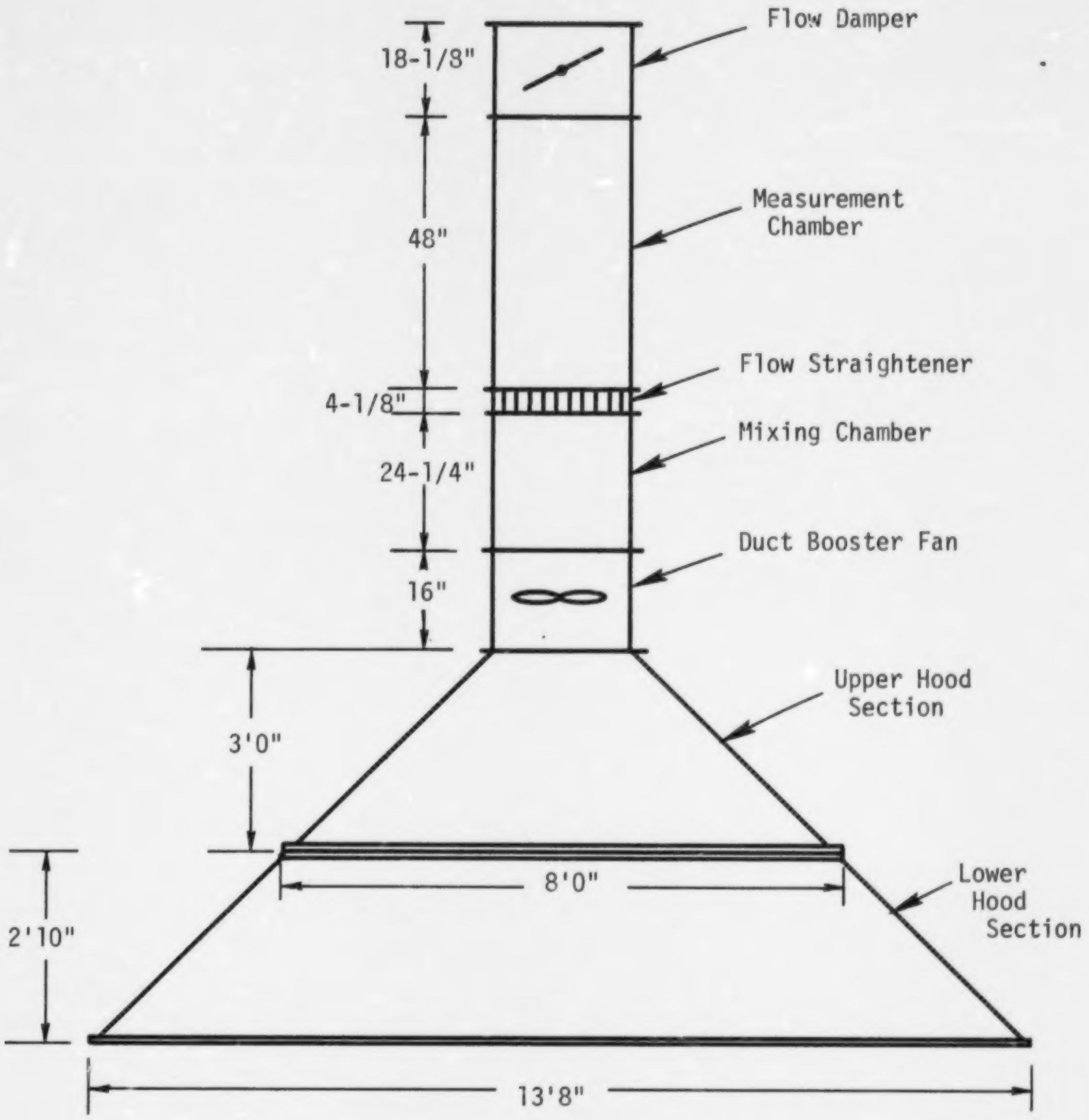
18-1/8"
48"
4-1/8"
24-1/4"
16"
3'0"
2'10"
8'0"
13'8"
Flow Damper
Measurement Chamber
Flow Straightener
Mixing Chamber
Duct Booster Fan
Upper Hood Section
Lower Hood Section

Figure 7-1. Sampling Hood Assembly.

flare gas rate at 2.8 ft/sec from the 6-inch flarehead (equivalent to about 17 times the plume of a 56 percent propane flame at stoichiometry combustion conditions).

The mixing chamber is a 4-feet long, 2-feet in diameter pipe with 9 flow directors to increase turbulence mixing. However, the duct booster fan changed the flow pattern in this chamber to highly swirling. A flow-straightener at the exit of the mixing chamber was used to reduce the swirling flow. The straightener is made of two banks of 2-inch wide steel bars at two-inch spacings oriented 90 degrees from each other.

The measurement chamber is 2-feet in diameter and 4-feet long and houses the sample probe, five velocity probes and a type-K thermocouple. A damper valve at the chamber outlet allows adjustments of the flow rate through the hood.

Probe Design

F 7-2

The hood probe is shown in Figure 7-2. It consists of a center sample passage made of 316 stainless steel, 1/8-inch, schedule 40 pipe. An external flow jacket, 1½-inch OD, carries steam to maintain the gas sample at the desired temperature. A stainless steel filter holder (Gelman 1209), welded to the probe tip, houses a glass fiber filter to collect solid particulates. The particulate loading of the combustion product is determined by measuring the combustible material captured on the filter after a known volume of sample has passed through the filter. The probe is designed to pull 50 cu. ft. of gas per hour. Various-sized tips are used to ensure that the sampling is nearly isokinetic.

7.3 Multiple Point Sampling

The hood sampling system provides average properties of the combustion products. Multiple point sampling determines local species concentrations and identifies the contribution of individual flame structures to the overall plume. It uses five separate probes and sampling trains to collect five samples simultaneously.

Support Gantry

The multiple probes are supported by a gantry which can be lifted by a 12-volt DC winch. It covers sample heights from 6 to 50 feet above ground-

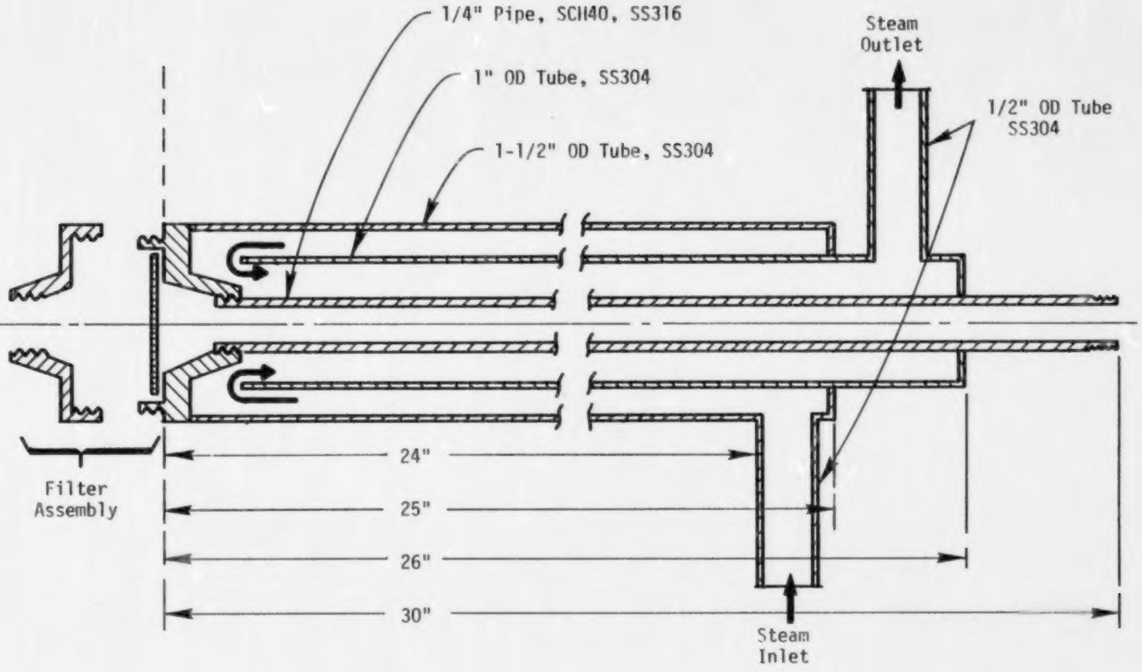
1/4" Pipe, SCH40, SS316
1" OD Tube, SS304
1-1/2" OD Tube, SS304
Steam Outlet
1/2" OD Tube SS304
Filter Assembly
24"
25"
26"
30"
Steam Inlet

Figure 7-2. Filter probe design.

level and can traverse a cross-section 15 feet by 25 feet. Figure 7-3 shows the probe positioning mechanism.

Probe Design

The probes used for the multiple point sampling are the same as the probe used in hood sampling. Refer to Figure 7-2 for the probe design.

7.4 Sample Conditions

The sample collected by the probes cannot be analyzed directly because it is likely to be too hot, laden with particulate and wet. The conditioning required depends on the specific property that is to be measured; namely, concentrations of O_2, CO, CO_2, SO_2 (or total gaseous sulfur), hydrocarbons and particulates. These concentrations can best be measured if the gas temperature is near 80°F and is free of particulates and moisture. Figure 7-4 shows the schematic of the sample train.

The sample temperature ranges from near ambient to over 1000°F depending on the sample location. Ideally, the moist samples should be maintained between 160 and 300°F so moisture does not condense which would remove a portion of the soluble gases. The sample temperature of the probes is controlled by passing water or steam through outer jackets. The moist sample is kept above 200°F by electrically-heated Teflon sample lines but drops to ambient levels downstream of the driers.

Particulate Removal

The probe tips contain the filters in stainless steel holders, to collect particulates, keep the sample line clean, and reduce the contact time between the sample gas and the potentially reactive particulates. Combustible particulate are determined by burning the filter and sample. Filters (Gelman GA Triacetate material with pore sizes 0.2, 0.45, 0.8, 1.2 and 5 μm are adequate for temperatures below 212°F and approach velocities from 1.64 to 16.4 ft/sec. Other glass-fibre filters are adequate up to 930°F (Whatman 934AH), but should not be necessary.

Drying

Moisture in the gas sample must be removed before it condenses and partially removes the soluble gases such as SO_2. In addition, water vapor interferes with infrared analysis of CO and CO_2.

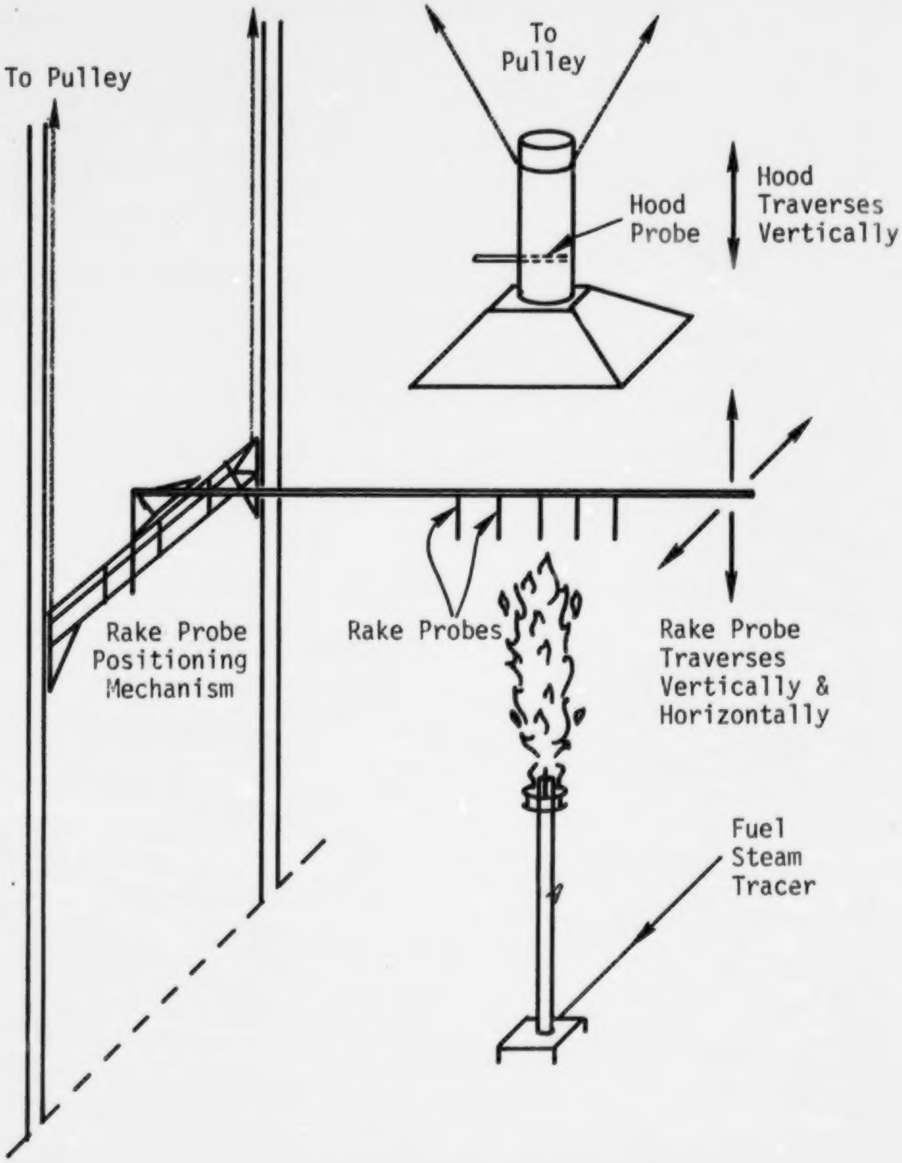

To Pulley
To Pulley
Hood Probe
Hood Traverses Vertically
Rake Probe Positioning Mechanism
Rake Probes
Rake Probe Traverses Vertically & Horizontally
Fuel Steam Tracer

Figure 7-3. Hood and probe rake positioning mechanism.

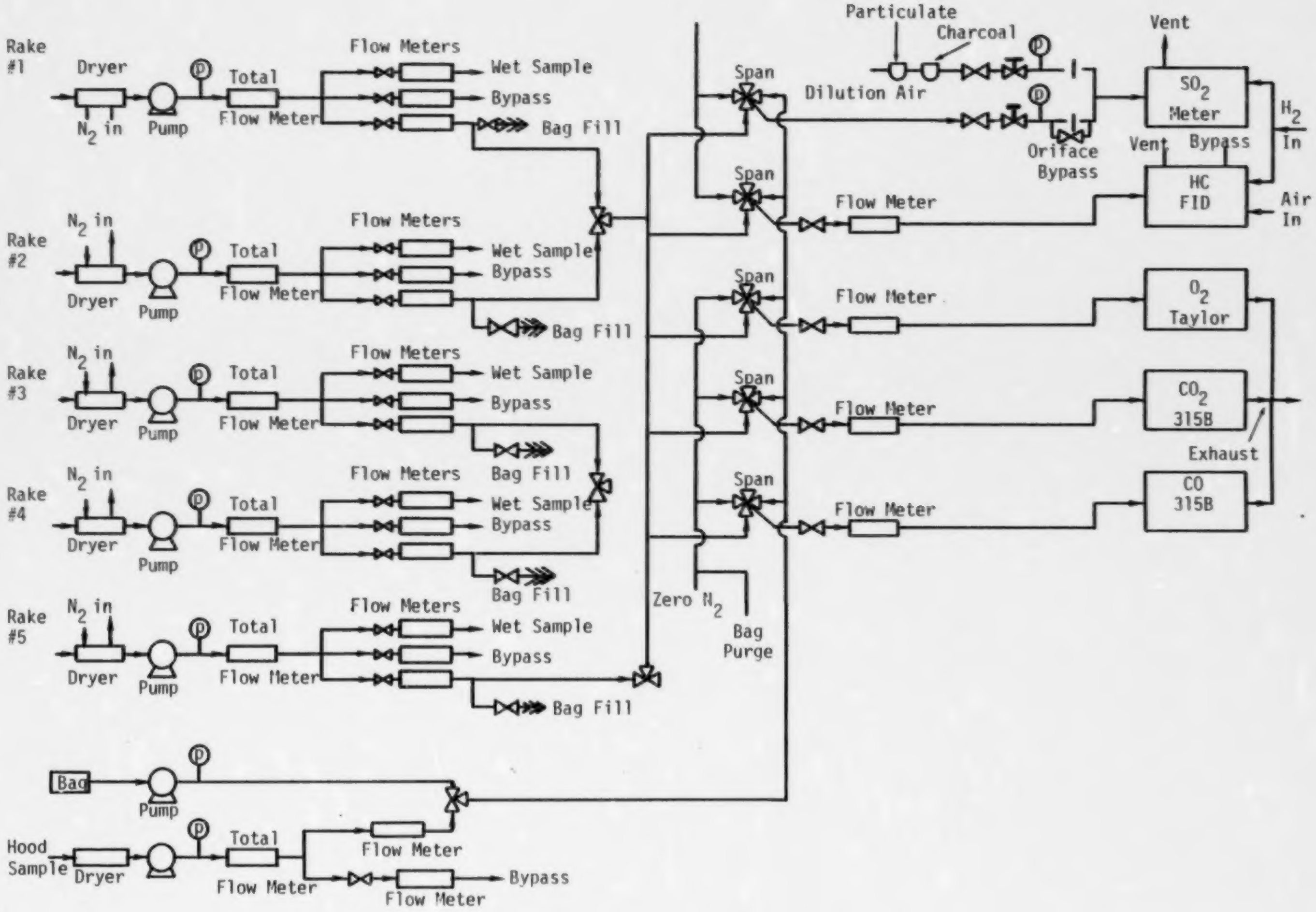
Rake #1
Dryer
N_2 in
Pump
Total Flow Meter
Flow Meters
Wet Sample
Bypass
Bag Fill
Rake #2
Rake #3
Rake #4
Rake #5
Bag
Hood Sample
Flow Meter
Span
Zero N_2
Bag Purge
Particulate
Charcoal
Dilution Air
Oriface Bypass
Vent
SO_2 Meter
H_2 In
Air In
HC FID
O_2 Taylor
CO_2 315B
CO 315B
Exhaust

Figure 7-4. Flare Sample System

The moisture is removed by Permapure driers (Model PD-1000-24SS) which uses a membrane tube bundle to transfer selectively water vapor from the gas stream. The water passes through the membrane where it is removed by dry nitrogen. The driers have 40 cu cm internal volume and can pass 9.95 to 51.1 cu. ft. of sample per hour at 0.15 and 0.75 psi pressure drop, respectively. The amount of purge-gas required is 117 cu. ft. per hour. The outlet sample is designed to achieve 40°F dew-point.

Continuous Analysis

Concentrations of CO, CO_2, O_2, SO_2, HC in the dry, clean gas are measured by continuous analytical instruments.

Bag Collection

One set of analyzers is available, consequently samples from the multiple-probe sampling will be simultaneously drawn and subsequently analyzed. The samples will be stored in 1.8 cu. ft. capacity Tedlar bags. Tedlar bags are fabricated on-site using a heat sealer. The bags include stainless steel valves through which the gas will enter, be trapped in the bag, and exit for analysis.

7.5 Analysis

The gas samples are analyzed for concentrations of O_2, CO, CO_2, SO_2 and hydrocarbons and the particulate filters are weighed to determine particulate loading in the sample gas. Table 7-1 lists the analyses, sensitivities, accessories and typical ranges of gas concentrations.

TABLE 7-1. ANALYTICAL METHODS AND ACCURACIES

SPECIE	INSTRUMENT	PRINCIPLE	RANGES	ACCURANCIES *	MEASURED CONCENTRATIONS
O_2	Taylor 570A	Paramagnetic	0-100%	±0.02%	Typical - 20.5% Range 18-21%
CO	Beckman 315A	Non-dispersive Infrared Absorption	0-500 ppm 0-2.0%	±01 ppm ±200 ppm	Typical 3-10 ppm Minimum 3 ppm Maximum 300 ppm
CO_2	Beckman 315B	Non-dispersive Infrared Absorption	0-5.0% 0-10% 0-20%	±0.02% ±0.1% ±0.2%	Typical 0.2-0.5% Minimum 0.07% Maximum 1.0%
HC	Beckman 400	Flame Ionization Detection	0-5 ppm 0-50 ppm 0-500 ppm 0-5000 ppm	±.05 ±0.5 ppm ±5 ppm ±50 ppm	Typical - 3 to 10 ppm Minimum - 3 ppm Maximum 200 ppm
SO_2	Meloy SA 260	Flame Photometric Detection	0.5 ppb to 10 ppm	±1% of measured	0.5 - 10 ppm
	Titration	Reaction with Perchlorate	1 to 100 ppm	±10% of measured value	
Particulate	Filter	Timed Collection	0 to 10^{-7} lb/ft^3	±5% of measured value	0-5 x 10^{-7} lb/ft^3

* Short-term accuracies within 20 minutes of instrumental calibration

8.0 VISUAL MONITORS

The flame behavior is recorded by a video recorder, a still camera and a high-speed, 16 mm movie camera.

8.1 Video System

The video system has been used to monitor and record gross-flame structures. A JVC color camera records the gross-flame characteristics on tape. The recorder uses a 3/4" wide magnetic cassette tape and provides frame-by-frame play-back. A 12-inch diagonal color monitor permits on-line monitoring and playback. The video monitor system is limited by its spatial and temporal resolution and narrow range of sensitivity to light.

8.2 Photography

A still camera is used to record the structure of the flames. Long time-exposures will record the average structure and short time-exposures will record the instantaneous structure of the flames. Both exposures are recorded with a 35 mm single-lens-reflex camera (Cannon Model AE-1) with a 50 mm focal length and an 80-200 mm zoom lens.

8.3 High-Speed Cinematography

High-speed motion pictures help in understanding the evolution of flare-flame structures. This information is used to understand the influence of flame structure on the combustion efficiency and scale of the head. The flame structure is recorded with a 16 mm Hycam camera using a rotating prism and lens with focal length of 10 to 100 mm. Motion pictures can be taken with this camera at speeds of 100 to 1000 frames/sec. Experience has shown that 200 frames per second is adequate to record flare flame structure.

A camera platform provides stable positioning for recording the flame structure (Figure 8-1). The platform is 15 feet above the ground and can be positioned up to 30 feet from the flarehead. The 30-foot distance produces acceptable flame resolution when using commonly available lenses.

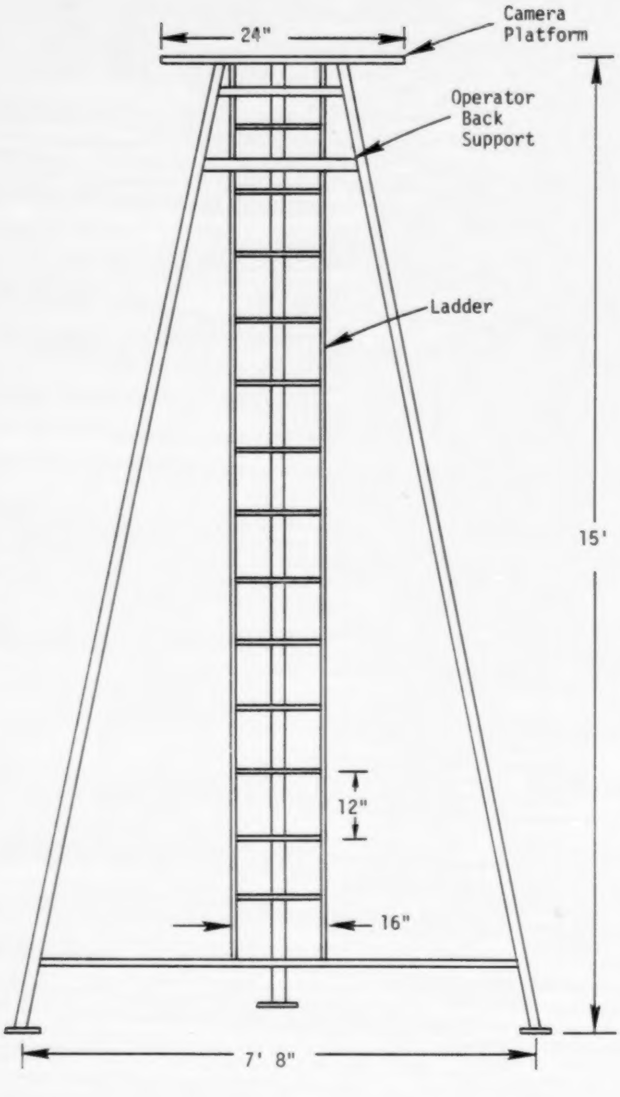

24"
Camera Platform
Operator Back Support
Ladder
15'
12"
16"
7' 8"

Figure 8-1. Camera platform.

9.0 AMBIENT MONITOR AND CONTROL

The flare-flame is not enclosed and is subjected to environmental variations in wind velocity. Screens are used to attenuate natural wind. The wind speed and ambient air temperature are monitored during tests and no tests are conducted during high wind conditions.

9.1 Windscreens

Perforated steel panels, 8 feet by 10 feet protect the flame from wind. Eighteen panels cover the four sides from 10 to 26-foot levels. Figure 9-1 shows a typical wind-screen panel. The panels have 22.7 percent open area with one-half-inch diameter holes on one-inch triangle pitch. Observations using smoke bombs showed that the windscreens effectively reduce the influence of the wind on the flare-flame.

9.2 Monitors

Wind speed and direction are monitored by a three-cup anemometer and wind vane (Climatronics Model Mark I). The velocity is recorded on a strip chart and dry-bulb thermometers used to measure ambient air temperature.

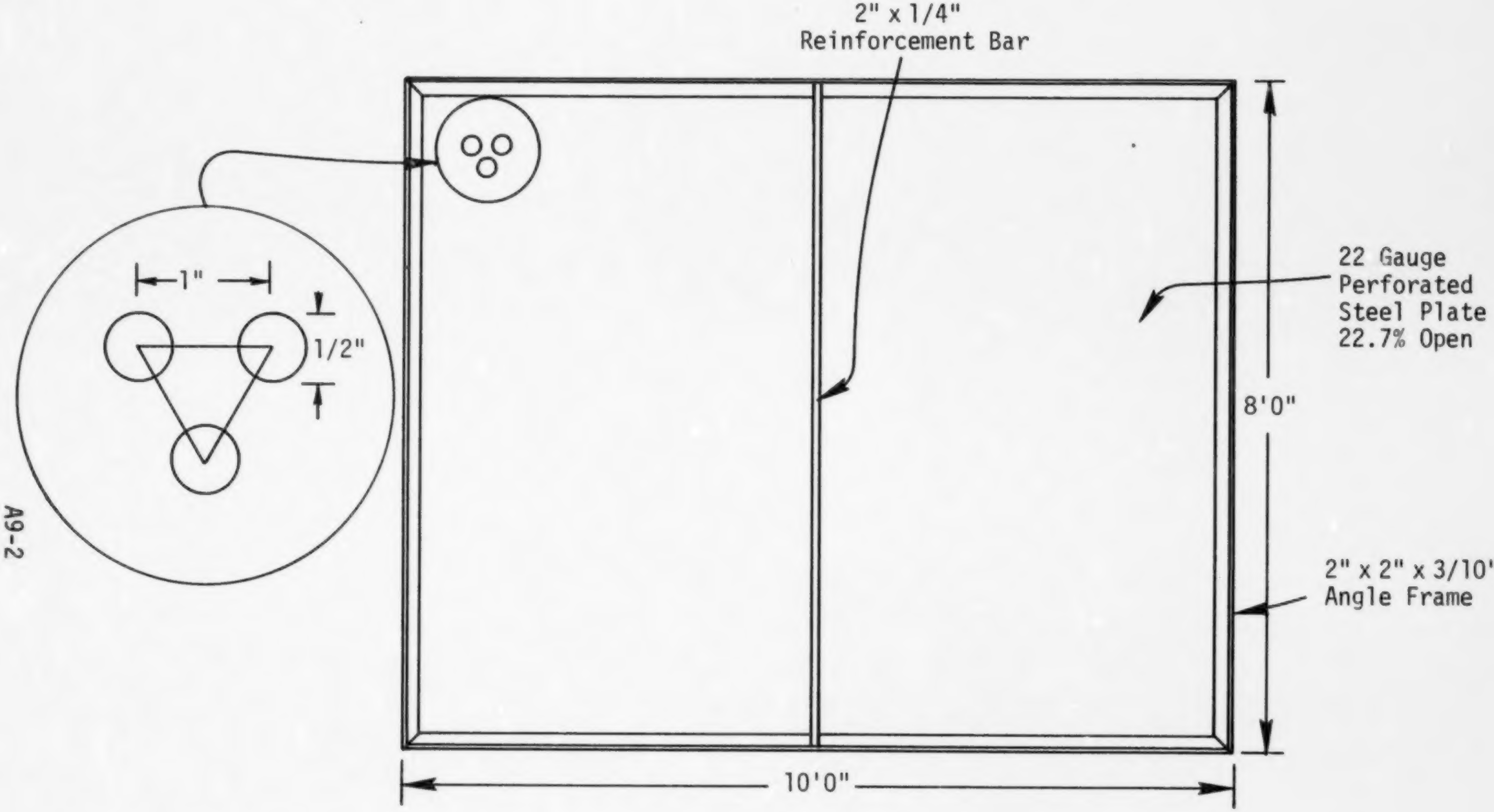
2" x 1/4"
Reinforcement Bar
22 Gauge
Perforated
Steel Plate
22.7% Open
8'0"
2" x 2" x 3/10"
Angle Frame
10'0"
1"
1/2"

Figure 9-1. Perforated plate windscreen.

10.0 SUPPORT STRUCTURE

The structure around the flarehead provides support for the hood, the rake probes and the windscreens and acts as the position reference for the flame and sampling probes.

10.1 Overall Structure

f10-1

The structure covers an area 20 feet by 30 feet. Figure 10-1 shows the schematic of the structure. The corner poles are 4" x 4" x ¼" box-tubing, the horizontal beams are 4" x 4" x ¼" H-beams supported by diagonal members. The structure is stabilized by 3/8"-diameter steel guy cables attached to the corners and anchored to the ground. The vertical and horizontal members are marked by paint stripes spaced at 2-foot intervals to provide a reference for flame observations and probe positions.

10.2 Hood Support

The hood, as shown in Figure 7-1, weighs about 2500 pounds. It is lifted at four points by 3/8"-diameter wire ropes. A system of pulleys guides the wire ropes to one corner where the wire ropes are bridled together. An electric winch is used to raise the hood , which can reach 50 feet above the ground.

10.3 Rake Probe Support

The Rake Probe Gantry weighs about 1200 pounds. It is guided at one end by trolleys and a tongue-in-grove arrangement at the other. It is lifted at two points near the ends by 3/8"-diameter wire rope. These are guided through pulleys to one end and are bridled together. An electric winch lifts the probe, which can reach 50 feet above the ground.

10.4 Windscreens Support

The windscreen panels weigh approximately 180 pounds each. Wire ropes hanging from pulleys at the top of the structure have thimble-loops spaced at 8-foot intervals. Hooks at the top of the panels secure them to the thimble loops. The windscreen assembly on each side of the structure is lifted and lowered to the appropriate height by electric winches.

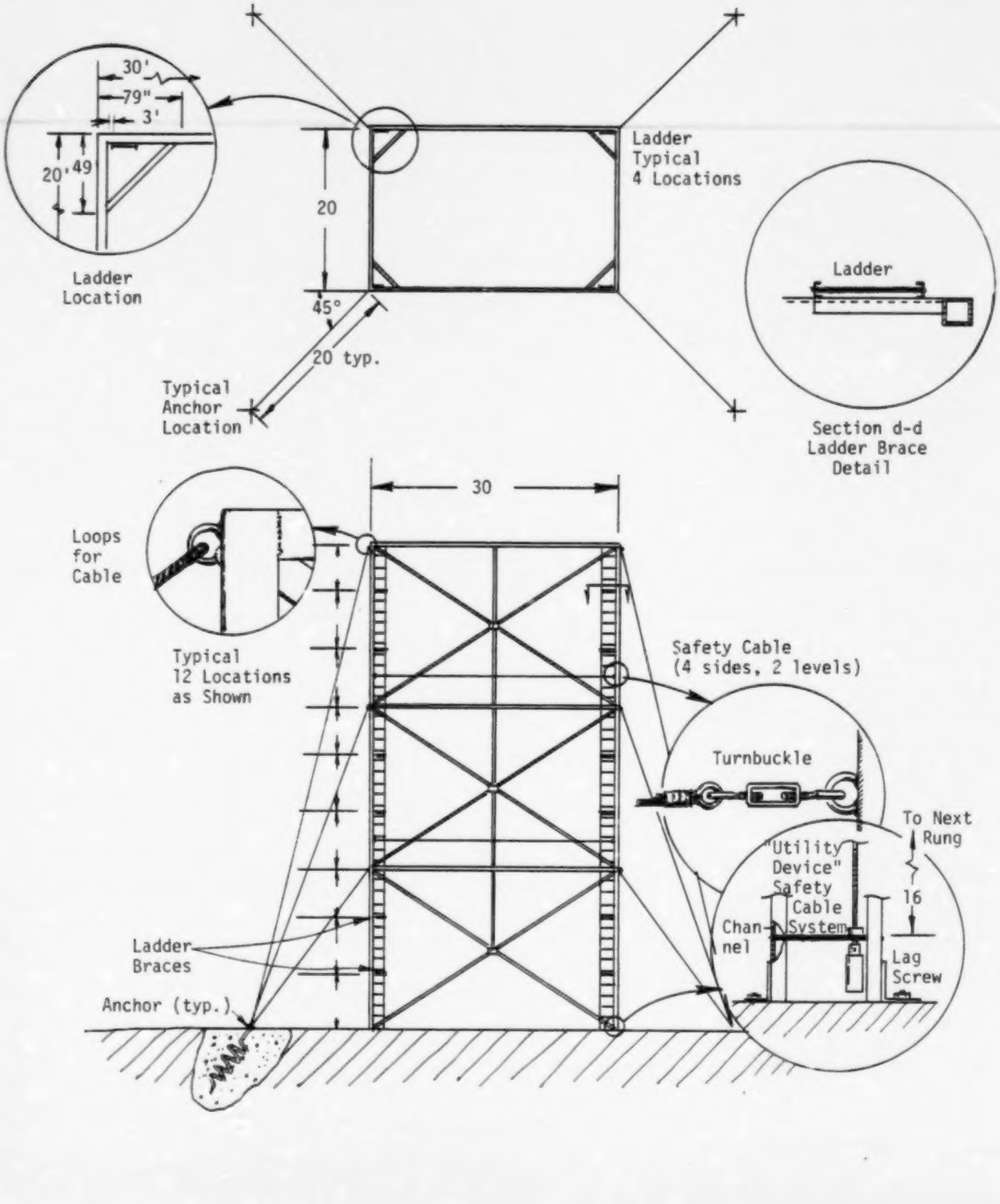
30'
79"
3'
20'
49
Ladder Location
20
45°
20 typ.
Typical Anchor Location
Ladder Typical 4 Locations
Ladder
Section d-d Ladder Brace Detail
30
Loops for Cable
Typical 12 Locations as Shown
Safety Cable (4 sides, 2 levels)
Turnbuckle
To Next Rung
"Utility Device" Safety Cable System
16
Chan-nel
Lag Screw
Ladder Braces
Anchor (typ.)

Figure 10-1. Support structure for sampling hood and rake probes.

11.0 DATA SYSTEM

Data are recorded manually and with the aid of a data logger, and strip-chart recorders.

11.1 Data Logger

A data-logger (Esterline-Angus Model D2020) is used to scan and print up to 20 voltage signals at 2 channels/second. It is used primarily to log the temperatures of the probe, structure, and fuel gases.

11.2 Strip Recorder

A 6-pen chart recorder (Soltec Model 3306) continuously records the output of the O_2, CO, CO_2, HC and the SO_2 analyzers. It also records the wind speed measured by the 3-cup anemometer.

12.0 Orifice Flowmeter Calibration

The orifice plates were calibrated using air and calibrated laminar flowmeters. The apparatus used to calibrate the orifice meters is shown in Figure A-1. The flow rate through the laminar flowmeters and orifices is adjusted with a control valve and the following data are recorded:

- P_1 - pressure at upstream tap of laminar flowmeter
- P_2 - pressure at upstream tap of orifice flowmeter
- ΔP_1 - differential pressure across laminar flowmeter
- ΔP_2 - differential pressure across orifice flowmeter
- T - air temperature upstream of laminar flowmeter

The flow rate of air is calculated from P_1, ΔP_1 and T using the equation with the following form:

$$\text{Flow Rate} = \left(a(\Delta P_1) + b(\Delta P_1)^2\right) \times \left(\frac{P_1 + 14.7}{14.7}\right) + \left(\frac{530}{460 + T}\right)$$

where flow rate is in SCFM (1 atmos, 70°F)

ΔP_1 - is in inches water column

P - is in psig

T - is in °F

Table A-1 lists the calibration constants for the laminar flowmeters. The calculated characteristics of the orifice flowmeters use the following equation:

$$q = K \times \frac{1}{\sqrt{MW}} \times F\,\text{gas} \times \sqrt{h_{H_2O}} \times \sqrt{\frac{P + 14.7}{T + 460}}$$

where

q = SCFM

TABLE A-1. CALIBRATION CONSTANTS OF LAMINAR FLOWMETERS

MODEL	SERIAL NO.	a	b	FLOW @ 8" W.C. /atm, 70°F (SCFM)
50 MY 15-6	S-4291-1	51.27	-0.4479	381.5
50 MW 20-2	R-3049-1	10.0125	-0.071875	75.5

K = orifice flow calibration content

MW = molecule weight of gas

F_{gas} = correction factor for gas other than air

$F_{air} = 1$, $F_{propane} - 1.14$

h_{H_2O} = pressure drop in inches of water

P = pressure of gas at orifice, psig

T = temperature of gas at orifice, °F

Table A-2 lists the orifice flow calibration constant, K, of the orifice flowmeters.

TABLE A-2. ORIFICE FLOWMETERS CALIBRATION CONSTANTS

ORIFICE NUMBER	UPSTREAM ID (inch)	BORE DIAMETER (inch)	FLOW FACTOR, K	STANDARD DEVIATION OF K	FLOW of AIR @ 20" WC 1 atm, 70°F (SCFM)
F1	2.469	1.91	7366	266	295.0
F2	1.610	1.03	1806	45	72.3
F3	0.824	0.52	460.5	5.6	18.4
F4	0.824	0.28	120.3	3.7	4.82
F5	2.469	1.68	5041	17	201.8
F6	1.610	0.87	1195	35	47.8
F7	0.824	0.44	310.7	10.3	12.4
F8	0.824	0.22	73.65	2.80	2.97
F9	2.469	1.92	7307	215	2930
F10	1.610	1.04	1821	36	72.9
F11	0.824	0.52	470.8	9.3	18.8
F12	0.824	0.28	135.2	10.3	5.41

$$\text{Flow} - K \times \frac{1}{\sqrt{MW}} \times F\,\text{gas} \times \sqrt{h} \times \sqrt{\frac{P + 14.7}{T + 460}}$$

Flow = SCFM
h = Inch of Water
P = psig
T = °F
MW = Molecular Weight

APPENDIX B
TESTING METHODOLOGY

The methodology used in testing is discussed in Appendix B in sections on:

- Background concentration determinations
- Test conditions
- Sample collection
- Analytical procedures
- Visual observations
- Data reduction

Background Concentration Determinations

During the early phases of the test program, the background concentrations of O_2, CO, CO_2 and HC were found to be comparable with those from the flare flame. Hence, local combustion efficiencies need to be corrected for the concentration of the species in the background. To accomplish this, the concentration of the species in the background is determined prior to each test.

The background samples are collected and analyzed following a procedure identical to that for sampling of the flare gases. The facility equipment is operated normally except that the flare flame and pilot flames are not lit. During sampling for the background concentrations, the probe is located in the same position as it is for sampling from the flare flame. Table B-1 lists the range of background concentrations for O_2, CO, CO_2, HC, soot, and SO_2 measured during the testing period.

Test Conditions

The flare test facility was designed to achieve the test operating conditions with ease. The operating parameters are:

- Flare head type and size
- Fuel composition
- Gas exit velocity
- Steam to combustible gas ratio
- Tracer flow (SO_2)

TABLE B-1. BACKGROUND SPECIES CONCENTRATIONS

SPECIES	MEAN	MINIMUM	MAXIMUM
O_2	21%	21%	21%
CO	2.22 ppm	0.0 ppm	6.7 ppm
CO_2	694 ppm	519 ppm	927 ppm
HC	3.17 ppm	1.5 ppm	7.15 ppm
Soot	0.50 ppm	0 ppm	1.32 ppm
SO_2	0.17 ppm	0 ppm	3.6 ppm

Although not a daily operation, changing the flare head was a simple procedure and could be accomplished in three to four hours. The supply for nitrogen, propane, and natural gas were set on a flow system designed to avoid transient fluctuations. The flow rates of these gases were held constant during testing, which usually lasted twenty minutes.

A small boiler supplied steam to the SO_2 vaporizer, the sample probes, and the flare head steam injectors. Steam used for the vaporizers and sample probes was a small fraction of the total boiler output. Steam flow to the flare head was held constant up to the boiler's capacity of about 400 lbs/hr. Steam lines were preheated and drained prior to trials using steam injection. The lines were heated using steam flow until no water was ejected from the nozzles. This typically required about twenty minutes. After heating and draining the trap, steam flow rate was set by a manual valve and determined from the differential pressure across a calibrated orifice.

The flow rate of tracer was monitored by rotameters and controlled by manual valves. The maximum safe flow rate of SO_2 was limited to 7 standard cubic feet per hour by the vaporizer capacity.

Sample Collection

Samples were collected by two methods. For small flare flames, the sample hood collected the entire plume into a mixing chamber where gas and particulates were sampled with a single probe. For larger flames, samples were drawn simultaneously by five probes spaced on a diameter above the flare flame.

The sample probes were of a uniform design, as shown in Appendix A. Gas was sampled at about 30- to 45-standard-cubic-feet per hour. A 6-inch-long, 0.250-inch OD, 0.19-inch ID, stainless steel tube was used as the probe nozzle. This resulted in gas entrance velocities of about 50 feet-per-second. This value was usually higher than the plume rise velocity. However, the soot particulates are small and the error caused by anisokinetic sampling is unimportant.

The probe tip held a glass fiber filter to capture solid particles. The probes were steam-heated to 212°F to minimize moisture condensation and loss of condensibles and soluble gas species. Moisture was removed by Permapure dryers and the samples cooled to room temperature downstream of the dryers.

Gas samples could be analyzed on a real-time basis for O_2, CO, CO_2, HC, and SO_2, but usually were stored temporarily in Tedlar bags for analysis. The method of continual analysis could give on-line information. However, experience showed that the real-time concentration readings fluctuated over a very wide range due to the intermittent nature of the flare flame. Integration of the traces could not determine the concentration as reliably as mixing the gas in the Tedlar bags prior to analysis. Hence, the gas samples were collected in Tedlar bags before analysis, for all tests. Mixing was accomplished by manipulating the bags and by normal diffusion. The contents of the mixed bags were subsequently analyzed for O_2, CO, CO_2, HC and SO_2 concentrations.

Sulfur dioxide was also analyzed by wet chemistry by diverting part of each sample to a bubbler containing 3 percent hydrogen peroxide solution to absorb the sulfur dioxide. The gas bubbling rate and bubbling time interval were recorded for subsequent calculations.

Analytical Procedures

Techniques for determining gas samples are listed in Appendix A. Those for soot and SO_2 concentrations are discussed in this Appendix.

Soot Concentrations

The procedure to determine soot was modified early in the trials. Initially, soot concentration was determined by weighing the filter before and after collection of a soot sample from a known volume of gas. This procedure was unsatisfactory because the filter substrates were fragile and small parts were lost to the filter holder. The procedure developed to eliminate this problem was:

1. Preparation of the filter substrate by baking in an oven at 700°C for one hour.
2. Installation of the filter substrate into the probe tip.
3. Sample collection.
4. Drying the filter on the sample specimen at 70°F for one hour in an oven.
5. Weighing the filter and specimen.

6. Burning the combustible material from the filter in an oven at 700^{0} for one hour.

7. Determination of the loss in weight of the filters on combustion.

This method yielded improved results because:

- Chances of losing part of the filter substrate are reduced, because the filters are protected throughout the steps that are critical in determining sample weight.
- Burning the sample will measure only the combustible products, and non-combustible materials, such as airborne soil, will not contribute to the weight loss.
- The only disadvantage is destruction of the solid sample.

For calculations of combustion efficiency, the gas and the solid must be converted to a consistent set of units. This is accomplished by converting the soot loading to the equivalent parts-per-million of gaseous carbon. The concentration of the solids in the gas sample is determined as pounds-of-solid per standard-cubic-foot of gas. This is converted to pound-moles-of-carbon per cubic-foot of gas by:

$$\chi \, \frac{\text{lb carbon}}{\text{ft}^3} = \chi \, \frac{\text{lb carbon}}{\text{ft}^3} \times \frac{\text{1 lb mole carbon}}{\text{12 lb carbon}} = \frac{\chi}{12} \, \frac{\text{lb moles carbon}}{\text{ft}^3} \tag{B-1}$$

The mole density of an ideal gas at standard conditions is:

$$\rho \text{ mole, gas} = \frac{P}{RT} = \frac{14.7}{10.73 \times 530} = \frac{\text{lb moles}}{\text{ft}^3} = 2.585 \times 10^{-3} \, \frac{\text{lb moles}}{\text{ft}^3} \tag{B-2}$$

Therefore, the equivalent solid concentration in parts per million by volume is:

$$[\text{soot}] = \frac{\frac{\chi}{12} \, \frac{\text{lb moles carbon}}{\text{ft}^3 \text{ gas}}}{2.585 \times 10^{-3} \, \frac{\text{lb moles}}{\text{ft}^3 \text{ gas}}} \times 10^6 \text{ ppm} = \frac{\chi}{3.1019 \times 10^{-2}} \times 10^6 \text{ ppm}$$

$$= 3.224 \times 10^6 \, \chi \text{ ppm} \tag{B-3}$$

where χ is the concentration of solids in pounds-per-standard-cubic-foot of sampled gas.

SO_2 Determinations

Sulfur dioxide is determined by withdrawing gas samples with a vacuum pump, bubbling them through 25 ml of 3-percent hydrogen peroxide solution for 20 minutes. Sulfur dioxide is absorbed in the solution which is chilled by an icewater bath.

After sampling, the solution is analyzed for sulfur dioxide in an in-house analytical laboratory. Isopropyl alcohol (IPA) is added to the sample to produce an 80-percent IPA solution. The solution is titrated with standardized barium perchloride solution using thorium as an indicator. To attain a Salmon endpoint, the background of the solution is determined by titrating the same amount of 80-percent IPA / 20-percent distilled water solution using the same IPA.

The concentration of SO_2 in the original gas sample is calculated as follows:

$$Vs(STP) = Vs \times 28.3 \times \frac{273}{273 + T} \times \frac{B\text{-}V.P.}{29.92} \qquad \text{(B-4)}$$

where Vs(STP) = Volume sampled corrected to standard conditions, liter

Vs = Volume sampled

T = average temperature during sampling in °C

B = barometer reading for atmospheric pressure

V.P. = average vacuum pressure during sampling

$$\text{ppm } SO_2 = \frac{(V_S - V_B)\ (N_{Ba(ClO_4)_2}\ (11.2 \times 10^3)}{V_S(STP)} \qquad \text{(B-5)}$$

where V_S = volume of $Ba(ClO_4)_2$ titrant added to sample to obtain endpoint (ml)

V_B = volume of $Ba(ClO_4)_2$ titrant added to obtain endpoint in a blank solution (ml)

$N_{Ba(ClO_4)_2}$ = normality of barium perchlorate

V_S(STP) = gas volume sampled, corrected to standard conditions

Visual Observations

The first phase of the test program focused on determining the visual characteristics of the flare flames under a wide range of operating conditions. Table B-2 lists the conditions used for photography, high-speed cinematography, and video recording.

The cameras were mounted on a platform 15-feet above the ground and 30-feet away from the flare head. From this position, the largest flame (40-feet) would subtend an angle of about 55°. However, most flames were less than 30-feet long and would subtend an angle less than 45°. Under these conditions the cameras were able to record three-quarters of the flame for the largest flames studied in this investigation.

The luminous flames, i.e., those produced from high-heating-value fuels, were capable of being recorded with all techniques. The non-luminous blue flames produced with low-heating-value fuels had insufficient luminosity for them to be photographed with time exposures less than 10 seconds. However, high-quality pictures of flames burning low-heat-value fuels were produced at night when interference from background light sources was reduced.

Operators recorded visual observations of the flame structure during the rest of the program. They recorded mean, minimum, and maximum flame lengths, deflection of the flame caused by crosswind, the spread angle of the flame, the maximum width of the flame, the flame liftoff distance from the flare head, the flame color, the density of smoke, and the amount of combustion noise. Estimates are based on the judgment of the operators, so fluctuations of the flame structure could result in potential errors. However, these errors are limited to less than 20-percent of the recorded observations.

Data Reduction

The procedure for calculating the operating conditions, the combustion efficiencies, and estimating the potential error in the combustion efficiencies are discussed in Appendix C.

TABLE B-2. PHOTOGRAPHIC SETTINGS

TECHNIQUE	EQUIPMENT	RECORD MEDIA	FRAME SPEED	EXPOSURE TIME	COMMENTS
Photography	Canon AE-1 with 1) 50 mm f 4 lens 2) 75-200m zoom f 3.5 lens	Kodacolor II ASA 100	N/A	10 sec	• For time-averaged flame shapes, lengths, color. • Needed for low-luminosity flames picture. • Must be used at night. Daylight overexposes pictures.
				0.001 sec	• For instantaneous flame features. • Cannot record images for low-luminosity flames. • Can be used day and night.
		Kodak Plus X	N/A	All	• Not useful in daylight. Interference by background images. • Not useful for discriminating flame features.
High-Speed Cinematography	Redlake Hycam with Canon 16-120 mm zoom f 2.0 lens	Kodak 7239 Video News film Daylight ASA 160 100- & 400-foot rolls	100 Frames/sec 200 Frames/sec 400 Frames/sec		• Film processing pushed to ASA 640. • Operation at low range of camera speed was not optimum. • Reflex view finder not available. Made aiming and focusing difficult. • Maximum iris opening f 4.0. • Brightness acceptable for luminous flames. • Images on successive frames can be tracked reasonably well. • Brightness marginally acceptable for luminous flames. • Images on successive frames clearly traceable. • Brightness not acceptable for non-luminous flames. • Images do not permit satisfactory discrimination of flame structures. • Does not provide color information.
Video Monitor	Panasonic Model Camera JVC Model Video Recorder Amder Color Monitor	Kodak Black & White Scotch Video Cassette Tape 1" wide, 1-hr. capacity.			• Light sensitivity range narrow. • Time resolution is slow. • Color faithfulness is arbitrary and can be tuned by viewer. • Cannot discriminate flame features. • Useful only for general flame appearance.

APPENDIX C

DATA SUMMARY TABLES

The summary tables of all test data are provided in this appendix and are grouped by the size of the flare head. The entries are self-explanatory, with the exception of the observations which require further clarification. The observations were made by the test operator during sampling.

Wind is the wind speed monitored by a three-cup anamometer located 10 feet above the roof of the 10-foot high control room. The anemometer is about 40 feet from the flare head and outside the windscreens. Hence the flare flames were affected by less wind than measured.

Flame Length is the "average" flame length observed using a 2-foot grid mark on the probe support structure.

Lift Off is the distance between the flare head and the ignition print, identified by onset of visible radiation.

Color is a subjective description by the operator.

Smoke is a subjective assessment. Particulate concentrations are determined by the filter procedure discussed in Appendix B.

TABLE C-1. DATA SUMMARY FOR 3-INCH FLARE HEAD, [illegible] LOW VELOCITY

FLARE HEAD: EER SIZE: 3-INCH*

Purpose of Test	Test Number	Flame Retention Ring	Actual Exit Velocity (ft/sec)	Nominal Exit Velocity (ft/sec)	Low Heating Value (Btu/ft^3)	Fuel in Nitrogen (Percent)	Steam Ratio (lb.Steam /lb.Fuel)	Observations					Sample Method R=Rake H=Hood	Probe Position (ft)	Combustion Efficiency (Percent)
								Wind Speed (MPH)	Flame Length (ft)	Lift Off (Inches)	Color	Smoke			
Combustion Efficiency 56 Percent C_3H_8	001	No	0.5	0.5	1311	55.8	0.0	Low	4	0	Yellow	Yes	R	7	99.49
	002		0.5	0.5	1311	55.8	0.0	Low	4	0	Yellow	Yes	H	10	98.37
	003		0.5	0.5	1309	55.7	0.0	Low	4	0	Yellow	Yes	R	9	98.77
	004		0.5	0.5	1311	55.8	0.0	Low	4	0	Yellow	Yes	R	3	99.06
	005		2.0	2.0	1318	56.1	0.0	Low	7	0	Dk.Yel	Yes	H	4	99.54
	006		2.0	2.0	1314	55.9	0.0	Low	7	0	Yellow	Yes	R	5	94.24
	007		2.0	2.0	1314	55.9	0.0	Low	6.5	0	Yellow	Yes	R	8	99.64
	008		2.0	2.0	1314	55.9	0.0	Low	6	0	Yellow	Yes	R	10	98.95
	009		9.9	9.9	1325	56.4	0.0	Low	15	0	Yellow	Yes	H	10	99.74
	010		10.0	10.0	1316	56.0	0.0	Low	15	0	Yellow	Yes	R	10	98.69
	011		10.0	10.0	1323	56.3	0.0	2-4	15	0	Yellow	Yes	R	13	95.66
	012		10.0	10.0	1323	56.3	0.0	2-4	15	0	Yellow	Yes	R	15	98.78
Effect of Steam	013	No	0.5	0.5	273	11.6	0.0	0-1	4	0	Barely Visible	No	H	0	90.19
	016		10.0	10.0	1323	56.3	0.142	0-8	10	0	Yellow	Little	H	7	99.83
	017		10.0	10.0	1323	56.3	0.300	0-6	10	2	Yellow	Little	H	9	99.96
	018		10.0	10.0	1321	56.2	0.500	-	9	2-4	Yellow	Little	H	9	99.89
	019		10.0	10.0	1323	56.3	1.000	-	6	4	Yellow	Little	H	9	98.94
Low Btu	020	No	12.0	12.0	620	26.4	0.0	-	-	-	Yellow	Yes	H	9	99.12
	021		2.1	2.1	343	14.6	0.0	3-5	4	4-10	Yellow	Yes	H	4	99.29
	051		2.1	2.1	362	15.4	0.0	0-5	4	0-5	Yel/Ora	No	R	3	91.81
	052		2.1	2.1	376	16.0	0.0	0-3	3-5	0-3	Yel/Ora	No	R	5	98.09

TABLE C-2. DATA SUMMARY FOR EER 3-INCH FLARE HEAD, HIGH VELOCITIES

FLARE HEAD: EER SIZE: 3-INCH*

Purpose of Test	Test Number	Flame Retention Ring	Actual Exit Velocity (ft/sec)	Nominal Exit Velocity (ft/sec)	Low Heating Value (Btu/ft^3)	Fuel In Nitrogen (Percent)	Steam Ratio (lb.Steam /lb.Fuel)	Wind Speed (MPH)	Flame Length (ft)	Lift Off (Inches)	Color	Smoke	Sample Method R=Rake H=Hood	Probe Position (ft)	Combustion Efficiency (Percent)
High-Velocity, No Flame Retention Ring	77	No	39.6	39.6	1316	56.0	0.0	0-3	24	5-9	Yellow	Yes	R	25	95.11
	78	No	80.0	80.0	1325	56.4	0.0	-	28	12-13	Yel/Ora	Yes	R	33	98.40
	79	No	118.5	118.5	1307	55.6	0.058	1-5	32	18	Yel/Ora	Yes	R	35	99.66
High-Vel, 56% C_3H_8	80	Div 40.0%	420.5	168.2	1255	53.4	0.015	0-1	33	24	Clr/Ora	No	R	34	99.20
	81		67.0	26.8	837	35.6	0.149	0-1	17.5	8-10	Orange	No	R	20	97.27
	82		248.3	99.3	1107	47.1	0.031	0-1	31	24	Orange	No	R	35	99.33
High-Vel, 100% C_3H_8	83	Div 40.0%	144.5	57.8	2350	100.0	0.131	0-1	29.5	12	Orange	No	R	33	99.87
High-Vel, 100% C_3H_8	92	Conv 46.3%	171.4	79.3	2350	100.0	0.060	0-3	30	12-15	Yellow	No	R	36	99.60
	93		84.7	39.2	2348	99.9	0.122	0-5	26.5	10	Orange	No	R	31	99.74
	94		171.4	79.3	2350	100.0	0.061	0-3	34.5	12	Yel/Ora	Little	R	37	99.83
High-Velocity, Stable Flame Limit	95	Conv 46.3%	114.8	53.1	792	33.7	0.087	0-2.5	23	12-18	Yellow	No	R	26	99.87
" " "	96		274.1	126.8	1043	44.4	0.028	0-1.5	33	18-28	Yel/Ora	No	R	37	99.85
High-Vel, 50% C_3H_8	97	Conv 46.3%	85.8	39.7	1156	49.2	0.142	1-5	20	8	Orange	No	R	24	99.72
" " "	98		172.3	79.7	1133	48.2	0.071	0-2	29	7	Yel/Ora	No	R	34	99.87
High-Vel, Stable Flame Limit	99	Conv 46.3%	428.2	198.1	1027	43.7	0.018	0-1	30.5	24-36	Orange	No	R	35	99.38
High-Vel, 50% C_3H_8	100	Conv 46.3%	343.1	158.7	1149	48.9	0.020	0-4	34	24-30	Orange	No	R	37	99.84
High-Vel, 77% C_3H_8	101	Conv 46.3%	85.8	39.7	1807	76.9	0.091	1-4	25	6	Orange	No	R	29	99.73
	102		170.1	78.7	1805	76.8	0.080	1-5	30.5	12	Yel/Ora	Little	R	34	99.74
	103		260.1	120.3	1795	76.4	0.060	0-1.5	37	8	Yellow	No	R	37	99.88
High-Vel, Stable Flame Limit	104	Conv 46.3%	375.5	173.7	921	39.2	0.023	0-1.5	29.5	36-48	Orange	No	R	30	94.81
High-Vel, 100% C_3H_8	105	Conv 46.3%	243.4	112.6	2350	100.0	0.049	0-5	40	12	Orange	Yes	R	42	99.77

TABLE C-3. DATA SUMMARY OF EER 6-INCH FLARE HEAD

FLARE HEAD: EER SIZE: 6-INCH*

Purpose of Test	Test Number	Flame Retention Ring	Actual Exit Velocity (ft/sec)	Nominal Exit Velocity (ft/sec)	Low Heating Value (Btu/ft^3)	Fuel in Nitrogen (Percent)	Steam Ratio (lb.Steam /lb.Fuel)	Wind Speed (MPH)	Observations				Sample Method R=Rake H=Hood	Probe Position (ft)	Combustion Efficiency (Percent)
									Flame Length (ft)	Lift Off (Inches)	Color	Smoke			
Combustion Efficiency 56 Percent C_3H_8	22	No	1.0	1.0	1293	55.0	0.0	0-5.5	8	0	Yellow	Yes	H	7	99.60
	23		2.8	2.8	1314	55.9	0.0	0-10	9	0	Yellow	Yes	H	11	99.81
	24		2.8	2.8	1314	55.9	0.0	0-5	15	0	Yel/Ora	Yes	H	5	99.81
	25		2.8	2.8	1314	55.9	0.0	0-10	15	0	Yel/Ora	Yes	H	8	99.75
	26		2.8	2.8	1314	55.9	0.0	0-15	15	0	Yel/Ora	Yes	H	15	99.76
Effect of Steam	27	No	2.8	2.8	1314	55.9	0.316	0-4	14	0	Lt Yel	No	H	9	99.92
56 Percent C_3H_8	28	No	2.9	2.9	1318	56.1	0.0	0-10	10	0	Yellow	Yes	R	7	94.15
	29		2.9	2.9	1318	56.1	0.0	NA	11	0	Yellow	Yes	R	13	99.56
	30		2.9	2.9	1323	56.3	0.0	NA	12	0	Yellow	Yes	R	17	98.47
	31		10.1	10.1	1316	56.0	0.0	NA	20	0	Yellow	Yes	R	21	98.90
Effect of Steam	32	No	2.9	2.9	1316	56.0	0.563	0-5	13	0	Yellow	No	H	8	99.89
Low Btu	33	No	1.1	1.1	338	14.4	0.0	NA	4	2-3	Yel/Blu	No	H	1	96.35
	34		3.1	3.1	414	17.6	0.0	NA	6	6-12	Yel/Blu	No	H	5	98.93
	35		3.1	3.1	451	19.2	0.0	NA	7	3-8	Yellow	No	R	6	86.93
	36		3.1	3.1	454	19.3	0.0	NA	7	3-6	Yellow	No	R	10	98.06
	37		3.1	3.1	451	19.2	0.0	NA	8	3-6	Yellow	No	R	15	92.24
	38		11.7	11.7	613	26.1	0.0	NA	13.5	6-8	Yellow	No	R	20	98.76
	69		3.0	3.0	336	14.3	0.0	0	5.5	0-5	Orange	No	R	10	97.11
	70		1.0	1.0	287	12.2	0.0	0-3	4	0-3	Orange	No	R	5	99.14
	71		10.3	10.3	343	14.6	0.0	0	15	0-5	Orange	No	R	17	99.36
	72		2.9	2.9	345	14.7	0.0	0-2	8	0	Clear	No	R	5	93.49
	73		1.0	1.0	291	12.4	0.0	0-4	5	0	Clear	No	R	10	97.97
	74		2.9	2.9	350	14.9	0.0	0-1	10	0-7	Orange	No	R	15	99.02
56 Percent C_3H_8	75	No	2.9	2.9	1321	56.2	0.0	0-2	13.5	0	Yellow	Yes	R	17	99.66
	76		1.0	1.0	1311	55.8	0.0	0-3	8	0	Orange	Yes	R	17	99.54

TABLE C-4. DATA SUMMARY FOR EER 12-INCH FLARE HEAD

FLARE HEAD: EER SIZE: 12-INCH*

Purpose of Test	Test Number	Flame Retention Ring	Actual Exit Velocity (ft/sec)	Nominal Exit Velocity (ft/sec)	Low Heating Value (Btu/ft^3)	Fuel in Nitrogen (Percent)	Steam Ratio (lb.Steam /lb.Fuel)	Wind Speed (MPH)	Observations				Sample Method R=Rake H=Hood	Probe Position (ft)	Combustion Efficiency (Percent)
									Flame Length (ft)	Lift Off (Inches)	Color	Smoke			
Combustion Efficiency 56 Percent C_3H_8	39	No	0.2	0.2	1309	55.7	0.0	NA	6	0	Yellow	Yes	R	13	98.29
	40		2.0	2.0	1323	56.3	0.0	NA	19	0	Yellow	Yes	R	23	99.24
	41		4.1	4.1	1314	55.9	0.0	NA	25	0	Yellow	Yes	R	29	99.50
	42		4.0	4.0	1314	55.9	0.0	NA	23	0	Yellow	Yes	R	22	99.48
	43		4.1	4.1	1318	56.1	0.0	NA	23	0	Yellow	Yes	R	35	99.50
Low Btu	44	No	2.1	2.1	378	16.1	0.0	NA	12	0	Yellow	No	R	22	99.73
City Gas	45	No	0.2	0.2	980	99.4 City Gas	0.0	NA	4	0	Orange	Little	R	9	99.91
Low Btu	46	No	0.2	0.2	451	19.2	0.0	NA	4	0	Orange	Little	R	9	98.62
	47		4.1	4.1	385	16.4	0.0	NA	13	10	Orange	No	R	23	94.89
	48		4.2	4.2	390	16.6	0.0	NA	15	0	Yellow	No	R	19	96.71
	49		4.2	4.2	385	16.4	0.0	NA	13	0	Orange	No	R	14	99.73
Steam, Smokeless	50	No	4.0	4.0	1323	56.3	0.457	NA	23	0	Yellow	Little	R	30	99.32

TABLE C-5. DATA SUMMARY FOR 12-INCH INDUSTRIAL FLARE HEAD A

FLARE HEAD: Industrial SIZE: 12-INCH*

Purpose of Test	Test Number	Flame Retention Ring	Actual Exit Velocity (ft/sec)	Nominal Exit Velocity (ft/sec)	Low Heating Value (Btu/ft^3)	Fuel in Nitrogen (Percent)	Steam Ratio (lb.Steam /lb.Fuel)	Wind Speed (MPH)	Observations				Sample Method R=Rake H=Hood	Probe Position (ft)	Combustion Efficiency (Percent)
									Flame Length (ft)	Lift Off (Inches)	Color	Smoke			
Combustion Efficiency 56 Percent C_3H_8	62	Yes	2.0	1.9	1269	54.0	0.0	0-3	18	0	Yellow	Yes	R	22	99.12
	63		4.3	4.0	1318	56.1	0.0	0-3	24	0	Yellow	Yes	R	25	99.37
Low Btu	64	Yes	4.5	4.2	392	16.7	0.0	0-2	21	0	Yellow	No	R	23	98.49
Steam, Smokeless	65	Yes	4.3	4.0	1318	56.1	0.511	0-4	25	0	Yellow	Vry Ltl	R	25	99.85
56 Percent C_3H_8	66	Yes	4.3	4.0	1316	56.0	0.0	0-4	23	0	Yellow	Yes	R	22	99.63
	67		4.3	4.0	1316	56.0	0.0	0-2	22	0	Yellow	Yes	R	28	99.61
	68		0.22	0.2	1309	55.7	0.0	0-2	6	0	Orange	Yes	R	8	99.78

TABLE C-6. DATA SUMMARY FOR 12-INCH INDUSTRIAL FLARE HEAD B

FLARE HEAD: Industrial SIZE: 12-INCH*

Purpose of Test	Test Number	Flame Retention Ring	Actual Exit Velocity (ft/sec)	Nominal Exit Velocity (ft/sec)	Low Heating Value (Btu/ft^3)	Fuel in Nitrogen (Percent)	Steam Ratio (lb.Steam /lb.Fuel)	Wind Speed (MPH)	Observations				Sample Method R=Rake H=Hood	Probe Position (ft)	Combustion Efficiency (Percent)
									Flame Length (ft)	Lift Off (Inches)	Color	Smoke			
Combustion Efficiency 56 Percent C_3H_8	84	Yes	2.9	1.9	1276	54.3	0.0	0	22.5	0	Yellow	Yes	R	27	99.54
	85		6.0	4.0	1316	56.0	0.0	NA	27	0	Yel/Ora	Yes	R	32	99.65
	86		0.3	0.2	1314	55.9	0.0	NA	5.5	0	Orange	Yes	R	10	99.48
	87		6.0	4.0	1314	55.9	0.0	0-2	25	0	Yel/Ora	Yes	R	28	99.58
Low Btu	88	Yes	3.0	2.0	317	13.5	0.0	0-3.5	10.5	0	Clr/Ora	No	R	15	99.21
	89		6.2	4.1	303	12.9	0.0	0-2	20	0	Orange	No	R	24	99.72
	90		0.3	0.2	315	13.4	0.0	0-3	4	0	Orange	No	R	6	99.59
Steam, Smokeless	91	Yes	5.9	3.9	1311	55.8	0.441	0-5	23	0	Orange	Very Little	R	27	99.84

TABLE C-7. DATA SUMMARY FOR 12-INCH INDUSTRIAL FLARE HEAD C

FLARE HEAD: Industrial SIZE: 12-INCH*

Purpose of Test	Test Number	Flame Retention Ring	Actual Exit Velocity (ft/sec)	Nominal Exit Velocity (ft/sec)	Low Heating Value (Btu/ft^3)	Fuel in Nitrogen (Percent)	Steam Ratio (lb.Steam /lb.Fuel)	Wind Speed (MPH)	Observations				Sample Method R=Rake H=Hood	Probe Position (ft)	Combustion Efficiency (Percent)
									Flame Length (ft)	Lift Off (Inches)	Color	Smoke			
Combustion Efficiency	53	Yes	0.65	0.2	1309	55.7	0.0	0-2	5.5	0	Yel/Ora	Yes	R	11	99.28
56 Percent C_3H_8	54		6.50	2.0	1316	56.0	0.0	0-2	15	3-5	Yellow	Yes	R	24	99.08
	55		13.3	4.1	1328	56.5	0.0	0-2	21	0	Yel/Ora	Yes	R	27	99.65
	56		13.0	4.0	1316	56.0	0.0	1-5	21	0	Yel/Ora	Yes	R	22	99.28
	57		13.0	4.0	1316	56.0	0.0	NA	21	0.0	Yel/Ora	Yes	R	20	98.18
Low Btu	58		6.8	2.1	371	15.8	0.0	0-1	15	0	Yellow	No	R	18	99.52
56 Percent C_3H_8 Steam	59		13.0	4.0	1314	55.9	0.456	NA	23.5	0	Yel/Ora	Little	R	27	99.55
Low Btu	60		14.63	4.5	522	22.2	0.0	0-3	15	0-12	Yellow	Little	R	25	91.16
Low Btu	61		0.65	0.2	458	19.5	0.0	0-2	3	0	Yellow	Little	R	6	99.50

APPENDIX D

INTEGRATED COMBUSTION EFFICIENCIES

The tables in this appendix list test conditions of the flare flames and the "integrated" combustion efficiencies calculated according to the procedure described in Section 3.3. Most of the designations are clear.

The SIZE column lists the nominal diameters of the various flare heads. The actual dimensions of the EER test flare heads are listed in Appendix A. The SIZES of the industrial flare heads are designations by the manufacturer and do not necessarily reflect their physical dimensions.

The VEL column lists the nominal velocity of the gas mixture exiting the flare heads. These are calculated from the measured component gas flow rates and the flow area based on the nominal SIZE of the flare heads. For the flare heads which have nozzle flow areas different from the nominal value, the gas velocity can be significantly higher. Both the nominal and actual gas exit velocities are tabulated in Appendix C.

STEAM RATIO indicates the mass flow of steam injected per pound of combustible. The mass flow of combustible gas, rather than the total gas flow (i.e., it excludes nitrogen), is used because only the combustible fraction has a tendency to smoke and nitrogen does not increase the fuel's tendency to smoke.

HT is the height of the probe tip above the flare heads.

The EFFICIENCIES are the results of the integration procedure described in Section 3.3.

DATA PRINTED ON 18-OCT-83 16:00:18 FILE : FLARE.DAT

PT NO	DATE	FLAREHEAD	SIZE (IN)	VEL (FPS)	C3H8 (%)	CH4 (%)	STEAM RATIO	SAMPLE METHOD	HT (FT)	EFFICIENCY (%) CO	HC	SOOT	TOTAL
1	12-14-82	EER-PROTO	3.0	0.5	55.8	0.0	0.000	RAKE	7.0	100.00	100.00	99.49	99.49
3	12-15-82	EER-PROTO	3.0	0.5	55.7	0.0	0.000	RAKE	9.0	99.50	99.61	99.66	98.77
4	12-16-82	EER-PROTO	3.0	0.5	55.8	0.0	0.000	RAKE	3.0	99.61	99.80	99.66	99.06
6	12-17-82	EER-PROTO	3.0	2.0	55.9	0.0	0.000	RAKE	5.0	97.07	97.36	99.81	94.24
7	12-20-82	EER-PROTO	3.0	2.0	55.9	0.0	0.000	RAKE	8.0	100.00	100.00	99.65	99.64
8	12-20-82	EER-PROTO	3.0	2.0	55.9	0.0	0.000	RAKE	10.0	99.58	100.00	99.37	98.95
10	12-21-82	EER-PROTO	3.0	10.0	56.0	0.0	0.000	RAKE	10.0	99.29	99.58	99.83	98.69
11	01-06-83	EER-PROTO	3.0	10.0	56.3	0.0	0.000	RAKE	13.0	99.77	96.14	99.76	95.66
12	01-06-83	EER-PROTO	3.0	10.0	56.3	0.0	0.000	RAKE	15.0	99.81	99.25	99.71	98.78
28	01-24-83	EER-PROTO	6.0	2.9	56.1	0.0	0.000	RAKE	7.0	97.45	97.07	99.63	94.15
29	01-25-83	EER-PROTO	6.0	2.9	56.1	0.0	0.000	RAKE	13.0	99.88	99.84	99.84	99.56
30	01-25-83	EER-PROTO	6.0	2.9	56.3	0.0	0.000	RAKE	17.0	99.83	98.87	99.77	98.47
31	01-25-83	EER-PROTO	6.0	10.1	56.0	0.0	0.000	RAKE	21.0	99.86	99.16	99.87	98.90
35	01-31-83	EER-PROTO	6.0	3.1	19.2	0.0	0.000	RAKE	6.0	96.04	91.03	99.86	86.93
36	01-31-83	EER-PROTO	6.0	3.1	19.3	0.0	0.000	RAKE	10.0	99.69	98.42	99.95	98.06
37	02-01-83	EER-PROTO	6.0	3.1	19.2	0.0	0.000	RAKE	15.0	99.88	92.41	99.96	92.24
38	02-01-83	EER-PROTO	6.0	11.7	26.1	0.0	0.000	RAKE	20.0	99.96	98.84	99.96	98.76
39	02-09-83	EER-PROTO	12.0	0.2	55.7	0.0	0.000	RAKE	13.0	99.87	98.70	99.71	98.29
40	02-14-83	EER-PROTO	12.0	2.0	56.3	0.0	0.000	RAKE	23.0	99.84	99.59	99.81	99.24
41	02-15-83	EER-PROTO	12.0	4.1	55.9	0.0	0.000	RAKE	29.0	99.87	99.92	99.71	99.50
42	02-15-83	EER-PROTO	12.0	4.0	55.9	0.0	0.000	RAKE	22.0	99.88	99.92	99.68	99.48
43	02-16-83	EER-PROTO	12.0	4.1	56.1	0.0	0.000	RAKE	35.0	99.93	99.93	99.63	99.50
44	02-16-83	EER-PROTO	12.0	2.1	16.1	0.0	0.000	RAKE	22.0	99.88	99.89	99.97	99.73
45	02-16-83	EER-PROTO	12.0	0.2	0.0	99.4	0.000	RAKE	9.0	99.99	99.99	99.94	99.91
46	02-17-83	EER-PROTO	12.0	0.2	19.2	0.0	0.000	RAKE	9.0	99.13	99.67	99.82	98.62

DATA PRINTED ON 18-OCT-83 16:00:18 FILE : FLARE.DAT

PT NO	DATE	FLAREHEAD	SIZE (IN)	VEL (FPS)	C3H8 (%)	CH4 (%)	STEAM RATIO	SAMPLE METHOD	HT (FT)	EFFICIENCY (%) CO	HC	SOOT	TOTAL
72	04-18-83	EER-PROTO	6.0	2.9	14.7	0.0	0.000	RAKE	5.0	99.80	93.72	99.96	93.49
73	04-20-83	EER-PROTO	6.0	1.0	12.4	0.0	0.000	RAKE	10.0	99.77	98.27	99.93	97.97
74	04-21-83	EER-PROTO	6.0	2.9	14.9	0.0	0.000	RAKE	30.0	99.71	99.35	99.97	99.04
75	04-21-83	EER-PROTO	6.0	2.9	56.2	0.0	0.000	RAKE	17.0	99.87	99.99	99.80	99.66
76	04-21-83	EER-PROTO	6.0	1.0	55.8	0.0	0.000	RAKE	17.0	99.84	99.97	99.73	99.54
77	05-19-83	EER-PROTO	3.0	39.6	56.0	0.0	0.000	RAKE	25.0	99.90	95.31	99.90	95.11
78	05-19-83	EER-PROTO	3.0	80.0	56.4	0.0	0.000	RAKE	33.0	99.84	98.57	99.99	98.40
79	06-09-83	EER-PROTO	3.0	118.5	55.6	0.0	0.058	RAKE	35.0	99.79	99.88	100.00	99.66
80	06-13-83	EER-RING DIV	3.0	168.2	53.4	0.0	0.015	RAKE	34.0	99.82	99.38	100.00	99.20
81	06-13-83	EER-RING DIV	3.0	26.8	35.6	0.0	0.149	RAKE	20.0	99.48	97.79	100.00	97.27
82	06-14-83	EER-RING DIV	3.0	99.3	47.1	0.0	0.021	RAKE	35.0	99.85	99.48	99.99	99.33
83	06-14-83	EER-RING CON	3.0	57.8	100.0	0.0	0.131	RAKE	33.0	99.87	100.00	100.00	99.87
84	06-15-83	INDUSTRY B	12.0	1.9	54.3	0.0	0.092	RAKE	27.0	99.69	99.96	99.90	99.54
85	06-15-83	INDUSTRY B	12.0	4.0	56.0	0.0	0.000	RAKE	32.0	99.71	99.94	100.00	99.65
86	06-15-83	INDUSTRY B	12.0	0.2	55.9	0.0	0.000	RAKE	10.0	99.54	99.94	100.00	99.48
87	06-16-83	INDUSTRY B	12.0	4.0	55.9	0.0	0.000	RAKE	28.0	99.74	99.85	100.00	99.58
88	06-16-83	INDUSTRY B	12.0	2.0	13.5	0.0	0.000	RAKE	15.0	99.44	99.78	100.00	99.21
89	06-17-83	INDUSTRY B	12.0	4.1	12.9	0.0	0.000	RAKE	24.0	99.76	100.00	99.97	99.72
90	06-17-83	INDUSTRY B	12.0	0.2	13.4	0.0	0.000	RAKE	6.0	99.66	99.93	100.00	99.59
91	06-17-83	INDUSTRY B	12.0	3.9	55.8	0.0	0.441	RAKE	27.0	99.85	99.99	100.00	99.84
92	06-21-83	EER-RING CON	3.0	79.3	100.0	0.0	0.060	RAKE	36.0	99.83	99.77	100.00	99.60
93	06-22-83	EER-RING CON	3.0	39.2	99.9	0.0	0.122	RAKE	31.0	99.77	99.98	100.00	99.74
94	06-23-83	EER-RING CON	3.0	79.3	100.0	0.0	0.061	RAKE	37.0	99.85	99.99	99.99	99.83
95	06-23-83	EER-RING CON	3.0	53.1	33.7	0.0	0.087	RAKE	26.0	99.90	99.98	100.00	99.87
96	06-23-83	EER-RING CON	3.0	126.8	44.4	0.0	0.028	RAKE	37.0	99.88	99.97	100.00	99.85

DATA PRINTED ON 18-OCT-83 16:00:18 FILE : FLARE.DAT

PT NO	DATE	FLAREHEAD	SIZE (IN)	VEL (FPS)	C3H8 (%)	CH4 (%)	STEAM RATIO	SAMPLE METHOD	HT (FT)	EFFICIENCY (%) CO	HC	SOOT	TOTAL
97	06-23-83	EER-RING CON	3.0	39.7	49.2	0.0	0.142	RAKE	24.0	99.76	99.96	100.00	99.72
98	06-24-83	EER-RING CON	3.0	79.7	48.2	0.0	0.071	RAKE	34.0	99.88	99.99	100.00	99.87
99	06-24-83	EER-RING CON	3.0	198.1	43.7	0.0	0.018	RAKE	35.0	99.92	99.97	100.00	99.88
100	06-24-83	EER-RING CON	3.0	158.7	48.9	0.0	0.020	RAKE	37.0	99.91	99.93	100.00	99.84
101	07-07-83	EER-RING CON	3.0	39.7	76.9	0.0	0.071	RAKE	29.0	99.77	99.96	100.00	99.73
102	07-07-83	EER-RING CON	3.0	78.7	76.8	0.0	0.080	RAKE	34.0	99.80	99.94	100.00	99.74
103	07-08-83	EER-RING CON	3.0	120.3	76.4	0.0	0.060	RAKE	37.0	99.90	99.98	99.99	99.88
104	07-08-83	EER-RING CON	3.0	173.7	39.2	0.0	0.023	RAKE	30.0	99.90	99.91	100.00	99.81
105	07-08-83	EER-RING CON	3.0	112.6	100.0	0.0	0.049	RAKE	42.0	99.83	99.95	99.99	99.77

APPENDIX

SAMPLES OF TEST DATA

Data for the 105 tests conducted in this program were compiled and analyzed via computer processing. Examples are show in the following tables:

- Input Flow Conditions
- Measurements
- Combustion Efficiency

Input Flow Conditions which list the flow rates of the propane natural gas, nitrogen, SO_2 and steam flows are in cubic foot (SCF) based on 1 atmosphere pressure and $70^{o}F$ temperature. The calculated concentrations are reported in volume percent (%) and parts per million (ppm). The mass flow rates are reported in pounds per hour based on the theoretical densities of the fuels. The STEAM/GAS ratio is calculated per pound of combustible in the fuel mixture.

Measurements lists the concentrations of O_2, CO, CO_2, HC, Soot, and SO_2 present in the ambient air and the sampled gas. These are reported as volume percent. The numbers following the "+ –" symbols are estimated maximum potential errors of the values reported in the units of the concentration. The numbers below the headings "AT SR=1 BY CO_2" and "AT SR=1 BY SO_2" are the species concentrations that would have been measured if the combustion products were not diluted by ambient air. The method of estimating the maximum potential errors and calculating the undiluted species concentrations are discussed in Section 3.3.

The sampling method and location are listed at the top. For the RAKE probes, the locations are those of the probe tips. For the HOOD probe, the location is that of the inlet of hood. The actual location of the probe is in the sampling chamber which can be 5 to 8 feet above the inlet depending on whether the hood extension is used.

Combustion Efficiency lists the calculated combustion efficiencies based on CO, CO_2, HC, and Soot. These are reported in volume percent (%). The maximum potential errors of each parameter follow the "+ –" symbols and reported in the units of efficiency.

Dilution Factors are the amounts of air entrained in the combustion products. A dilution factor of zero means that no additional air is entrained into the stoichiometries combustion products. A dilution factor of 1 means that the stoichiometries combustion products are diluted by an equal volume of ambient air. The respective maximum potential errors follow the "+ –" symbols and are reported in the unit of the dilution factors.

Other Comments

1. If a dilution factor is zero, it means that the measured CO_2 or SO_2 concentrations is less than those measured in the background. The dilution factor is also zero when the measured O_2 concentration is higher than that in the background. This occurs for extremely dilute plumes. Consequently, the corresponding species concentrations at SR=1 and the combustion efficiencies are small and difficult to determine. This is evident when an entire column consists of only zeros.
2. The "***" indicates that the corresponding number is too large to be printed in the allocated space.

```
DATA PRINTED ON 20-OCT-83   08: 04: 35        FILE : FLARE. DAT

POINT:  1  DATE: 12-14-82   FLAREHEAD: EER-PROTO              SIZE:  3. 0 IN
============================================================================
INPUT FLOW CONDITIONS
VELOCITY =   0. 50 FPS   HV = 1311. 2 BTU/CU FT
PROPANE      0. 824 SCFM  55. 8 %       5. 6 LB/HR     STEAM     =   0. 0 LB/HR
N GAS        0. 000 SCFM   0. 0 %       0. 0 LB/HR     STEAM/GAS = 0. 000
NITROGEN     0. 645 SCFM  43. 7 %       2. 8 LB/HR
SO2          0. 470 SCFH 5304.  PPM    0. 08 LB/HR
============================================================================
MEASUREMENTS WITH  RAKE  AT HEIGHT   7. 0 FT  2. 0 FT FROM FLAREHEAD AXIS
SPECIE       BACKGROUND         MEASURED         AT SR=1 BY CO2   AT SR=1 BY SO2
O2 (%)       21. 00+-  0. 00    20. 90+-  0. 02    0. 00+-   0. 00    0. 00+-  0. 00
CO (PPM)      4. 31+-  0. 40     2. 70+-  0. 40   -0. 00+-1998. 91   -0. 00+-608. 89
CO2(PPM)      742. +-  150.      960. +-  174.  132733 +-401526.  115095. +-******
HC (PPM)      3. 59+-  2. 55     3. 50+-  0. 05   -0. 00+-1656. 06   -0. 00+-******
SOOT(PPM)     0. 86+-  0. 39     1. 28+-  0. 03  258. 77+- 439. 49  224. 30+- 83. 56
SO2(PPM)      0. 00+-  0. 00     0. 80+-  0. 10  485. 48+- 814. 91  420. 61+- 52. 58

COMBUSTION EFFICIENCY (%)
```

```
DATA PRINTED ON 20-OCT-83   08:06:56         FILE : FLARE.DAT

POINT:  1  DATE: 12-14-82   FLAREHEAD: EER-PROTO                 SIZE:  3.0 IN
==============================================================================
INPUT FLOW CONDITIONS
VELOCITY =  0.50 FPS   HV = 1311.2 BTU/CU FT
PROPANE     0.824 SCFM  55.8 %        5.6 LB/HR     STEAM      =   0.0 LB/HR
N GAS       0.000 SCFM   0.0 %        0.0 LB/HR     STEAM/GAS = 0.000
NITROGEN    0.645 SCFM  43.7 %        2.8 LB/HR
SO2         0.470 SCFH 5304. PPM     0.08 LB/HR
==============================================================================
MEASUREMENTS WITH  RAKE  AT HEIGHT   7.0 FT  2.0 FT FROM FLAREHEAD AXIS
SPECIE       BACKGROUND        MEASURED        AT SR=1 BY CO2   AT SR=1 BY SO2
O2 (%)       21.00+-  0.00     20.90+-  0.02     0.00+-   0.00    0.00+-  0.00
CO (PPM)      4.31+-  0.40      2.70+-  0.10    -0.00+-1998.91   -0.00+-608.89
CO2(PPM)      742.+-  150.      960.+-  174.   132733.+-401526.  115095.+-******
HC (PPM)      3.59+-  2.55      3.50+-  0.05    -0.00+-1656.06   -0.00+-******
SOOT(PPM)     0.86+-  0.39      1.28+-  0.03    258.77+- 439.49  224.30+- 83.56
SO2(PPM)      0.00+-  0.00      0.80+-  0.10    485.48+- 814.91  420.61+- 52.58

COMBUSTION EFFICIENCY (%)
SPECIE    BY O2         BY CO2         BY SO2          DILUTION FACTOR
CO     100.00+- 0.51 100.00+- 1.50 100.00+- 0.53       BY O2  =  209.0+-  42.0
HC     100.00+- 1.18 100.00+- 1.25 100.00+- 1.19       BY CO2 =  605.9+- 942.8
SOOT    99.81+- 0.39  99.81+- 0.92  99.81+- 0.41       BY SO2 =  524.8+- 117.5
TOTAL   99.81+- 2.07  99.81+- 3.66  99.81+- 2.12
------------------------------------------------------------------------------
MEASUREMENTS WITH  RAKE  AT HEIGHT   7.0 FT  1.0 FT FROM FLAREHEAD AXIS
SPECIE       BACKGROUND        MEASURED        AT SR=1 BY CO2   AT SR=1 BY SO2
O2 (%)       21.00+-  0.00     20.80+-  0.02     0.00+-   0.00    0.00+-  0.00
CO (PPM)      4.31+-  0.40      2.32+-  0.40    -0.00+- 770.80   -0.00+-768.27
CO2(PPM)      742.+-  150.     1163.+-  174.   132733.+-211686.  253407.+-******
HC (PPM)      3.59+-  2.55      3.50+-  0.05    -0.00+- 836.01   -0.00+-******
SOOT(PPM)     0.86+-  0.39      1.77+-  0.04    288.06+- 267.39  550.65+-185.83
SO2(PPM)      0.00+-  0.00      0.70+-  0.10    219.72+- 214.73  420.61+- 60.09

COMBUSTION EFFICIENCY (%)
SPECIE    BY O2         BY CO2         BY SO2          DILUTION FACTOR
CO     100.00+- 0.23 100.00+- 0.58 100.00+- 0.30       BY O2  =  104.0+-  10.5
HC     100.00+- 0.60 100.00+- 0.63 100.00+- 0.62       BY CO2 =  312.9+- 261.9
SOOT    99.78+- 0.23  99.78+- 0.55  99.78+- 0.29       BY SO2 =  599.9+- 145.0
TOTAL   99.78+- 1.06  99.78+- 1.75  99.78+- 1.21
------------------------------------------------------------------------------
MEASUREMENTS WITH  RAKE  AT HEIGHT   7.0 FT  0.0 FT FROM FLAREHEAD AXIS
SPECIE       BACKGROUND        MEASURED        AT SR=1 BY CO2   AT SR=1 BY SO2
O2 (%)       21.00+-  0.00     20.40+-  0.02     0.00+-   0.00    0.00+-  0.00
CO (PPM)      4.31+-  0.40      3.86+-  0.40    -0.00+- 330.61   -0.00+-283.73
CO2(PPM)      742.+-  150.     1199.+-  174.   132733.+-195646.  148440.+-******
HC (PPM)      3.59+-  2.55      5.50+-  0.07    557.08+-1182.84  622.95+-953.38
SOOT(PPM)     0.86+-  0.39      3.52+-  0.09    771.40+- 646.94  863.10+-208.12
SO2(PPM)      0.00+-  0.00      1.30+-  0.10    375.88+- 319.72  420.61+- 32.35

COMBUSTION EFFICIENCY (%)
SPECIE    BY O2         BY CO2         BY SO2          DILUTION FACTOR
CO     100.00+- 0.17 100.00+- 0.25 100.00+- 0.19       BY O2  =   34.0+-   1.2
HC      99.58+- 0.83  99.58+- 1.49  99.58+- 1.00       BY CO2 =  288.1+- 223.7
SOOT    99.44+- 0.45  99.42+- 1.33  99.42+- 0.64       BY SO2 =  322.5+-  56.8
TOTAL   99.02+- 1.43  99.01+- 3.04  99.01+- 1.82
------------------------------------------------------------------------------
```

```
DATA PRINTED ON 20-OCT-83   08:06:56        FILE : FLARE.DAT

POINT:  1  DATE: 12-14-82   FLAREHEAD: EER-PROTO                SIZE:  3.0 IN
==========================================================================

MEASUREMENTS WITH  RAKE  AT HEIGHT   7.0 FT -1.0 FT FROM FLAREHEAD AXIS
SPECIE       BACKGROUND         MEASURED        AT SR=1 BY CO2   AT SR=1 BY SO2
O2 (%)       21.00+-  0.00     20.80+-  0.02      0.00+-   0.00    0.00+-  0.00
CO (PPM)      4.31+-  0.40      3.28+-  0.40     -0.00+- 261.68   -0.00+-751.07
CO2(PPM)      742.+-  150.      1424.+-  174.   132733.+-133788. 478482.+-******
HC (PPM)      3.59+-  2.55      3.50+-  0.05     -0.00+- 509.96   -0.00+-******
SOOT(PPM)     0.86+-  0.39      5.76+-  0.14    950.84+- 568.00 3439.32+-******
SO2(PPM)      0.00+-  0.00      0.60+-  0.10    116.21+-  82.04  420.61+- 70.10

COMBUSTION EFFICIENCY (%)
SPECIE    BY O2          BY CO2          BY SO2          DILUTION FACTOR
CO     100.00+- 0.13 100.00+- 0.20 100.00+- 0.16        BY O2  =  104.0+-  10.5
HC     100.00+- 0.37 100.00+- 0.38 100.00+- 0.38        BY CO2 =  192.7+- 104.5
SOOT    99.29+- 0.51  99.29+- 1.14  99.29+- 0.76        BY SO2 =  700.0+- 185.9
TOTAL   99.29+- 1.01  99.29+- 1.71  99.29+- 1.29
--------------------------------------------------------------------------
MEASUREMENTS WITH  RAKE  AT HEIGHT   7.0 FT -2.0 FT FROM FLAREHEAD AXIS
SPECIE       BACKGROUND         MEASURED        AT SR=1 BY CO2   AT SR=1 BY SO2
O2 (%)       21.00+-  0.00     20.73+-  0.02      0.00+-   0.00    0.00+-  0.00
CO (PPM)      4.31+-  0.40      4.25+-  0.40     -0.00+-  94.68   -0.00+-130.36
CO2(PPM)      742.+-  150.      1880.+-  174.   132733.+- 83477. 184758.+-79591.
HC (PPM)      3.59+-  2.55      3.50+-  0.05     -0.00+- 302.61   -0.00+-420.12
SOOT(PPM)     0.86+-  0.39      5.00+-  0.12    481.82+- 196.62  671.40+-139.90
SO2(PPM)      0.00+-  0.00      2.60+-  0.13    301.69+- 120.30  420.61+- 21.03

COMBUSTION EFFICIENCY (%)
SPECIE    BY O2          BY CO2          BY SO2          DILUTION FACTOR
CO     100.00+- 0.07 100.00+- 0.07 100.00+- 0.07        BY O2  =   76.8+-   5.8
HC     100.00+- 0.22 100.00+- 0.23 100.00+- 0.23        BY CO2 =  115.0+-  40.5
SOOT    99.64+- 0.18  99.64+- 0.37  99.64+- 0.23        BY SO2 =  160.8+-  24.0
TOTAL   99.64+- 0.47  99.64+- 0.67  99.64+- 0.53
--------------------------------------------------------------------------
```

```
DATA PRINTED ON 20-OCT-83   08:06:56        FILE : FLARE.DAT

POINT:  2  DATE: 12-14-82   FLAREHEAD: EER-PROTO             SIZE:  3.0 IN
=========================================================================
INPUT FLOW CONDITIONS
VELOCITY =  0.50 FPS   HV = 1311.2 BTU/CU FT
PROPANE     0.824 SCFM  55.8 %       5.6 LB/HR     STEAM     =   0.0 LB/HR
N GAS       0.000 SCFM   0.0 %       0.0 LB/HR     STEAM/GAS = 0.000
NITROGEN    0.645 SCFM  43.7 %       2.8 LB/HR
SO2         0.470 SCFH 5304. PPM    0.08 LB/HR
=========================================================================
MEASUREMENTS WITH  HOOD  AT HEIGHT   0.0 FT  0.0 FT FROM FLAREHEAD AXIS
SPECIE       BACKGROUND        MEASURED        AT SR=1 BY CO2   AT SR=1 BY SO2
O2 (%)      21.00+-  0.00    21.00+-  0.02      0.00+-   0.00     0.00+-  0.00
CO (PPM)     4.31+-  0.40     6.57+-  0.40    518.62+- 500.94 1194.78+-686.28
CO2(PPM)     742.+-  150.     1324.+-  174.   132733.+-155472.  306261.+-******
HC (PPM)     3.59+-  2.55     4.35+-  0.05    177.19+- 696.89  405.42+-******
SOOT(PPM)    0.86+-  0.39     7.49+-  0.19   1507.01+-1020.88 3487.16+-975.81
SO2(PPM)     0.00+-  0.00     0.80+-  0.10    181.71+- 135.64  420.61+- 52.58

COMBUSTION EFFICIENCY (%)
SPECIE     BY O2          BY CO2          BY SO2          DILUTION FACTOR
CO       0.00+- 0.00  99.62+- 0.82  99.62+- 0.52       BY O2  =    0.0+-   0.0
HC       0.00+- 0.00  99.87+- 0.67  99.87+- 0.57       BY CO2 =  226.1+- 141.2
SOOT     0.00+- 0.00  98.88+- 2.04  98.88+- 1.18       BY SO2 =  524.8+- 117.5
TOTAL    0.00+- 0.00  98.37+- 3.50  98.37+- 2.24
-------------------------------------------------------------------------
```

```
DATA PRINTED ON 20-OCT-83   08:06:56        FILE : FLARE.DAT

POINT:  3  DATE: 12-15-82  FLAREHEAD: EER-PROTO              SIZE:  3.0 IN
==========================================================================
INPUT FLOW CONDITIONS
VELOCITY =  0.50 FPS   HV = 1310.1 BTU/CU FT
PROPANE     0.825 SCFM  55.7 %       5.6 LB/HR    STEAM     =   0.0 LB/HR
N GAS       0.000 SCFM   0.0 %       0.0 LB/HR    STEAM/GAS = 0.000
NITROGEN    0.647 SCFM  43.7 %       2.8 LB/HR
SO2         0.470 SCFH 5293.  PPM    0.08 LB/HR
==========================================================================
MEASUREMENTS WITH  RAKE  AT HEIGHT   9.0 FT  2.0 FT FROM FLAREHEAD AXIS
SPECIE        BACKGROUND        MEASURED       AT SR=1 BY CO2   AT SR=1 BY SO2
O2 (%)        21.00+-  0.00    20.78+-  0.02    0.00+-    0.00    0.00+-  0.00
CO (PPM)       3.29+-  0.40     5.41+-  0.40  791.39+-1063.92  747.16+-414.91
CO2(PPM)       693.+-  150.    1049.+-  174. 132724.+-248612. 125314.+-******
HC (PPM)       3.08+-  2.55     3.90+-  0.05  309.05+-1259.74  291.87+-960.11
SOOT(PPM)      0.86+-  0.39     1.61+-  0.04  280.86+- 302.55  265.15+- 76.20
SO2(PPM)       0.00+-  0.00     1.20+-  0.10  445.05+- 470.57  420.07+- 35.01

COMBUSTION EFFICIENCY (%)
SPECIE    BY O2         BY CO2         BY SO2          DILUTION FACTOR
CO      99.41+- 0.84  99.41+- 1.89  99.41+- 0.96       BY O2  =   94.5+-   8.7
HC      99.77+- 0.95  99.77+- 1.37  99.77+- 1.00       BY CO2 =  369.9+- 361.2
SOOT    99.79+- 0.24  99.79+- 0.62  99.79+- 0.29       BY SO2 =  349.1+-  63.7
TOTAL   98.97+- 2.02  98.97+- 3.85  98.97+- 2.24
--------------------------------------------------------------------------
MEASUREMENTS WITH  RAKE  AT HEIGHT   9.0 FT  1.0 FT FROM FLAREHEAD AXIS
SPECIE        BACKGROUND        MEASURED       AT SR=1 BY CO2   AT SR=1 BY SO2
O2 (%)        21.00+-  0.00    20.92+-  0.02    0.00+-    0.00    0.00+-  0.00
CO (PPM)       3.29+-  0.40     5.25+-  0.40  577.27+- 681.40  920.44+-565.24
CO2(PPM)       693.+-  150.    1145.+-  174. 132724.+-197569. 211661.+-******
HC (PPM)       3.08+-  2.55     6.25+-  0.08  930.51+-1489.19 1484.99+-******
SOOT(PPM)      0.86+-  0.39     2.01+-  0.05  338.24+- 292.70  539.94+-159.86
SO2(PPM)       0.00+-  0.00     0.90+-  0.10  262.89+- 234.45  420.07+- 46.67

COMBUSTION EFFICIENCY (%)
SPECIE    BY O2         BY CO2         BY SO2          DILUTION FACTOR
CO      99.57+- 0.69  99.57+- 1.14  99.57+- 0.66       BY O2  =  261.5+-  65.6
HC      99.31+- 1.39  99.31+- 2.12  99.31+- 1.34       BY CO2 =  291.1+- 228.0
SOOT    99.75+- 0.32  99.75+- 0.59  99.75+- 0.31       BY SO2 =  465.7+-  97.8
TOTAL   98.63+- 2.39  98.63+- 3.82  98.63+- 2.29
--------------------------------------------------------------------------
MEASUREMENTS WITH  RAKE  AT HEIGHT   9.0 FT  0.0 FT FROM FLAREHEAD AXIS
SPECIE        BACKGROUND        MEASURED       AT SR=1 BY CO2   AT SR=1 BY SO2
O2 (%)        21.00+-  0.00    20.83+-  0.02    0.00+-    0.00    0.00+-  0.00
CO (PPM)       3.29+-  0.40     5.33+-  0.40  717.58+- 936.92  361.22+-192.78
CO2(PPM)       693.+-  150.    1071.+-  174. 132724.+-234625.  66854.+-66384.
HC (PPM)       3.08+-  2.55     4.15+-  0.05  378.56+-1252.09  191.23+-480.79
SOOT(PPM)      0.86+-  0.39     2.88+-  0.07  708.16+- 701.68  355.29+- 77.77
SO2(PPM)       0.00+-  0.00     2.40+-  0.12  838.29+- 814.01  420.07+- 21.00

COMBUSTION EFFICIENCY (%)
SPECIE    BY O2         BY CO2         BY SO2          DILUTION FACTOR
CO      99.47+- 0.77  99.47+- 1.63  99.47+- 0.81       BY O2  =  122.5+-  14.5
HC      99.72+- 0.96  99.72+- 1.42  99.72+- 0.99       BY CO2 =  348.3+- 321.7
SOOT    99.48+- 0.60  99.47+- 1.45  99.48+- 0.63       BY SO2 =  174.0+-  26.0
TOTAL   98.66+- 2.31  98.66+- 4.46  98.66+- 2.41
--------------------------------------------------------------------------
```

```
DATA PRINTED ON 20-OCT-83   08: 06: 56        FILE : FLARE. DAT

POINT:  3  DATE: 12-15-82   FLAREHEAD: EER-PROTO                 SIZE:  3. 0 IN
================================================================================

MEASUREMENTS WITH  RAKE  AT HEIGHT   9. 0 FT -1. 0 FT FROM FLAREHEAD AXIS
SPECIE       BACKGROUND         MEASURED         AT SR=1 BY CO2   AT SR=1 BY SO2
O2 (%)       21. 00+-  0. 00    20. 80+-  0. 02     0. 00+-   0. 00    0. 00+-  0. 00
CO (PPM)      3. 29+-  0. 40     4. 05+-  0. 40   260. 95+- 498. 48  156. 31+-182. 35
CO2(PPM)      693. +-  150.      1085. +-  174.   132724. +-226541.  79106. +-76305.
HC (PPM)      3. 08+-  2. 55     3. 85+-  0. 05   264. 11+-1105. 59  158. 10+-540. 56
SOOT(PPM)     0. 86+-  0. 39     2. 88+-  0. 07   682. 90+- 655. 74  405. 92+- 88. 88
SO2(PPM)      0. 00+-  0. 00     2. 10+-  0. 10   707. 31+- 665. 17  420. 07+- 21. 00

COMBUSTION EFFICIENCY (%)
SPECIE    BY O2           BY CO2          BY SO2            DILUTION FACTOR
CO      99. 80+- 0. 40  99. 81+- 0. 70  99. 80+- 0. 42      BY O2  =  104. 0+-  10. 5
HC      99. 80+- 0. 84  99. 80+- 1. 16  99. 80+- 0. 87      BY CO2 =  335. 8+- 299. 9
SOOT    99. 49+- 0. 54  99. 49+- 1. 36  99. 49+- 0. 60      BY SO2 =  199. 0+-  29. 7
TOTAL   99. 10+- 1. 77  99. 10+- 3. 20  99. 10+- 1. 87
--------------------------------------------------------------------------------
MEASUREMENTS WITH  RAKE  AT HEIGHT   9. 0 FT -2. 0 FT FROM FLAREHEAD AXIS
SPECIE       BACKGROUND         MEASURED         AT SR=1 BY CO2   AT SR=1 BY SO2
O2 (%)       21. 00+-  0. 00    20. 84+-  0. 02     0. 00+-   0. 00    0. 00+-  0. 00
CO (PPM)      3. 29+-  0. 40     7. 73+-  0. 40  1792. 55+-2203. 39 1870. 50+-706. 29
CO2(PPM)      693. +-  150.      1021. +-  174.   132724. +-269128. 138476. +-******
HC (PPM)      3. 08+-  2. 55     4. 50+-  0. 06   576. 69+-1649. 82  601. 67+-******
SOOT(PPM)     0. 86+-  0. 39     2. 56+-  0. 06   687. 18+- 773. 26  717. 07+-195. 87
SO2(PPM)      0. 00+-  0. 00     1. 00+-  0. 10   402. 53+- 463. 60  420. 07+- 42. 01

COMBUSTION EFFICIENCY (%)
SPECIE    BY O2           BY CO2          BY SO2            DILUTION FACTOR
CO      98. 69+- 1. 80  98. 68+- 4. 24  98. 68+- 2. 03      BY O2  =  130. 3+-  16. 4
HC      99. 58+- 1. 26  99. 58+- 2. 06  99. 58+- 1. 34      BY CO2 =  401. 5+- 423. 3
SOOT    99. 50+- 0. 64  99. 49+- 1. 58  99. 49+- 0. 73      BY SO2 =  419. 1+-  83. 4
TOTAL   97. 76+- 3. 67  97. 75+- 7. 79  97. 75+- 4. 05
--------------------------------------------------------------------------------
```

```
DATA PRINTED ON 20-OCT-83   08:06:56        FILE : FLARE.DAT

POINT:  4  DATE: 12-16-82   FLAREHEAD: EER-PROTO               SIZE:  3.0 IN
===============================================================================
INPUT FLOW CONDITIONS
VELOCITY =  0.50 FPS   HV = 1310.8 BTU/CU FT
PROPANE     0.826 SCFM  55.8 %        5.6 LB/HR    STEAM     =   0.0 LB/HR
N GAS       0.000 SCFM   0.0 %        0.0 LB/HR    STEAM/GAS = 0.000
NITROGEN    0.647 SCFM  43.7 %        2.8 LB/HR
SO2         0.470 SCFH 5290.  PPM    0.08 LB/HR
===============================================================================
MEASUREMENTS WITH  RAKE  AT HEIGHT   3.0 FT  2.0 FT FROM FLAREHEAD AXIS
SPECIE       BACKGROUND         MEASURED       AT SR=1 BY CO2   AT SR=1 BY SO2
O2 (%)       21.00+-  0.00     20.90+-  0.02     0.00+-   0.00     0.00+-  0.00
CO (PPM)      4.63+-  0.40      7.73+-  0.40   1086.72+-1275.54 *******+-******
CO2(PPM)      785.+-  150.      1163.+-  174.  132730.+-234477.1586794.+-******
HC (PPM)      2.42+-  2.55      2.85+-  0.05    150.78+-1041.65 1785.64+-******
SOOT(PPM)     0.86+-  0.39      1.26+-  0.03    142.22+- 152.17 1700.15+-******
SO2(PPM)      0.00+-  0.00      0.10+-  0.10     34.91+-  67.06  419.58+-419.58

COMBUSTION EFFICIENCY (%)
SPECIE     BY O2          BY CO2         BY SO2          DILUTION FACTOR
CO      99.19+- 1.21  99.19+- 2.37  99.19+- 2.67       BY O2  =  209.0+-  42.0
HC      99.89+- 0.81  99.89+- 0.97  99.89+- 1.02       BY CO2 =  348.1+- 321.5
SOOT    99.89+- 0.15  99.89+- 0.30  99.89+- 0.34       BY SO2 = 4194.8+-4609.1
TOTAL   98.97+- 2.15  98.97+- 3.62  98.97+- 4.01
-------------------------------------------------------------------------------
MEASUREMENTS WITH  RAKE  AT HEIGHT   3.0 FT  1.0 FT FROM FLAREHEAD AXIS
SPECIE       BACKGROUND         MEASURED       AT SR=1 BY CO2   AT SR=1 BY SO2
O2 (%)       21.00+-  0.00     20.80+-  0.02     0.00+-   0.00     0.00+-  0.00
CO (PPM)      4.63+-  0.40      5.02+-  0.40     76.30+- 183.54  130.50+-279.88
CO2(PPM)      785.+-  150.      1503.+-  174.  132730.+-127367.  232522.+-******
HC (PPM)      2.42+-  2.55      3.00+-  0.05    108.09+- 529.68  188.01+-869.16
SOOT(PPM)     0.86+-  0.39      2.92+-  0.07    380.33+- 222.26  667.34+-163.97
SO2(PPM)      0.00+-  0.00      1.30+-  0.10    238.90+- 141.45  419.58+- 32.28

COMBUSTION EFFICIENCY (%)
SPECIE     BY O2          BY CO2         BY SO2          DILUTION FACTOR
CO      99.94+- 0.15  99.94+- 0.19  99.94+- 0.15       BY O2  =  104.0+-  10.5
HC      99.92+- 0.41  99.92+- 0.47  99.92+- 0.42       BY CO2 =  182.8+-  94.7
SOOT    99.72+- 0.20  99.71+- 0.44  99.71+- 0.25       BY SO2 =  321.8+-  56.6
TOTAL   99.57+- 0.75  99.58+- 1.10  99.58+- 0.82
-------------------------------------------------------------------------------
MEASUREMENTS WITH  RAKE  AT HEIGHT   3.0 FT  0.0 FT FROM FLAREHEAD AXIS
SPECIE       BACKGROUND         MEASURED       AT SR=1 BY CO2   AT SR=1 BY SO2
O2 (%)       21.00+-  0.00     20.50+-  0.02     0.00+-   0.00     0.00+-  0.00
CO (PPM)      4.63+-  0.40     21.52+-  0.43    813.54+- 186.22 1316.98+-259.01
CO2(PPM)      785.+-  150.      3540.+-  174.  132730.+- 39321.  214848.+-56814.
HC (PPM)      2.42+-  2.55     11.35+-  0.14    429.87+- 203.97  695.90+-309.59
SOOT(PPM)     0.86+-  0.39      9.31+-  0.23    405.79+-  95.57  657.81+-133.50
SO2(PPM)      0.00+-  0.00      5.40+-  0.27    258.62+-  59.88  419.58+- 20.98

COMBUSTION EFFICIENCY (%)
SPECIE     BY O2          BY CO2         BY SO2          DILUTION FACTOR
CO      99.39+- 0.15  99.39+- 0.32  99.39+- 0.28       BY O2  =   41.0+-   1.7
HC      99.68+- 0.16  99.68+- 0.25  99.68+- 0.23       BY CO2 =   46.9+-   8.7
SOOT    99.70+- 0.08  99.70+- 0.16  99.70+- 0.14       BY SO2 =   76.7+-  11.5
TOTAL   98.77+- 0.37  98.77+- 0.72  98.77+- 0.64
-------------------------------------------------------------------------------
```

```
DATA PRINTED ON 20-OCT-83   08:06:56        FILE : FLARE.DAT

POINT:  4  DATE: 12-16-82   FLAREHEAD: EER-PROTO                SIZE:  3.0 IN
=============================================================================

MEASUREMENTS WITH  RAKE  AT HEIGHT   3.0 FT -1.0 FT FROM FLAREHEAD AXIS
SPECIE       BACKGROUND        MEASURED         AT SR=1 BY CO2  AT SR=1 BY SO2
O2 (%)       21.00+-  0.00    20.30+-  0.02      0.00+-    0.00    0.00+-  0.00
CO (PPM)      4.63+-  0.40    16.65+-  0.40    525.99+- 123.16  651.21+-138.65
CO2(PPM)      785.+-  150.    3827.+-  174.   132730.+- 36393. 164421.+-41579.
HC (PPM)      2.42+-  2.55     8.70+-  0.11    274.60+- 159.16  339.97+-190.60
SOOT(PPM)     0.86+-  0.39    11.37+-  0.28    456.94+- 102.11  566.48+-114.29
SO2(PPM)      0.00+-  0.00     7.80+-  0.39    338.32+-  74.58  419.58+- 20.98

COMBUSTION EFFICIENCY (%)
SPECIE    BY O2          BY CO2          BY SO2           DILUTION FACTOR
CO      99.61+- 0.09  99.61+- 0.20  99.61+- 0.18        BY O2  =    29.0+-    0.9
HC      99.79+- 0.12  99.80+- 0.17  99.80+- 0.17        BY CO2 =    42.4+-    7.4
SOOT    99.66+- 0.07  99.66+- 0.17  99.66+- 0.15        BY SO2 =    52.8+-    8.0
TOTAL   99.06+- 0.27  99.06+- 0.54  99.06+- 0.50
-----------------------------------------------------------------------------
MEASUREMENTS WITH  RAKE  AT HEIGHT   3.0 FT -2.0 FT FROM FLAREHEAD AXIS
SPECIE       BACKGROUND        MEASURED         AT SR=1 BY CO2  AT SR=1 BY SO2
O2 (%)       21.00+-  0.00    20.70+-  0.02      0.00+-    0.00    0.00+-  0.00
CO (PPM)      4.63+-  0.40     4.63+-  0.40      4.63+- 141.10    4.63+-479.12
CO2(PPM)      785.+-  150.    1531.+-  174.   132730.+-122898. 447936.+-******
HC (PPM)      2.42+-  2.55     3.25+-  0.05    148.34+- 530.02  496.93+-******
SOOT(PPM)     0.86+-  0.39     5.69+-  0.14    856.02+- 476.26 2898.95+-869.87
SO2(PPM)      0.00+-  0.00     0.70+-  0.10    123.81+-  79.37  419.58+- 59.94

COMBUSTION EFFICIENCY (%)
SPECIE    BY O2          BY CO2          BY SO2           DILUTION FACTOR
CO      99.99+- 0.11 100.00+- 0.11 100.00+- 0.11        BY O2  =    69.0+-    4.7
HC      99.89+- 0.40  99.89+- 0.50  99.89+- 0.44        BY CO2 =   175.9+-   88.1
SOOT    99.36+- 0.39  99.36+- 0.95  99.36+- 0.62        BY SO2 =   598.4+-  144.7
TOTAL   99.24+- 0.89  99.25+- 1.54  99.25+- 1.17
-----------------------------------------------------------------------------
```

```
DATA PRINTED ON 20-OCT-83   08:06:56        FILE : FLARE.DAT

POINT:  5  DATE: 12-16-82   FLAREHEAD: EER-PROTO             SIZE:  3.0 IN
==============================================================================
INPUT FLOW CONDITIONS
VELOCITY =   2.00 FPS    HV = 1319.0 BTU/CU FT
PROPANE      3.302 SCFM  56.1 %        22.5 LB/HR     STEAM     =    0.0 LB/HR
N GAS        0.000 SCFM   0.0 %         0.0 LB/HR     STEAM/GAS = 0.000
NITROGEN     2.573 SCFM  43.7 %        11.2 LB/HR
SO2          0.470 SCFH 1332. PPM      0.08 LB/HR
==============================================================================
MEASUREMENTS WITH  HOOD  AT HEIGHT   4.0 FT  0.0 FT FROM FLAREHEAD AXIS
SPECIE       BACKGROUND         MEASURED        AT SR=1 BY CO2   AT SR=1 BY SO2
O2 (%)       21.00+-  0.00     20.50+-  0.02      0.00+-   0.00     0.00+-  0.00
CO (PPM)      5.79+-  0.40      8.12+-  0.40    184.32+- 105.86   359.32+-203.99
CO2(PPM)     700.+-  150.      2424.+-  174.   132796.+- 57944.  259325.+-******
HC (PPM)      2.80+-  2.55      5.00+-  0.06    171.37+- 240.08   332.83+-469.03
SOOT(PPM)     0.86+-  0.39      4.26+-  0.11    261.75+-  81.92   511.65+-155.15
SO2(PPM)      0.00+-  0.00      0.70+-  0.10     53.64+-  21.17   105.01+- 15.00

COMBUSTION EFFICIENCY (%)
SPECIE     BY O2          BY CO2          BY SO2          DILUTION FACTOR
CO      99.86+- 0.08   99.86+- 0.14   99.86+- 0.14       BY O2  =   41.0+-   1.7
HC      99.87+- 0.18   99.87+- 0.24   99.87+- 0.23       BY CO2 =   75.6+-  19.3
SOOT    99.80+- 0.06   99.80+- 0.15   99.80+- 0.14       BY SO2 =  149.0+-  36.2
TOTAL   99.53+- 0.32   99.54+- 0.52   99.54+- 0.51
------------------------------------------------------------------------------
```

```
DATA PRINTED ON 20-OCT-83   08:06:56        FILE : FLARE.DAT

POINT:  6  DATE: 12-17-82   FLAREHEAD: EER-PROTO              SIZE:  3.0 IN
=============================================================================
INPUT FLOW CONDITIONS
VELOCITY =  2.00 FPS   HV = 1314.8 BTU/CU FT
PROPANE     3.302 SCFM  55.9 %      22.5 LB/HR     STEAM     =   0.0 LB/HR
N GAS       0.000 SCFM   0.0 %       0.0 LB/HR     STEAM/GAS = 0.000
NITROGEN    2.592 SCFM  43.9 %      11.3 LB/HR
SO2         0.470 SCFH 1327. PPM    0.08 LB/HR
=============================================================================
MEASUREMENTS WITH  RAKE  AT HEIGHT   5.0 FT  2.0 FT FROM FLAREHEAD AXIS
SPECIE       BACKGROUND         MEASURED        AT SR=1 BY CO2   AT SR=1 BY SO2
O2 (%)       21.00+-  0.00    21.00+-  0.02     0.00+-   0.00    0.00+-  0.00
CO (PPM)      3.27+-  0.40     5.79+-  0.40   375.01+- 275.77 1473.04+-******
CO2(PPM)      589. +-  150.    1485. +-  174. 132762. +-103879. 523174. +-******
HC (PPM)      3.23+-  2.55     3.60+-  0.05    57.37+- 404.02  217.28+-******
SOOT(PPM)     0.97+-  0.39     3.20+-  0.08   329.63+- 163.35 1300.43+-943.19
SO2(PPM)      0.00+-  0.00     0.18+-  0.10    26.55+-  26.05  104.98+- 58.32

COMBUSTION EFFICIENCY (%)
SPECIE     BY O2          BY CO2          BY SO2          DILUTION FACTOR
CO       0.00+- 0.00  99.72+- 0.43  99.72+- 0.55       BY O2  =    0.0+-   0.0
HC       0.00+- 0.00  99.96+- 0.34  99.96+- 0.36       BY CO2 =  146.5+-  62.8
SOOT     0.00+- 0.00  99.75+- 0.32  99.75+- 0.43       BY SO2 =  582.2+- 381.5
TOTAL    0.00+- 0.00  99.43+- 1.07  99.43+- 1.33
-----------------------------------------------------------------------------
MEASUREMENTS WITH  RAKE  AT HEIGHT   5.0 FT  1.0 FT FROM FLAREHEAD AXIS
SPECIE       BACKGROUND         MEASURED        AT SR=1 BY CO2   AT SR=1 BY SO2
O2 (%)       21.00+-  0.00    20.60+-  0.02     0.00+-   0.00    0.00+-  0.00
CO (PPM)      3.27+-  0.40    22.49+-  0.45  1102.52+- 272.50    0.00+-  0.00
CO2(PPM)      589. +-  150.    2900. +-  174. 132762. +- 45350.      0. +-    0.
HC (PPM)      3.23+-  2.55    13.15+-  0.16   570.41+- 268.43    0.00+-  0.00
SOOT(PPM)     0.97+-  0.39     2.92+-  0.07   112.38+-  31.01    0.00+-  0.00
SO2(PPM)      0.00+-  0.00     0.00+-  0.10     0.00+-   5.72    0.00+-  0.00

COMBUSTION EFFICIENCY (%)
SPECIE     BY O2          BY CO2          BY SO2          DILUTION FACTOR
CO      99.18+- 0.23  99.18+- 0.48   0.00+- 0.00       BY O2  =   51.5+-   2.6
HC      99.58+- 0.21  99.58+- 0.34   0.00+- 0.00       BY CO2 =   56.2+-  11.7
SOOT    99.92+- 0.03  99.92+- 0.05   0.00+- 0.00       BY SO2 =    0.0+-   0.0
TOTAL   98.67+- 0.46  98.67+- 0.87   0.00+- 0.00
-----------------------------------------------------------------------------
MEASUREMENTS WITH  RAKE  AT HEIGHT   5.0 FT  0.0 FT FROM FLAREHEAD AXIS
SPECIE       BACKGROUND         MEASURED        AT SR=1 BY CO2   AT SR=1 BY SO2
O2 (%)       21.00+-  0.00    19.30+-  0.02     0.00+-   0.00    0.00+-  0.00
CO (PPM)      3.27+-  0.40   188.30+-  3.77  4490.59+- 653.93 ********+-******
CO2(PPM)      589. +-  150.    6039. +-  174. 132762. +- 24005.1907789. +-******
HC (PPM)      3.23+-  2.55   171.50+-  2.14  4084.02+- 614.45 ********+-******
SOOT(PPM)     0.97+-  0.39     9.95+-  0.25   218.71+-  38.66 3142.78+-******
SO2(PPM)      0.00+-  0.00     0.30+-  0.10     7.28+-   3.32  104.98+- 34.99

COMBUSTION EFFICIENCY (%)
SPECIE     BY O2          BY CO2          BY SO2          DILUTION FACTOR
CO      96.84+- 0.31  96.83+- 1.00  96.82+- 2.91       BY O2  =   11.4+-   0.1
HC      97.12+- 0.30  97.11+- 0.92  97.11+- 2.67       BY CO2 =   23.3+-   3.0
SOOT    99.85+- 0.02  99.85+- 0.05  99.85+- 0.15       BY SO2 =  348.9+- 151.1
TOTAL   93.81+- 0.61  93.79+- 1.92  93.77+- 5.54
-----------------------------------------------------------------------------
```

```
DATA PRINTED ON 20-OCT-83   08:06:56        FILE : FLARE.DAT

POINT:  6  DATE: 12-17-82  FLAREHEAD: EER-PROTO               SIZE:  3.0 IN
===========================================================================

MEASUREMENTS WITH  RAKE  AT HEIGHT   5.0 FT -1.0 FT FROM FLAREHEAD AXIS
SPECIE       BACKGROUND        MEASURED       AT SR=1 BY CO2   AT SR=1 BY SO2
O2 (%)       21.00+-  0.00     20.20+-  0.02     0.00+-   0.00     0.00+-  0.00
CO (PPM)      3.27+-  0.40     51.45+-  1.03  1540.34+- 263.54     0.00+-  0.00
CO2(PPM)      589.+-  150.     4732.+-  174.  132762.+- 28962.       0.+-    0.
HC (PPM)      3.23+-  2.55     36.00+-  0.45  1048.59+- 241.66     0.00+-  0.00
SOOT(PPM)     0.97+-  0.39     27.96+-  0.70   861.96+- 166.21     0.00+-  0.00
SO2(PPM)      0.00+-  0.00      0.00+-  0.10     0.00+-   3.19     0.00+-  0.00

COMBUSTION EFFICIENCY (%)
SPECIE     BY O2          BY CO2          BY SO2         DILUTION FACTOR
CO       98.87+- 0.17  98.87+- 0.44   0.00+- 0.00       BY O2  =   25.3+-   0.7
HC       99.23+- 0.16  99.23+- 0.34   0.00+- 0.00       BY CO2 =   30.9+-   4.5
SOOT     99.37+- 0.11  99.37+- 0.26   0.00+- 0.00       BY SO2 =    0.0+-   0.0
TOTAL    97.47+- 0.44  97.47+- 1.02   0.00+- 0.00
---------------------------------------------------------------------------
MEASUREMENTS WITH  RAKE  AT HEIGHT   5.0 FT -2.0 FT FROM FLAREHEAD AXIS
SPECIE       BACKGROUND        MEASURED       AT SR=1 BY CO2   AT SR=1 BY SO2
O2 (%)       21.00+-  0.00     20.63+-  0.02     0.00+-   0.00    0.00+-  0.00
CO (PPM)      3.27+-  0.40      8.89+-  0.40   473.11+- 192.77  593.28+-200.72
CO2(PPM)      589.+-  150.     2170.+-  174.  132762.+- 62463. 166568.+-66815.
HC (PPM)      3.23+-  2.55      7.50+-  0.09   359.96+- 314.35  451.20+-363.93
SOOT(PPM)     0.97+-  0.39     16.16+-  0.40  1270.70+- 408.43 1595.46+-400.96
SO2(PPM)      0.00+-  0.00      1.00+-  0.10    83.60+-  30.83  104.98+- 10.50

COMBUSTION EFFICIENCY (%)
SPECIE     BY O2          BY CO2          BY SO2         DILUTION FACTOR
CO       99.65+- 0.16  99.65+- 0.31  99.65+- 0.26       BY O2  =   55.8+-   3.1
HC       99.73+- 0.24  99.73+- 0.36  99.73+- 0.32       BY CO2 =   82.6+-  22.5
SOOT     99.06+- 0.34  99.06+- 0.74  99.06+- 0.61       BY SO2 =  104.0+-  20.8
TOTAL    98.44+- 0.73  98.44+- 1.39  98.44+- 1.18
---------------------------------------------------------------------------
```

APPENDIX F

GRAPHS OF LOCAL COMBUSTION EFFICIENCIES AND DILUTION FACTORS

Concentrations of CO, CO_2, HC, O_2, soot, and SO_2 were measured at several radial positions for most of the flare flames studied. Local dilution factors can be calculated as shown in Appendix C using the measured concentrations of O_2, CO_2, soot, and SO_2. Each dilution factor can then be used to calculate a local combustion efficiency. Examples of the numerical results of the calculations are shown in Appendix E and the graphical results in this Appendix.

Two types of graphs are shown. Combustion efficiencies are plotted for each condition as a function of radial probe position. The base of the axes of each graph denote the axial position of probe sampling above the flare head and the horizontal axes show the radial position of probe sampling.

Dilution factors are plotted in a similar fashion. In some cases, the dilution factors at the edge of the plume are large and are omitted so that the scale of the graph is not excessively compressed.

The dilution factors calculated using different species can vary considerably because of the range of accuracy for different species. The dilution factors calculated from each species are shown in the graphs. However, the line is drawn through those determined from CO_2 concentrations. These values are thought to be the most reliable. However, calculation of dilution factors based on CO_2 assumes a complete carbon balance and verification of a carbon balance was one of the objectives of this program. Carbon balances have been verified in this program using SO_2 as a tracer and by capturing the entire flare plume in a hood.

The local combustion efficiencies calculated using different dilution factors estimated from different species concentrations are similar. (See examples in Appendix E.) For consistency, the local combustion efficiencies calculated using CO_2 as the tracer are plotted.

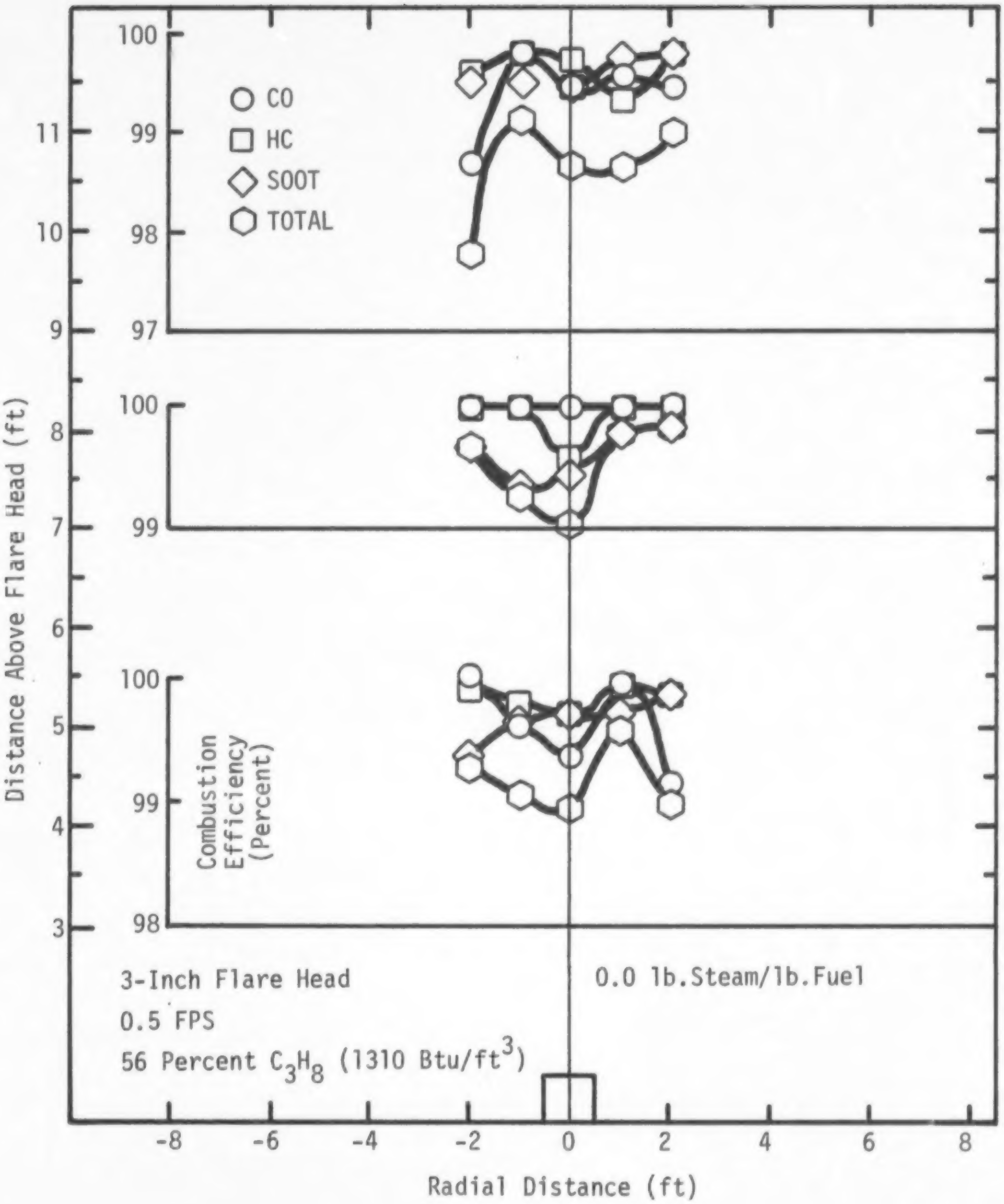

Figure F-1. Local combustion efficiencies of the 3-inch EER test flare head burning 56 percent propane in nitrogen at 0.5 ft/sec with 0.0 lb steam per lb of fuel.

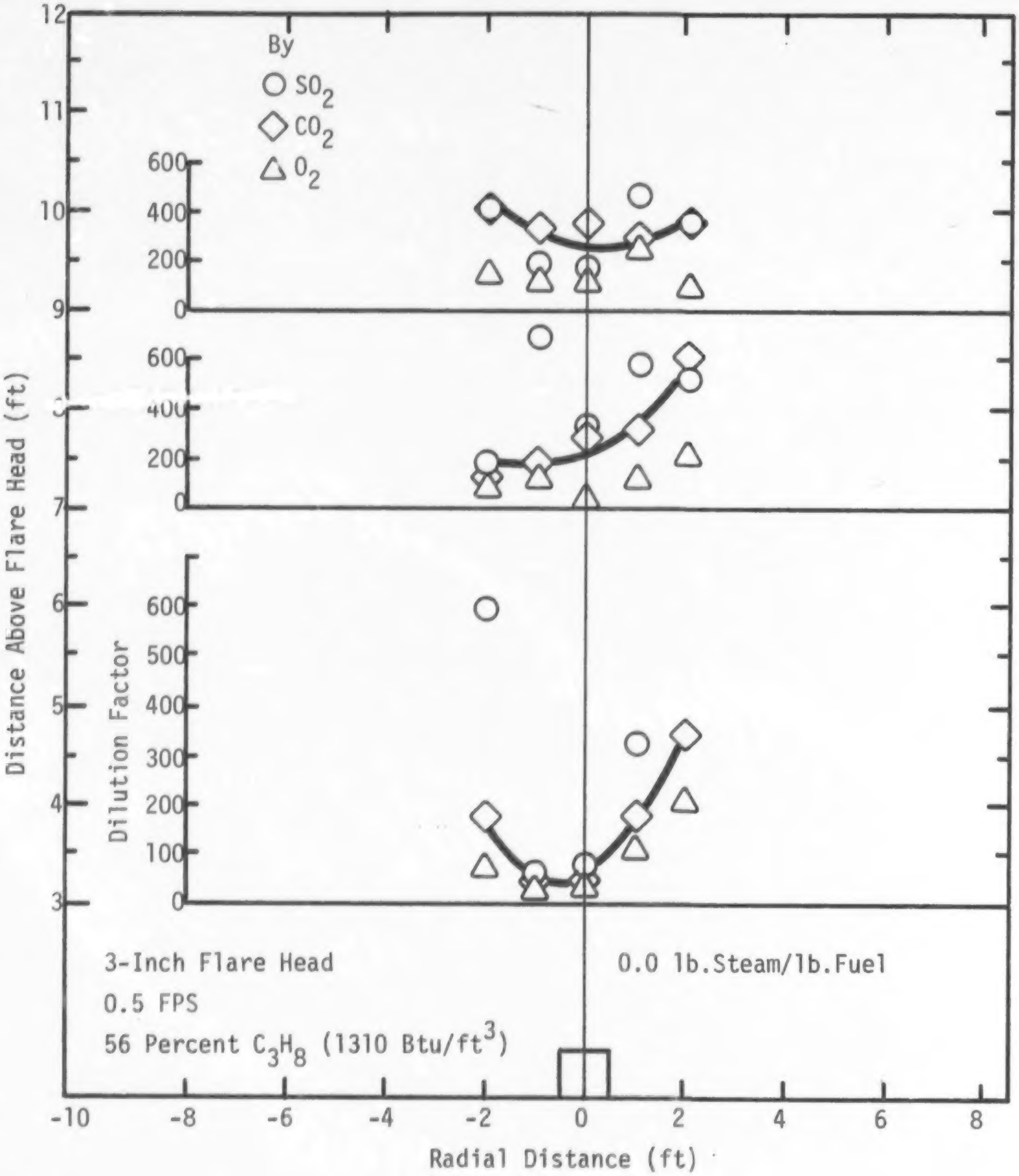

Figure F-2. Dilution factor of the 3-inch EER test flare head burning 56 percent propane in nitrogen at 0.5 ft/sec with 0.0 lb steam per lb of fuel.

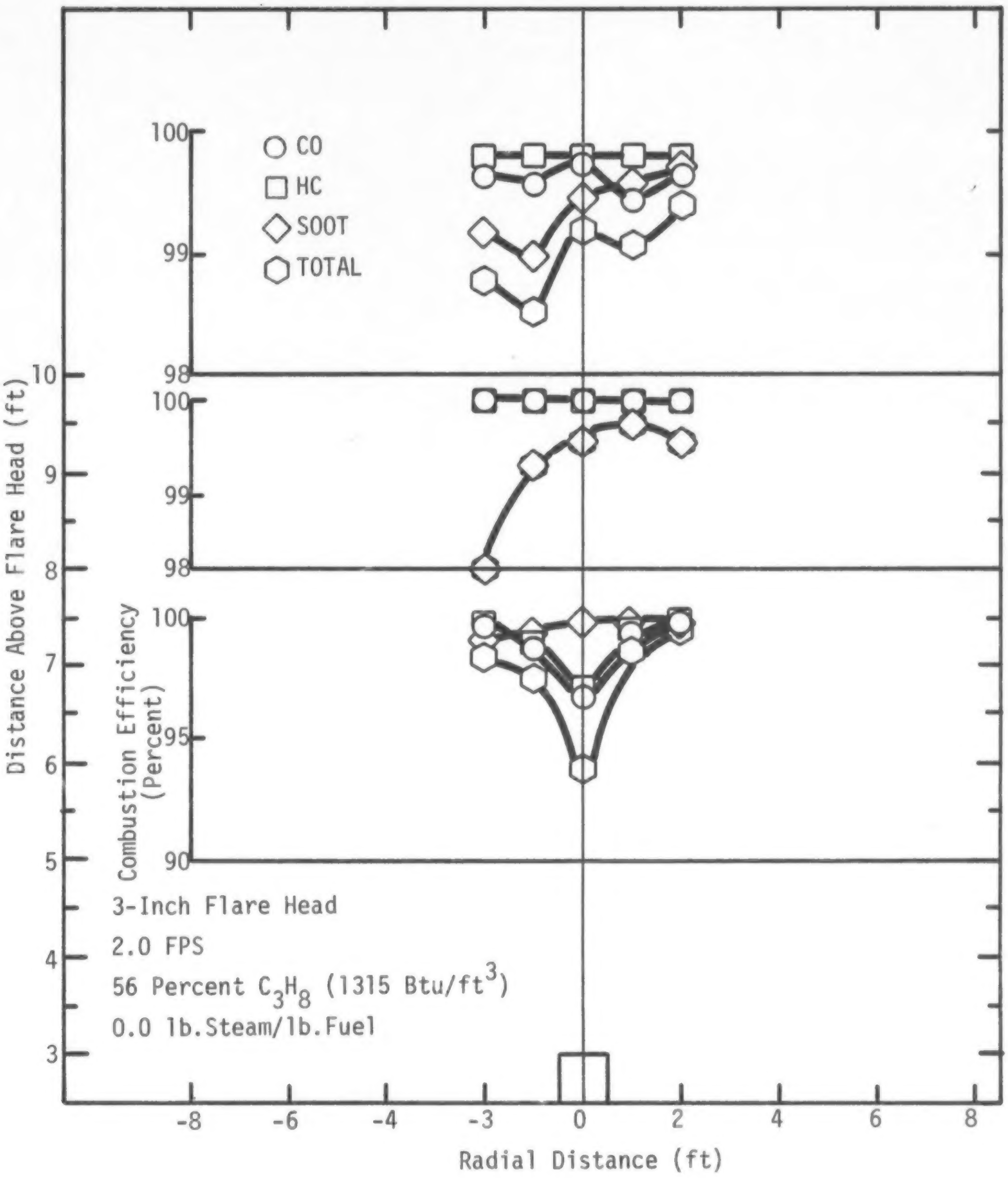

Figure F-3. Local combustion efficiencies of the 3-inch EER test flare head burning 56 percent propane in nitrogen at 2.0 ft/sec with 0.0 lb steam per lb of fuel.

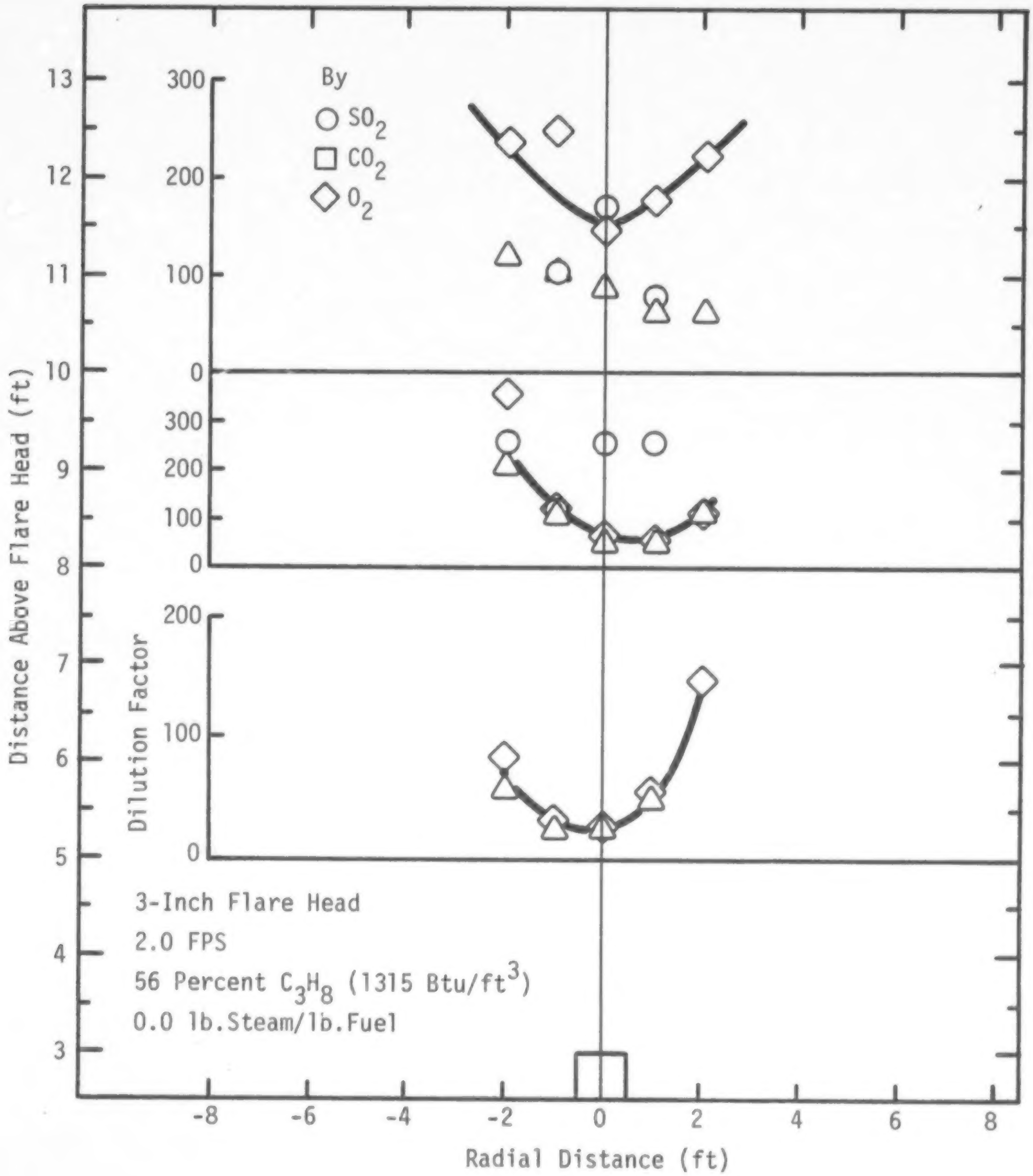

Figure F-4. Dilution factor of the 3-inch EER test flare head burning 56 percent propane in nitrogen at 2.0 ft/sec with 0.0 lb steam per lb of fuel.

APPENDIX G
QUALITY ASSURANCE

G.0 ASSESSMENT OF DATA QUALITY

The data taken in this study was carefully evaluated to establish the maximum error bounds. Procedures used to take the data are described in Appendix B. Reduction of the data and analysis of errors are discussed in Section 3.3. Examples of the data and analysis procedures are presented in Appendices C, D, E, and F.

Data

The expected precision, accuracy, and completeness of the data is shown in Table G-1. The representativeness of the data is demonstrated by the correlations and statistical analysis of these correlations in the text of the report. The reproducibility of the data was demonstrated by repeating all the conditions on the 6 inch flare head which had resulted in low combustion efficiencies. In addition, material balances were closed for a number of test conditions (see Section 3.2).

Limitations

The data is strictly limited to the conditions of this study. These were:

- Propane-nitrogen mixtures.
- 3, 6, 12 inch simple pipe flares.
- 3 - 12 inch commercial pipe flares.
- Velocities from 0.2 to 428 ft/second.
- Gas heating values from 386 - 2350 Btu/ft^3.
- No pilot flames.
- Steam injection to 1 lb steam/lb fuel.

G.1 Results of Audit

This program was initiated prior to fiscal year 1982. Consequently, no Quality Assurance Project Plan was submitted nor were any audits conducted. However, the nature of the program and use of the results required that strict QC/QA procedures be applied. These procedures have been fully documented in the text and appendices of this report.

TABLE G-1. MEASUREMENT PRECISION, ACCURACY, AND COMPLETENESS

Measurement	Method	Reference	Experimental Condition	Precision	Accuracy	Completeness
Flow Rate	Calibrated Orifices	None	Gases, Steam	±3% Reading	± 5% Reading	100%
Flame Structure	Visual, Photograph	None	Observation	±10% Reading	±20% Reading	100%
O_2	Paramagnetic	EPA Spec. 3	Flame	±0.02%	± 0.04%	90%
CO	NDIR	EPA Spec. 3	Flame	±4 ppm	±8 ppm	90%
CO_2	NDIR	EPA Spec. 3	Flame	±0.02%	±0.04%	90%
HC	FID	None	Flame	±0.5 ppm	±1.0 ppm	90%
SO_2	FPD	EPA Spec. 2	Flame	±20% Reading	±40% Reading	90%
SO_2	Titration	EPA Method 6	Flame	±10% Reading	±20% Reading	90%
NO_x	Chem. Lumin.	EPA Spec. 2	Flame	±5% Reading	±20% Reading	90%
NH_3	Chem. Lumin.	None	Flame	±20% Reading	±40% Reading	90%
Particulate	Filter	EPA 600/4-76-004	Flame	±5% Reading	±10% Reading	90%
Individual HC	Tenax/ Charcoal GC	None	Flame	±30% Reading	±50% Reading	90%

G.2 Quality Problems and Solutions

Several problems with quality control were encountered and corrected during the course of this program.

The concentration of carbon species in the ambient air was recognized to be a problem and a procedure is described in Section 3.3 to correct for it.

Determination of soot concentration by weighing proved difficult. Accurate measurements of soot were obtained by burning the material from prebaked filters.

The instrument for measurement of SO_2 proved unsatisfactory. It was returned to the factory for repair and performance was improved but was still less than desired. Instrument measurements of SO_2 were supplemented by absorption and titration of SO_2 throughout these tests.

Continuous monitoring of emissions from the flare flame proved to be undesirable because of flame fluctuations. Gas samples were drawn through Teflon® lines into Tedlar® bags for 20 minutes to average flame fluctuations, mixed and analyzed using continuous analyzers.

A video recorder was used to record the structure of the flame flames. However, the spacial and temporal resolution were insufficient to make this technique useful. Excellent results were obtained using still photography and high speed motion pictures.